NORTH-WEST UNIVERSITY
YUNIBESITI YA BOKONE-BOPHIRIMA
NOORDWES-UNIVERSITEIT
POTCHEFSTROOMKAMPUS

Recovery of gold from spent matrices using supercritical carbon dioxide

P.G. van Zyl

Thesis submitted for the degree Philosophiae Doctor in Chemistry
at the North-West University, Potchefstroom Campus

Promoter: E.L.J. Breet

2007
Potchefstroom

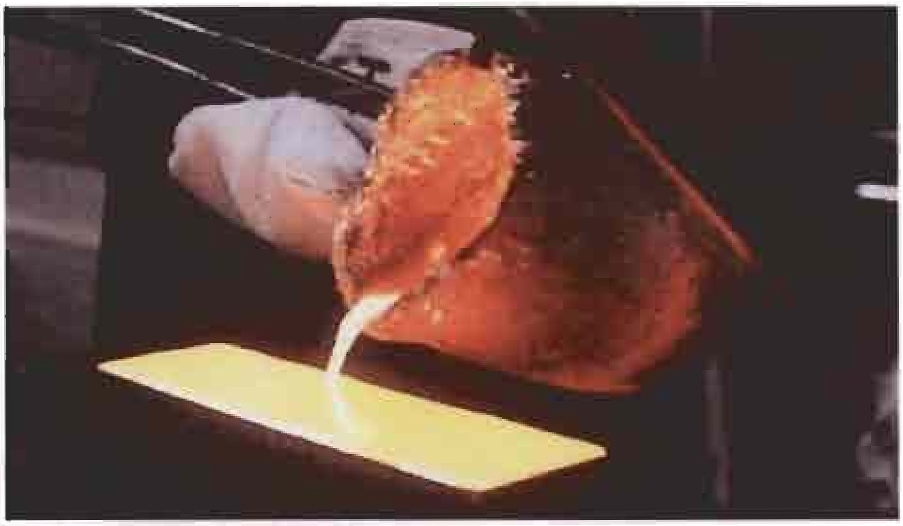

Gold is a child of Zeus, neither moth not rust devoured it, but mind of man is devoured by this supreme possession. (Pindar; 522 - 443 B.C.)

CONTENTS

CHAPTER 0

Gold Recovery by *sc*-CO_2?

Gold has always been precious to mankind, and the acquisition and recovery of gold has been an important issue since the earliest times. In South Africa, the cyanide process[1] for the extraction of gold from ore had its centenary in 1997 and has been developed and refined to a high level of perfection.

A problem which has arisen in the gold industry in time relates to gold residues (with gold prevailing as Au^{3+}) entrapped in spent ion exchange resin in the course of uranium recovery processes. The removal of such gold residues from spent matrices requires a new method of gold extraction and recovery which is both economically viable and environmentally friendly. Furthermore, gold(I) cyanide adsorbed onto activated carbon in the cyanidation gold recovery process is currently stripped from the matrix by environmentally hazardous processes such as acid and base elution. Clean technology to desorb gold from activated carbon is of interest to the mining industry.

Recent figures show that approximately 3 500 tons of such spent ion exchange resin are available in South Africa. On an average, 100 g of gold per ton of spent resin is potentially recoverable. This amounts to a total value of 50 million Rand. The 200 g/ton of uranium and other radioactive nuclides also entrapped in these resins represent a major environmental hazard. Stricter laws controlling the treatment of radioactive waste therefore also necessitate a new approach to the problem.

A few recent papers have reported on the dissolution of gold and gold complexes in supercritical carbon dioxide (*sc*-CO_2).[2-6] Although not yet fully understood and sufficiently explored, supercritical fluid technology could be a solution to the problem of removing/recovering adsorbed gold from different matrices. The intention with this project was to make a contribution towards such a recovery process to the potential advantage of the mining industry by conducting a fundamental study on the complex formation of gold and the solubility characteristics of gold complexes in *sc*-CO_2. The knowledge acquired in such a fundamental study could then serve as a basis for designing and optimising a potentially feasible gold recovery process from gold containing matrices.

0.1 Objectives

The specific objectives were to

1. acquire samples of pure gold and of activated carbon and to successfully load the metal in a suitable form onto the carbon matrix;
2. prepare a variety of gold complexes, analyse/characterise these complexes and measure the solubility of the complexes in *sc*-CO_2 in order to establish the preferred species to load onto activated carbon for removal by *sc*-CO_2;
3. to develop several methods to monitor gold removal in order to achieve reliable results in the anticipated event that removal may be limited and that yields of removed gold may be quite small;
4. perform trial extraction runs by *sc*-CO_2 to explore the possibility of metal recovery from the activated carbon surface;
5. optimise removal of gold by *sc*-CO_2 (should the process be viable) in terms of major role-playing conditions by virtue of a statistical design and surface response analysis;
6. investigate the influence of cosolvents in *sc*-CO_2 for the removal of gold from activated carbon;
7. propose a plausible mechanism (formation of carbonato complex,[7] for instance) whereby gold is removed by *sc*-CO_2.

General objectives of the investigation included

1. a contribution to the chemistry of gold and coordination chemistry of gold complexes;
2. added value to the development of supercritical fluid technology in general and to the application possibilities of *sc*-CO_2 in particular;
3. promotion of the concept of clean technology and development of processes for green chemistry.

0.2 Strategy

The realisation of the objectives outlined above required specific strategies comprising the following steps:

a. purchase of or sponsorship for pure gold from a gold supplier or refinery and location of industrial suppliers of activated carbon to obtain the most suitable quality carbon available for gold adsorption;

b. synthesis and characterisation of gold(I) and gold(III) complexes with selected ligands and measurement of the solubilities of these complexes in *sc*-CO_2 as a directive of which species should preferably be loaded onto activated carbon to investigate the feasibility of gold recovery from a matrix by *sc*-CO_2;

c. customisation of analytical techniques such as uv/visible spectrophotometry (for monitoring absorbance maxima and determining molar absorption coefficients), scanning electron microscopy (for surface analysis of activated carbon) and atomic absorption and/or inductively coupled plasma spectrometry (for gold analysis);

d. proof of the viability of gold removal from activated carbon by *sc*-CO_2 using a laboratory-size supercritical fluid extractor and samples of activated carbon preloaded with selected gold complex species,[8]

e. optimisation of recovery of a selected complex in terms of conditions (temperature, pressure, time) derived from a statistical experimental design,[9]

f. investigation into other substances (organophosphates, β-diketones) that could also recover adsorbed gold either as a primary extractant or as a cosolvent for *sc*-CO_2.

0.3 Methodologies

The utilisation of various physical/chemical, analytical and statistical/mathematical approaches were envisaged. These included

1. standard techniques for synthesis of coordination compounds;
2. characterisation of complex species of gold and analysis of extract composition by spectrometric methods;
3. solubility data for gold(I) and gold(III) complexes by virtue of concentration-time curves at selected conditions;
4. percentage recovery of adsorbed species by *sc*-CO_2 as a function of different variables (time, temperature, pressure, density, flow rate, % modifier);
5. optimisation of gold recovery by surface response analysis using a statistical software package.

0.4 Infrastructure

The infrastructure offered by the Separation Science and Technology (SST) research laboratory at the North-West University (Potchefstroom Campus) was accessible for the execution of the envisaged project. These included labware, chemicals, basic facilities, small instrumentation, a state-of-the-art laboratory-size supercritical extractor and analytical instrumentation (uv/visible spectrophotometer, atomic absorption spectrometer, ICP-MS). A scanning electron microscope (SEM) connected to an energy dispersive detector system (EDS) was available as an interdepartmental facility on campus, while some analyses were performed by an independent accredited laboratory. Two essential chemicals for the investigation (gold, activated carbon) were donated by companies.

0.5 Envisaged Output

In addition to a thesis in fulfilment of the requirements for the doctoral degree, the results of this research project were envisaged to be published in accredited journals, to be presented at conferences and to be utilised in the design of a potentially feasible gold recovery process in the interest of the gold mining industry. It might further contribute to the protection of the environment by presenting a less harsh process than acid and base elution for the recovery of adsorbed gold from matrices, and to safe and efficient handling of radioactive waste.

References:

1 http://www.bullion.org.za

2 Otu, E.O.; Wilson, W.W., *Separation Science and Technology*, **2000**, *35(12)*, 1879.

3 Otu, E.O., *Separation Science and Technology*, **1997**, *32(6)*, 1107.

4 Glennon, J.D.; Harris, S.J.; Walker, A.; McSweeney, C.C.; O'Connell M., *Gold Bulletin*, **1999**, *32(2)*, 52.

5 Arai, M.; Nishiyama, Y.; Ikushima, Y., *Journal of Supercritical Fluids*, **1998**, *13*, 149.

6 Wang, J.S.; Wai, C.M., *Industrial and Engineering Chemistry Research*, **2005**, *44*, 922.

7 Cloete, E.; Breet, E.L.J.; Van Eldik, R., *Journal of Chemical Society Dalton Transactions*, **1995**, 3591.

8 LECO TFE 2000™ Instruction Manual, Copyright LECO® Corporation, **2002**.

9 CSS Statistica User Manual, Copyright© StatSoft Inc., **1991**.

CHAPTER 1

Recovery and Chemistry of Gold

Historians believe that gold was the first metal known to man ca. 6 000 years ago. Man desired gold for its sheer beauty and for precious objects into which it can be converted. Over centuries, gold has been used as a currency, and in modern times it is increasingly used in industry, for instance in dentistry, computers and electronic circuits.

Most of the gold discovered until the last century was alluvial (gold found in riverbeds), and panning for such gold was relatively easy. Although gold mining began in the Urals (Russia) as early as 1744, most of the world's major discoveries were made in the second half of the 19th century.

With the Witwatersrand discovery in 1886 South Africa became the largest source of gold. The gold is embedded in rock and could not be recovered by simple panning. As a result the whole nature of gold mining changed. It was carried out by corporations. The large mining houses of modern times were born.[1,2]

1.1 RECOVERY OF GOLD

1.1.1 Gold Mining in South Africa – Brief Historical Overview

History records that gold was first discovered on the Witwatersrand in 1834. The discoveries in the then Eastern Transvaal in the 1870's gave rise to the first gold rushes, but the gold deposits found in this area proved to be small in relation to those of the gold bearing Witwatersrand reefs. An outcrop of these reefs was discovered in 1885 on the farm "Langlaagte" on the western outskirts of Johannesburg.[2]

The full extent of these reefs has emerged gradually over the years. At present they are being mined over an arc of about 500 kilometres extending from beyond Virginia in the Free State, through Klerksdorp in the North-West Province, Carletonville, Krugersdorp and Johannesburg in Gauteng to Kinross in Mpumalanga. South Africa has about 35 percent of known world gold reserves. This constitutes by far the largest known deposits of gold in the world and is the source of about 40 percent of the annual world production of newly mined gold.[3]

1.1.2 Importance of Gold Mining[1]

Infrastructure

Gold is one of the main export commodities of South Africa, and gold mining is the nation's largest single industry and second largest employer. Through gold mining, many towns and cities have come into being. Much of the infrastructural development of roads, electricity generation, water reticulation, telecommunications, housing and supporting industries have resulted from gold mining.

Gross domestic/geographic product

Gold mining has played a pivotal role in the development of the domestic economy. Although its relative importance has diminished over the last decade, it still contributes just under 4 percent directly to the gross domestic product (GDP). This is substantially lower than the 17 percent direct contribution recorded in 1980 when the gold price was at peak, but taking in consideration the indirect contribution to the economy and the multiplier effects, gold mining's total contribution to GDP is closer to 10 percent. It also contributes substantially to the national fiscus, both directly and indirectly.

The contribution of gold mining to economic growth in certain provinces is significantly larger than the contribution to the overall economy. The mining sector was responsible for approximately 20 percent of the gross geographic product (GGP) of the Free State, 40.5 percent of North-West Province, 24.6 percent of

Northern Cape, 20.4 percent of Mpumalanga and 20.1 percent of Limpopo. One realises that closure of certain gold mines would have a significant impact on the economy and socio-economic welfare of certain mining towns.

Foreign exchange earnings

Gold has been South Africa's largest export commodity for years. While gold mining is a very high nett generator of foreign exchange, it is also a very low nett user of foreign exchange since much of the required materials and technology has been developed locally.

Employment

In 1996 gold mines employed 2.3 percent of the total economically active population or 3.5 percent of those formally employed in the economy. Approximately R8.8 billion was paid to these mine workers as wages. Estimates indicate that for every three people employed at a mine, one other person is employed by industries serving the mining industry directly or indirectly. It is also estimated that every worker in the gold mining industry has between 7 and 10 dependants, thereby highlighting the social importance of the industry.

Challenges

The most fundamental challenge facing the mining industry is productivity of labour and control over costs. For most minerals, including gold, prices are set on international markets. In order to remain competitive, the mining industry has to focus on productivity and cost saving. Current inhibiting factors include restrictive legislation, government intervention in the domestic economy, domestic price instability and high domestic taxation.

1.1.3 Basic Processes of Gold Mining and Processing

Modern prospecting culminates in drilling holes into the earth at selected sites to precisely locate the gold reef. When payable deposits are found, a mine is developed. A shaft is sunk to reach the gold-bearing rock. Tunnels are driven at various levels from the shaft, until the inclined plane of the gold bearing reef is struck. These "cross-cuts" are excavated by drilling holes at various angles into the face of the tunnel. These holes are filled with explosives and the rock is blasted out. When the cross-cuts reach the gold bearing conglomerate, other tunnels are developed along the plane of the reef. The process of drilling and blasting is known as stoping. Gold bearing ore is hoisted up the shaft and sent for extraction of gold.[2]

The major commercially viable extraction processes for gold include cyanide leaching (cyanidation), gravity concentration, flotation, refractory ore processing, amalgamation and alternative lixiviants. Today, the standard method used for extracting most of the gold throughout the world is cyanide leaching. The reason is mainly economical, since cyanide leaching is capable of recovering about 90 percent of the available gold as opposed to about 60 percent recovery in amalgamation plants. Many of the old tailing piles from other processes have been economically reprocessed by cyanide leaching.[4]

The standard cyanide leach process entails grinding of the ore to about 80 percent 200 mesh, mixing the ore/water slurry with about 1 kg per ton sodium cyanide and sufficient quick lime to keep the pH of the solution at about 11.0. At a level of 50 percent solids, the slurry passes through a series of agitated mixing tanks with a residence time of 24 hours. The gold bearing liquid is then separated from the leached solids in thickener tanks or vacuum filters, and the tailings are washed to remove gold and cyanide prior to disposal. The separation and washing take place in a series of units by counter-current decantation. Gold is then precipitated from the pregnant solution by addition of zinc or by adsorption onto activated carbon. In the zinc precipitation process the precipitate is filtered off and melted with fluxes at the mine to recover the gold bullion as doré bars, which are refined later to more than 99 percent purity. Gold adsorbed onto carbon is recovered by elution and submitted to the same pyrometallurgical process as the precipitate.[1]

The recovery of gold by adsorption onto activated carbon in cyanide solution is based upon the physical affinity carbon has for gold (it can attract 7 percent of its mass in gold). There are several variations to the carbon adsorption process:

1. Carbon-In-Column (CIC): The leach solution flows through a series of fluidised bed carbon columns in an up-flow direction. The major advantage of these columns is the ability to process solutions containing as much as 2 to 3 mass percent solids. Down-flow columns are rarely used for gold recovery, since they act like sand filters suffering frequent plugging.[4]

2. Carbon-In-Pulp (CIP): This process was developed in South Africa during the 1970's and is considered to be the most significant advance in gold recovery technology in recent years. The slurry of finely ground ore (75 µm particle size) and water (the 'pulp') is treated with cyanide in large tanks stirred mechanically or by air-agitation. Instead of separating solids from the pregnant solution as in the traditional cyanidation process, activated carbon is used to adsorb gold directly from the cyanided pulp while it is flowing continually from one vessel to another and the carbon is transferred in the counter-current direction. The gold value of the pulp decreases downstream and the gold loading on the carbon increases upstream.[1]

3. Carbon-In-Leach (CIL): The process integrates leaching and carbon-in-pulp into a single operation by fitting leach tanks with carbon retention screens so that gold is adsorbed onto carbon almost as soon as it is dissolved by the cyanide solution. CIL is often used when native carbon present in the gold ore adsorbs the leached gold and prevents its recovery. The carbon added in CIL is more active than the native carbon, so that gold will be preferentially adsorbed by carbon that can be recovered for stripping. The CIL process is used in small cyanide mills to reduce the complexity and cost of the circuit, but carbon loading is 20 to 30 percent less than with CIP and thus requires a larger carbon inventory.[4]

The final stage of gold processing is pyrometallurgical conversion of gold concentrate to bullion. Generally, South African mine doré contains about 10 percent silver and 2 to 3 percent copper, iron and other base metals. The removal of non-gold material is achieved in refineries. As a result, mine metallurgy plants are restricted to production of suitable quality bullion that can be accurately sampled and assayed.[1]

1.1.4 Activated Carbon in Gold Recovery[5]

Activated carbon is a generic term for highly porous carbonaceous materials that cannot be defined by a structural formula or by chemical analysis. It is a piece of carbon with millions of tiny interlocking holes occupying space within the carbon and constituting high internal surface area. Typical activated carbons used in the Carbon-in-Pulp (CIP) and Carbon-in-Leach (CIL) processes discussed in **Section 1.1.3** have surface areas of about 1 000 m^2/g, which means that one gram of activated carbon has the same surface area as two football fields.

The pores in activated carbon are classified into the following groups depending on the diameter of the pores:

macropores (500 - 20 000 Å) running from the surface of the activated carbon into the interior and allowing rapid movement of adsorbates into the activated carbon;

mesopores (100 - 500 Å) branching off the macropores and allowing the adsorbates to leave the macropores;

micropores (8 - 100 Å) constituting 95% of the total internal surface area and allowing adsorbates transported by the meso- and macropores to be strongly adsorbed.

Activated carbon is inert and carries no charge. Its internal surface area is therefore neutral, so that only neutral species from water, industrial solutions and gases are adsorbed and charged species are left behind. Gold leached from ore in the cyanidation process

$$Au + 2CN^- \longrightarrow Au(CN)_2^- \qquad (1.1)$$

is present in water as gold cyanide ion. An ion-pair is formed when a positive ion such as Ca^{2+}, Mg^{2+}, Na^+, K^+ combines with the gold cyanide ion to form neutral species.[6,7]

$$K^+ + Au(CN)_2^- \longrightarrow [K^+.....Au(CN)_2^-] \qquad (1.2)$$

Equilibrium is established between the gold cyanide ion and the ion-pair. The neutral ion-pair is adsorbed by the activated carbon while gold cyanide ion remains in solution.

The adsorption of the ion-pair onto activated carbon is depicted as physical adsorption. It results from the action of Van der Waals forces causing some distortion of electron distributions of adsorbate molecules and solid phase surface molecules in mutual proximity but with the electrons maintaining their association with the original nuclei. There is no chemical reaction between the ion-pair and the carbon surface. Important factors that determine the extent of adsorption are the concentration, mole mass, molecular size and polarity of the adsorbate. The only factor that can be varied during gold adsorption is the concentration of the adsorbate in solution. The higher the concentration of gold in solution is, the larger the amount of gold adsorbed onto activated carbon will be.

Removal of adsorbed gold from activated carbon can be done by reversing adsorption. This requires a stable ion-pair present on the carbon surface, such as $Ca(Au(CN)_2)_2$, to be converted to a less stable ion-pair, such as $NaAu(CN)_2$. This is achieved by washing the carbon with a hot NaOH/NaCN solution. The high concentration of sodium ion causes ion exchange between calcium and sodium to form a less stable sodium gold cyanide ion-pair. The high pH and high cyanide concentration further destabilises the $NaAu(CN)_2$ ion-pair as the $Au(CN)_2^-$ ion is stabilised under these conditions. Since the adsorption of gold is an exothermic process, presence of heat promotes elution.

The two subsequent process steps involve regeneration of the carbon to a gold activity (affinity which carbon has for gold) as close as possible to that of virgin carbon, and acid washing to remove scaling by converting $CaCO_3$ to $CaCl_2$ soluble in water. Regeneration entails removal of organic poisons by heating to above their boiling points (~ 700 °C) and addition of steam to etch away pyrolysed matter caused by organics breaking down during heating. Acid washing is a rapid reaction which does not require heat and which removes base metals such as Ni, Fe and Zn. It is generally undertaken prior to elution, but it may be performed after regeneration.

1.2 CHEMISTRY OF GOLD

Gold has a characteristic brilliant yellow colour in bulk, but when finely divided, it can be black, purple, ruby red or blue. Although oxidation states from -1 to +7 are claimed for gold, the chemistry of gold is dominated by the +1 and +3 oxidation states.[8] Types of complex compounds in which gold exists in different oxidation states are summarised in **Table 1.1**:

Table 1.1 Types of complex compounds with gold in different oxidation states[8]

Oxidation state	Type of complex
-1	With very electropositive metals (e.g. Cs^+)
+1	With wide range of ligands, mostly 2-coordinate
+2	Rare, stabilised by suspect ligands
+3	Common with wide range of ligands, usually square-planar
+4	One example with a suspect ligand
+5	Fluorine as ligand, 6-coordinate
+7	Not confirmed, F^- as ligand

The ionisation energies of gold are listed in **Table 1.2**. The high I_1 value for gold (890 kJ mol^{-1}) compared to that of silver (731 kJ mol^{-1}) is attributed to the relatively high energy of the 6s shell (from which an electron is removed), while the low I_3 value for gold (2 900 kJ mol^{-1}) compared to that of silver (3 361 kJ mol^{-1}) stems from the stability of the +3 state reinforced by the large ligand field splitting of the $5d^8$ ion[8]. The preference for the +3 state is attributed to relativistic effects according to Hartree-Fock calculations.[9]

Table 1.2 Ionisation energy values for Au[8]

Ionisation energy (kJ mol^{-1})	Electronic configuration change
$I_1 = 890$	$6s^1 \rightarrow 5d^{10}$
$I_2 = 1\,978$	$5d^{10} \rightarrow 5d^9$
$I_3 = 2\,900$	$5d^9 \rightarrow 5d^8$
$I_4 = 4\,200$	$5d^8 \rightarrow 5d^7$

Mixing of atomic orbitals of gold to give hybrid orbitals capable of generating diagonal 2-coordination[10] is illustrated in **Figure 1.1**. The $5d_z{}^2$ and 6s atomic orbitals of gold can mix as a result of the small d^{10}-d^9s separation and the large d^9s-d^9p separation to form two molecular orbitals Ψ_1 and Ψ_2. Ψ_1 lies away from the two incoming ligands along the z-axis and can occupy the electron pair which was initially in the $5d_z{}^2$ orbital. Ψ_2 can mix with $6p_z$ to form the orbitals Ψ_3 and Ψ_4 which have empty lobes pointing along the z-axis and which can accept electron pairs from the two incoming ligands. This mixing of orbitals generates diagonal 2-coordination.

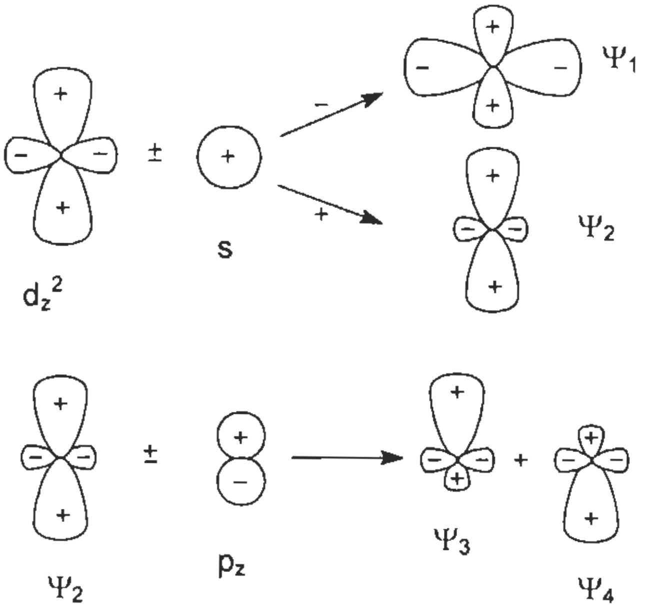

Figure 1.1 Illustration of orbital mixing for diagonal 2-coordination.[10]

1.2.1 Gold Halides and Oxides

In **Table 1.3** the characteristics of different halides of gold are listed. AuCl and AuBr are prepared by cautious heating of Au_2X_6. In **Reaction 1.3** the synthesis of gold trichloride is illustrated. When heated, gold(I) chloride is formed as shown in **Reaction 1.4**. In **Reaction 1.5** the direct synthesis of AuI is shown.

$$2Au + 3Cl_2 \xrightarrow{240°C} Au_2Cl_6 \qquad (1.3)$$

$$Au_2Cl_6 \xrightarrow{150°C} 2Cl_2 + 2AuCl \qquad (1.4)$$

$$2Au + I_2 \longrightarrow 2AuI \qquad (1.5)$$

Table 1.3 Characteristics of gold halides[8]

	F	Cl	Br	I
AuX		Yellow-white, decomposes at 170°C	Light yellow, decomposes at 115°C	Lemon, decomposes at 120°C
AuX_2		Black; is in fact Au_4Cl_8 containing Au(I) and Au(III)		
AuX_3	Gold-yellow, decomposes at 500°C	Red, decomposes at 254°C	Dark brown, decomposes at 97°C	
AuX_5	Yellow-brown			
AuX_7	Pale yellow			

All three gold(I) halides have a zig-zag chain structure with linear coordination to gold as shown in **Figure 1.2**. Gold(III) coordination compounds, such as Au_2Cl_6, have a square-planar structure shown in **Figure 1.3**. Two types of structures are involved in 4-coordinated gold. AuF_3 has a fluorine-bridged helical structure (**Figure 1.4**),[11] while the corresponding chloride[9] and bromide[12] species are dimeric Au_2X_6 with Au - Cl 2.243 - 2.249 Å (terminal) and 2.334 Å (bridged)

(**Figure 1.3**). Some ligands cause the bridges to break and to form adducts $AuX_3.L$, while other ligands reduce the bridged compounds to gold(I) species.

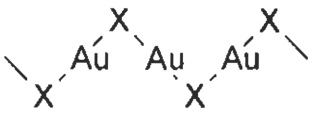

Figure 1.2 Structure of gold(I) halides in the solid state

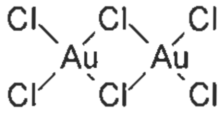

Figure 1.3 Structure of Au_2Cl_6

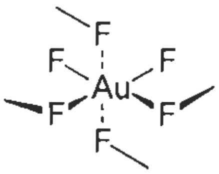

Figure 1.4 Structure of AuF_3

The only important gold oxide is Au_2O_3 (brown), which is obtained by alkaline precipitation of Au^{3+}. Single ruby crystals have been synthesised by hydrothermal crystallisation at 235 - 275 °C from $HClO_4/KClO_4$. It has a polymeric structure with square-planar coordinated Au^{3+}.[13] It decomposes to the elements on gentle heating and exists in strong alkali as $Au(OH)_4^-$.

1.2.2 Aqua Ions

Gold is traditionally dissolved in aqua regia to yield $AuCl_4^-$, in alkali cyanides to produce $Au(CN)_2^-$ or in thiocyanates to form $Au(SCN)_2^-$.[14] The Au^{3+} ion is the only stable species in aqueous solution and it is always complexated. The relevant reduction potentials in acidic solution are given below:

$$Au^+ (aq) + e^- \longrightarrow Au (s) \qquad E^0 = +1.83\ V \qquad (1.5)$$

$$Au^{3+} (aq) + 2e^- \longrightarrow Au^+ (aq) \qquad E^0 = -1.36\ V \qquad (1.6)$$

The electrode potentials for selected gold(I) and gold(III) complexes are listed in **Table 1.4**. These potentials predict the disproportionation

$$3Au^+ (aq) \longrightarrow Au^{3+} (aq) + 2Au (s) \qquad E^0 = +0.47\ V \qquad (1.7)$$

of Au^+ in aqueous solution. AuCl, for example, immediately decomposes into gold and gold(III) chloride. $(AuCN)_2^-$ is formed by oxidation of gold in the presence of CN^-.

$$Au + 2CN^- \longrightarrow Au(CN)_2^- + e^- \qquad E^0 = +0.61\ V \qquad (1.8)$$

Table 1.4 Selected electrode potentials for gold(I) and gold(III) complexes[8] $[Au(L^{n-})_2]^{(1-2n)+}$ and $[Au(L^{n-})_4]^{(3-4n)+}$

Ligand	E^0/V	
	Gold(I)	**Gold(III)**
H_2O	-1.83	-1.52
Cl^-	-1.15	-1.00
Br^-	-0.96	-0.85
I^-	-0.66	
SCN^-	-0.58	-0.64
NH_3	-0.56	-0.33
CN	+0.61	+0.20

1.2.3 Gold(I) Complexes

A molecular orbital (MO) scheme for a typical σ-bonded gold(I) complex, $[AuL_2]^+$, is shown in **Figure 1.5**. The 5d orbitals of the Au atom are completely filled and the atomic orbitals of the two ligands each accommodate an electron-pair for donation to the central metal atom. The atomic orbitals lead to the formation of seven molecular orbitals according to the linear combination of atomic orbitals (LCAO) principle in which the fourteen electrons are arranged according to Hund's rule.[15]

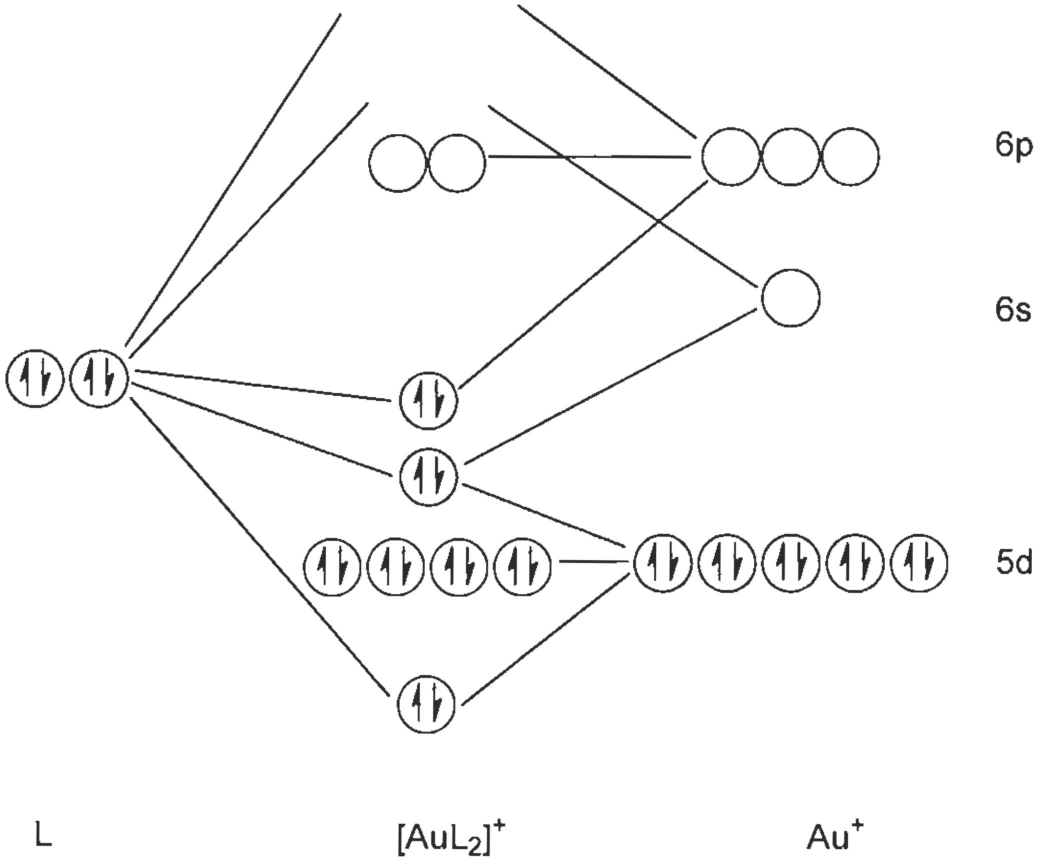

Figure 1.5 MO diagram for a σ-bonded complex $[AuL_2]^+$.[16]

Complexes of O-, N- and halogen-donors

Very little is known about O-donor complexes of gold(I). The most important Au-O bond is formed in $[(Ph_3P)Au]_3O^+$, which is used as a starting material in the synthesis of a hetero-atom oxo-centred gold cluster compound.[17] Most similar type complexes reported involve other supporting ligands, such as in $(Ph_3P)Au(OSi(CH_3)_3)$.

Complexes with ammines, nitriles and diazoles, like $Au(NH_3)_2^+$ and $Au(RCN)_2^+$, are known but little studied.

The ions AuX_2^- (X = Cl, Br, I) are well known but very unstable in water unless excess halide ion is present. The series $(C_4H_9)_4NAuX_2$ was prepared by reactions like[8]

$$2R_4NAuCl_4 + PhNHNH_2HCl \longrightarrow R_4NAuCl_2 + R_4NPhAuCl_3 + N_2 + 4HCl \qquad (1.9)$$

Au-X bond lengths are 2.257 Å (Cl), 2.376 Å (Br) and 2.529 Å (I).

Tertiary phosphine and arsine complexes

These complexes of gold(I) have been intensively studied since the early 1970's. The usual starting material is $AuCl_4^-$, which can be reduced with a tertiary phosphine

$$AuCl_4^- + 2R_3P \longrightarrow R_3PAuCl + R_3PCl_2 + Cl^- \qquad (1.10)$$

to yield a complex with a coordination number between 2 and 4.[18] An alternative method for the synthesis of tertiary phosphine or arsine gold complexes involves cheaper *in situ* preparation with 2,2'-thiodiethanol, (bis-2-hydroxyethylsulphide) (1.11).

$$AuCl_4^- + 2(HOCH_2CH_2)_2S \longrightarrow AuCl[S(CH_2CH_2OH)_2] + (HOCH_2CH_2)_2SO + Cl^- + 2HCl \qquad (1.11)$$

$(Ph_3P)AuX$ (X = Cl, Br, I, NO_3, SCN, Ph, CN) are linear 2-coordinated 1:1 complexes with Au - P bond lengths ranging between 2.199 and 2.325 Å. Complexes with more than one phosphine (2:1; 3:1 and 4:1) have been prepared by varying the stoichiometry of the reaction mixture.[18]

Complexes of C-donors

The most important complexes with C-donors are cyanides. AuCN has a linear structure and dissolves in excess KCN to form $K^+Au(CN)_2^-$, which is important for the extraction of gold. It has been characterised as various salts (Tl, K, $(C_4H_9)_4N$, Cs) with an Au - C bond length of 1.964 Å.[19] Isocyanides are C-donor ligands forming stable complexes with gold, for example

$$AuCl(S(CH_3)_2) + CH_3NC \longrightarrow AuCl\{(CH_3)NC\} + (CH_3)_2S \quad (1.12)$$

$$AuCl_4^- + (C_4H_9)NC + C_2H_5OH \longrightarrow AuCl\{(C_4H_9)NC\} \quad (1.13)$$

Excess isocyanide leads to $Au(RNC)_2^+$ and possibly $Au(RNC)_4^+$. Linear Au(CO)Cl, which is a useful synthetic intermediate, is prepared according to

$$HAuCl_4 + CO + SOCl_2 \longrightarrow Au(CO)Cl + COCl_2 \quad (1.14)$$

Complexes of S-donors

The most important complexes of S-donors are thiolates, $[Au(SR)]_n$. Allthough little is known about their structures, EXAFS and Mossbauer measurements indicate that they coordinate diagonally with gold (Au - S bond length of 2.30 Å) and are thiolate-bridged polymers.[20] Hexameric structures have been suggested for some complexes with long alkyl groups soluble in organic solvents.[21] Reaction with phosphines lead to monomeric R_3PAuSR and contains diagonally coordinated gold. Sulphate and thiosulphate bind through sulphur, such as in $Na_3Au(S_2O_3)_2.2H_2O$, which has a linear 2-coordinated gold structure.

Among neutral ligands, thioethers form important complexes $AuCl(SR_2)$ which are synthetically useful since the sulphide is easily replaced by strong donors like tertiary phosphines. Thiourea complexes with a linear coordination structure are also important. $[Au(S{=}C(NH_2)_2]^+X^-$ (X = Cl, ClO_4, NO_3)[22] is formed when gold reacts with thiourea in acidic solution[23]. Gold thiourea was introduced as a possible extracting ligand for gold because of its adsorption onto activated carbon. It leaches gold at a much faster rate than cyanide.[24]

$$HAuCl_4 + 2(NH_2)_2CS \xrightarrow{HX} [Au(S{=}C(NH_2)_2]X \qquad (1.15)$$

1.2.4 Gold(III) complexes

Complexes of halogens

Gold(III) has a d^8 electron configuration and forms square-planar complexes with halogens. The tetrahalometallates are normally starting materials. The oxidising agent is usually concentrated HNO_3.

$$Au \xrightarrow[\text{oxidising agent}]{HX} HAuX_4 \text{ (X = Cl, Br)} \qquad (1.16)$$

Typical bond lengths are 2.27 - 2.29 Å (Cl), 2.404 Å (Br), 2.633 - 2.648 Å (I) and 1.915 Å (F).[8]

Complexes of N-donors

Gold(III) forms complexes with a variety of N-donor ligands. These complexes have a square-planar structure. Examples include $AuCl_3py$ and $Au(NH_3)Cl_3$.[8] Ethylene-1,2-diamine forms $Au(en)_2Cl_3$ with an ionic nature (**Figure 1.6**) which distorts to $Au(en)_2Cl_2^+$ in the solid state.[25] 1.10-phenanthroline monohydrate reacts with gold(III) to form $[Au(phen)Cl_2]Cl$ (**Figure 1.7**).[26]

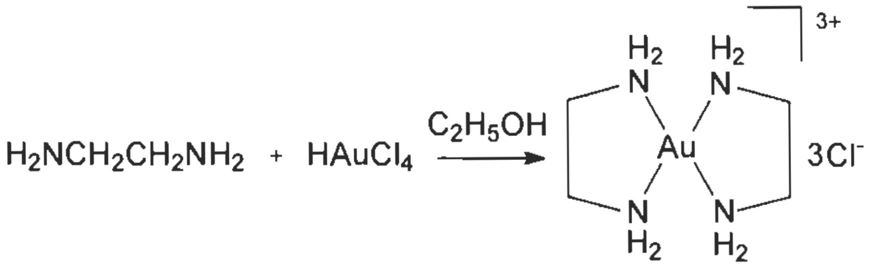

Figure 1.6 Synthesis of $Au(en)_2Cl_3$

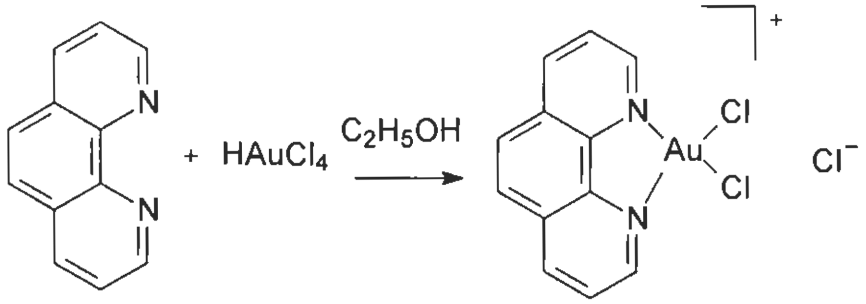

Figure 1.7 Synthesis of $[Au(phen)Cl_2]Cl$

$Au(en)_2^{3+}$ reacts with β-diketones in template reactions to afford complexes of tetradentate macrocycles as illustrated in **Figure 1.8**.[8] Macrocyclic complexes include the porphyrin complex Au(TPP)Cl, and cyclam-type macrocyclic ligands have a very high affinity for gold(III).[27] Fluorinated crown ethers of gold(III) were also synthesised to form macrocyclic compounds.[28]

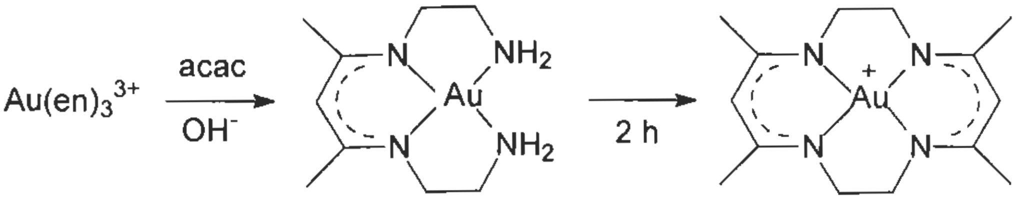

Figure 1.8 Synthesis of a gold(III) macrocycle complex

Other complexes

Tertiary phosphines and arsines tend to reduce gold(III) to gold(I), although reverse reactions can be used to synthesise these complexes[29]:

$$Ph_3PAuCl + Cl_2 \longrightarrow (Ph_3P)AuCl_3 \qquad (1.17)$$

Oxidation of gold(I) complexes gives unexpected results with the formation of a Au-C bond. Gold(I) complexes of bidentate phosphines and arsines, like $Au(diphos)_2^+$ and $Au(diars)_2^+$, can be oxidised to gold(III) species[30].

Thiols and other sulphur ligands can be used to reduce Au^{3+} to Au^+, but gold(III) complexes can be made with tetramethylthiourea, for example. Various dithiocarbamates and dithiolene complexes have been synthesised. Square-planar coordination generally occurs in these compounds. The most important complex with an inorganic C-donor is $Au(CN)_4^-$, captured as a potassium salt.[8]

$$Na^+AuCl_4^- \xrightarrow{\text{conc. KCN(aq)}} K^+Au(CN)_4^- \qquad (1.18)$$

Abbreviations

acac - acetylacetonate
diars - diarsene
diphos - diphosphine
en - ethylenediamine
EXAFS - Extended X-ray Absorption Fine Structure
Ph - phosphine
phen - phenanthroline
py - pyridine
R - alkanes, alkenes, alkynes
TPP - tetraphenylporphyrin
X - halogen

References

1 http://www.bullion.org.za

2 Stanley, G.G., *The Extractive Metallurgy of Gold in South Africa, Volume 1*, Chamber of Mines: Johannesburg, **1987**.

3 Directorate: Mineral Economics, *Operating Gold Mines and Recovery Plants in the Republic of South Africa 2006*, Department: Minerals and Energy of the Republic of South Africa, Pretoria, **2006**.

4 http://www.denvermineral.com/ basicp~1.html

5 Rogan, J.; Van Rensburg, D., *An introduction to activated carbon in gold recovery utilizing carbon-in-pulp or carbon-in-leach technology*, **1989**.

6 McDougall, G.J.; Adams, M.D.; Hancock, R.D., *Hydrometallurgy*, **1987**, *19*, 95.

7 Adams, M.D.; Fleming, C.A., *Metallurgical Transactions B*, **1989**, *20B*, 315.

8 Cotton, S.A., *Chemistry of Precious Metals*, Blackie Academic & Professional, Chapman & Hall: London, **1997**.

9 Schwerdtfeger, P.; Boyd, P.D.W.; Brienne, S.; Burrell, A.K., *Inorganic Chemistry*, **1992**, *31*, 3411.

10 Huheey, J.E., *Inorganic Chemistry*, Harper and Row: London, **1975**.

11 Einstein, F.W.B.; Rao, P.R.; Trotter, J.; Bartlett, N., *Journal of the Chemical Society (A)*, **1967**, 478.

12 Lörcher, K-P.; Strähle, J., *Z. Naturforsch. Teil.*, **1975**, *30*, 662.

13 Jones, P.G.; Rumpel, H.; Schwarzmann, E.; Sheldrick, G.M.; Paulus, H., *Acta Crystallographica Section B*, **1979**, *35*, 1435.

14 Wang, J.S.; Wai, C.M., *Industrial and Engineering Chemistry Research*, **2005**, *44*, 922.

15 Shriver, D.F.; Atkins, P.W., *Inorganic Chemistry 3rd Edition*, Oxford University Press: Oxford, **1999**.

16 Bancroft, G.M.; Chan, T.; Puddephatt, R.J.; Tse, J.S., *Inorganic Chemistry*, **1982**, *21*, 2946.

17 Yang, Y.; Ramamoorthy, V.; Sharp, P.R., *Inorganic Chemistry*, **1993**, *32*, 1946.

18 Colburn, C.C.; Hill, W.E.; McAuliffe, C.A.; Parish, R.V., *Journal of the Chemical Society Chemical Communications*, **1979**, 218.

19 Schubert, R.J.; Range, K-J., *Z. Naturforsch*, **1990**, *45B*, 1118.

20 Al-Sa'ady, A.K.H.; Moss, K.; McAuliffe, C.A.; Parish, R.V., *Journal of the Chemical Society: Dalton Transactions*, **1984**, 1609.

21 Schröter, I.; Strähle, J., *Chemische Berichte*, **1991**, *124*, 2161.

22 Kazakov, V.P.; Lapshin, A.L.; Peschchevitski, B.I., *Russian Journal of Inorganic Chemistry*, **1964**, *9*, Nr. 5, 708.

23 Zhang, H.; Ritchie, I.M.; La Brooy, S.R., *Hydrometallurgy*, **2004**, *72*, 291.

24 Broadhurst, J.L.; Du Perez, J.G.H., *Hydrometallurgy*, **1993**, *32*, 317.

25 Minacheva, L.Kh.; Sadikov, G.G.; Sakharova, V.G.; Gladkaya, A.S.; Porai-Koshits, M.A., *Koordinatsionnaya Khimiya*, **1983**, *9*, 566.

26 Block, B.P.; Bailar, J.C., *Journal of the American Chemical Society*, **1951**, *73*, 4722.

27 Kimura, E.; Kurogi, Y.; Takahashi, T., *Inorganic Chemistry*, **1991**, *30*, 4117.

28 Glennon, J.D.; Harris, S.J.; Walker, A.; McSweeney, C.C.; O'Connell, M., *Gold Bulletin*, **1999**, *32 (2)*, 52.

29 Staples, R.J.; Grant, T.; Fackler, J.P., *Acta Crystallographica Section C*, **1994**, *50*, 39.

30 Warren, L.F.; Bennett, M.A., *Inorganic Chemistry*, **1976**, *15*, 3126.

CHAPTER 2

SUPERCRITICAL TECHNOLOGY

Supercritical fluids refer to substances at conditions above their critical temperature and pressure.[1] At these conditions substances do not exhibit two clearly distinguishable phases (liquid and gas) anymore, but exists as a single new (supercritical) phase which can be depicted as either a highly compressed gas or a highly mobile liquid.[2] Although supercritical fluids have only recently been introduced as industrial solvents, the ability of a supercritical fluid to dissolve solids was described as early as 1879.[3] Supercritical fluid technology has been used industrially since the early 1980's to extract caffeine from coffee and tea, nicotine from tobacco and flavourants from hops and spices.[4]

2.1 A Brief History

The phenomenon of a supercritical fluid phase was first noted in 1822 when it was observed that the liquid phase vanishes when different liquids where heated in closed containers. The definition of a critical point was postulated in 1869. In the decades to follow the main aim of this research was to determine the solubility of inorganic and organic substances in supercritical fluids.[5] The solubility characteristics of supercritical fluids has thus been known to man for the past century!

The first industrial use of a supercritical fluid was the removal of asphalt from heavy mineral oil fractions with supercritical propane in the petrochemical industry in the 1930's. In the 1950's research was focused on the development of new techniques to separate substances by using the unique properties of supercritical fluids. The Max Planck Institute registered a patent according to the successful use of supercritical fluids as extraction solvents.[5]

It was only in the 1960's when the first commercial application of supercritical fluids emerged when a patent was granted to *Studiengesellschaft Kohle GmbH* (Mülheim/Ruhr).[6] The first large scale industrial application was the decaffeination of tea and coffee in 1978 when *Hag AG* (Bremen) built a supercritical carbon dioxide (sc-CO_2) plant. In 1982 Germany built the first plant for the extraction of hops with sc-CO_2. In 1985 and 1988 facilities for the extraction of hops and coffee, respectively, were built in the United States of America. In both these countries *sc*-H_2O plants were also built for the oxidation of organic materials in industrial effluent. The process is known as supercritical water oxidation (SCWO) where organic compounds are oxidised to CO_2 and H_2O.[2,7]

2.2 Fundamental Characteristics

A substance is regarded as a supercritical fluid when it exists at conditions above its critical point.[1] This point denotes the conditions (T_c, p_c) at which the phase boundary between the liquid and gaseous phases disappears and only a single phase exists as shown on the phase diagram in **Figure 2.1**. The critical conditions for a few different substances are listed in **Table 2.1**.

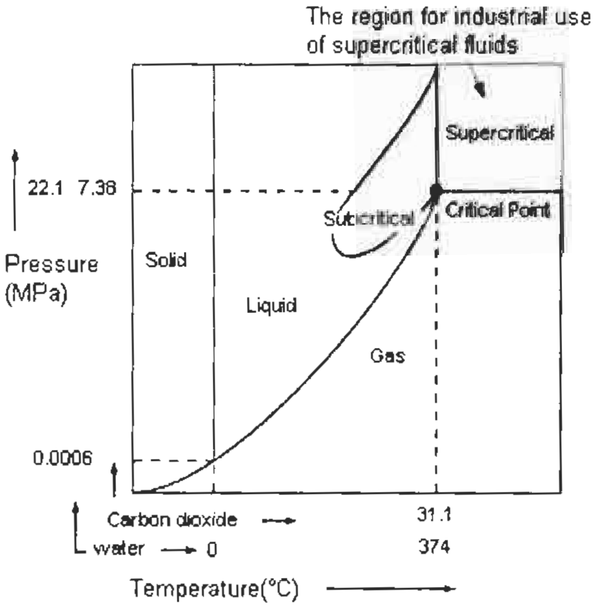

Figure 2.1 Generic phase diagram presenting critical constants for carbon dioxide and water

Table 2.1 Critical constants of different substances

Solvent	**T_c/°C**	**p_c/atm**
Carbon dioxide	31.1	72.8
Water	374	218
Ammonia	132	111
Ethane	32.2	48.1
Ethene	9.3	49.7
Propane	96.6	41.9
Toluene	319	40.6
Chlorotrifluoromethane	28.9	38.7
Methanol	240	78

The compressibility of a substance increases indefinitely as the critical point is approached, and a change in density and therefore in solvent strength is observed as the pressure increases. The variable solvent strength of supercritical fluids make them suitable for a variety of solubility related applications. The phase diagram in **Figure 2.1** shows the supercritical domain within which density, and thus solvent strength, can be adjusted by varying pressure and/or temperature.

The reduced density ($\rho_r = \rho/\rho_c$) can change from values typical for a gas (0.1) to that of a liquid (2.5) if the reduced pressure ($\rho_r = p/p_c$) increases to above ~1.0 at reduced temperatures ($T_r = T/T_c$) between 0.9 and 1.2. The solubility of a substance in a fluid is predominantly governed by the density of the fluid, and selective variation of pressure and temperature close to the critical point can therefore yield the desired solvent strength.

Apart from unique solvent strengths, supercritical fluids also possess other properties which make them viable solvents for a number of applications. Diffusivity is typically one to two orders of magnitude higher and viscosity an order of magnitude lower than those of organic liquids, even at high pressure (300-400 atm).[8] Negligible surface tension allows supercritical fluids to penetrate easily into microporous substances or into amorphous polymer matrices. The diffusion and mass transfer properties of supercritical fluids are comparable with those of gases, and the density and solvent strength with those of liquids. These characteristics, together with low viscosity and negligible surface tension, make supercritical fluids ideal solvents for a number of applications.

The solubility of substances in supercritical fluids can be improved by adding a modifier, entrainer or cosolvent. Polar (acetone, methanol) and non-polar (propane, n-hexane) modifiers are added in small quantities (2 - 5% per volume) to adjust the polarity of a supercritical fluid.[9] Supercritical carbon dioxide (*sc*-CO_2), for instance, does not have a dipole moment and is only weakly polarisable. The addition of a cosolvent improves the polarisability and increases the solubility of polar solids with an order of magnitude.[10] A cosolvent, like methanol, can act as a Lewis acid or base and react with functional groups of the dissolved substance, or it can participate in solvent sphere formation.[11] Acid-base interactions between *sc*-CO_2 and an aqueous system cause pH to have a definite influence on any process occurring in such medium. The presence of water in many extractions stresses the importance of acid-base interactions within systems involving supercritical fluids.[12]

Cosolvent modification of supercritical fluids represents a compromise in the sense that, on the one hand, the solvent impact of a given process is largely reduced but, on the other hand, the technology still relies on a volatile organic component in the system. Another limitation of cosolvents is that they are not effective for near-critical and supercritical fluid applications relying on dispersed phases.

2.3 Choice of Fluid

A variety of organic liquids and a selection of inorganic substances, noble gases and water, may be used as supercritical fluids. **Table 2.2** gives a comparison of the solubility parameters of common organic solvents with those of a selection of supercritical fluids.

Table 2.2 Comparison of solubility parameters of organic solvents and supercritical fluids. Solubility parameter is calculated as

$$\delta = \sqrt{\frac{\Delta E_v}{V}} = \sqrt{\frac{\rho(\Delta H_v - RT)}{M}}$$

with ΔE_v the energy of evaporation, V the molar volume, ρ the density, ΔH_v the heat of evaporation, M the molar mass of the dissolved substance, R the gas constant and T the temperature. a, b, c refers to δ of CO_2 with ρ = 0.6 g/L, 0.9 g/L and 1.23 g/L, respectively.

Solvent	**Solubility parameter**		**Supercritical fluid**
Methanol	14 – 15		
	13 – 14		NH_3
Ethanol	12 – 13		NO_2
2-Propanol	11 – 12		H_2S, HBr, HCl
Pyridine, Dioxane	10 – 11		N_2O, CH_3SH, Cl_2, CH_3Cl
Benzene, Chloroform	9 – 10	↑ c	$CH_2CHF/(CH_3)_2NH$
Ethyl acetate, Acetone		│	
Cyclohexane, Toluene	8 – 9	a ↑ │	CH_3CHF_2, CHF_3, Freon
Carbon tetrachloride		↓ │	C_2H_4
Ethyl ether, Pentane	7 – 8	b ↕ ↓	CCl_2F_2, $CClF_3$, SF_6, CO

The choice of supercritical fluid is determined by the polarity of the substance to be extracted and the technical feasibility of the conditions required to exist as a supercritical fluid. Corrosive, environmentally hazardous, flammable and explosive substances are typically unsuitable as supercritical fluids. The relatively mild critical conditions, abundance, affordability, non-toxicity and inert nature of CO_2 make it a suitable supercritical fluid for a variety of processes.[9] It can be used for the removal/extraction of non-polar and weakly polar compounds like alkenes, terpenes, aldehydes, esters, alcohols and fats. Variation of temperature and/or pressure, or density for that matter, allows the solvent strength of *sc*-CO_2 to be adjusted to dissolve specific substances better than common organic solvents. The addition of small amounts of cosolvent allows *sc*-CO_2 to dissolve more polar compounds. Highly polar compounds are insoluble in *sc*-CO_2, though water is soluble up to 0.3 mass % in *sc*-CO_2 at 250 atm and 50 °C as a result of the hydrophilic nature of CO_2.[13] Two classes of polymers are notable exceptions, viz. amorphous fluoropolymers and silicones. These materials, which have been found to be CO_2-philic, serve as essential building blocks for surfactants designed for application in near-critical and *sc*-CO_2.[14] Numerous developments have been made in the field of active surfactants.[15]

2.4 Instrumentation

The apparatus needed for supercritical fluid extraction (SFE) is relatively simple, and the basic components have not dramatically changed since the invention of the technique.[16] An SFE system basically consists of five components, viz. a gas cylinder, a high pressure pump, a modifier pump, a thermostatted sample vessel and a restrictor/collector.[8,9,16,17] **Figure 2.2** shows the basic components of a supercritical fluid extractor.

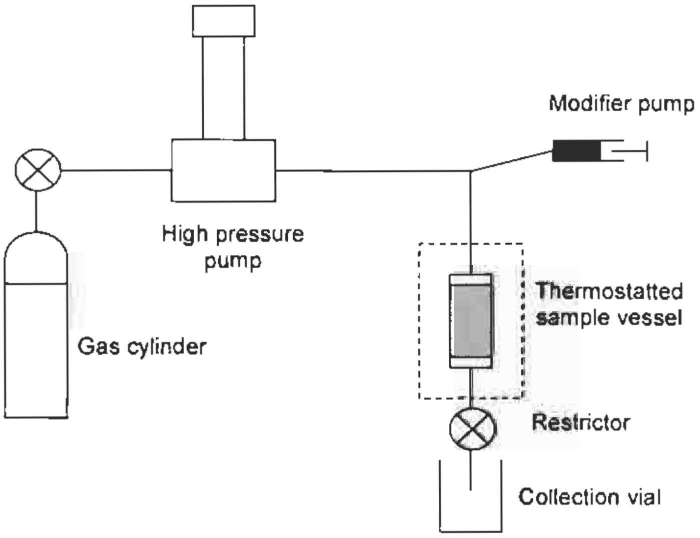

Figure 2.2 Schematic diagram of a supercritical fluid extractor

A laboratory-size gas cylinder supplies the gas to be used as a supercritical fluid. The gas is pressurised to the required level with a high-pressure pump, and a small quantity of modifier, if necessary, is added via a modifier pump. The resulting compressed gas is pumped to a sample vessel thermostatted to a temperature warranting supercritical conditions. An extraction of a desired component/ingredient from a sample/matrix within the sample vessel is performed in either a dynamic mode if the fluid is continuously pumped through the vessel at a constant flow rate, or in static mode if a fixed volume of fluid is kept in the vessel for a given residence time. These modes of extraction can be selected by means of opening and closing valves either automatically (by microprocessor control) or manually. The type of vessel used depends on the material to be extracted and the supercritical fluid and/or modifier used. It may be constructed from high-grade stainless steel or teflon for use with conventional extractions, or from special corrosion resistant materials, like Inconel®, Nimonic® and Hastelloy®, for extraction of highly corrosive substances. High-pressure vessels and autoclave reactors are sometimes fitted with sapphire windows to enable visual and/or spectroscopic monitoring. The vessel can be thermostatted in an oven, immersed in a circulation bath or heated with an internal or external heating element.

The supercritical fluid is allowed to return to ambient conditions after extraction by means of an adjustable vent valve or restrictor. The restrictor can be a simple fused silica tube with small internal diameter, or a more sophisticated needle-valve and seat, electronically controlled by a stepper motor. Clogging of the restrictor is a common problem, but it can be alleviated or prevented by heating the restrictor. Automatic variable flow restrictors are encased in a stainless steel or aluminium block, which can be set to a specific temperature. The dissolved substance, reaction product or destroyed waste is collected in a suitable solvent, adsorbed onto an appropriate adsorbent or transported via a heated line into a chromatographic column for direct analysis by means of a flame ionization detector, ultraviolet spectrophotometer, mass spectrometer or infrared spectrophotometer.[17,18] The collection process is a simple, though important step of the extraction procedure and a number of reports comparing different collection methods are available in the literature.[19,20]

2.5 Current Industrial Applications

Ill-fated developments in the early 1980's caused supercritical fluids to be regarded with scepticism, regardless of the successful implementation of large-scale industrial processes such as the decaffeination of coffee and tea and the extraction of flavourants from hops and spices. Systematic, well-planned investigation and evaluation of process parameters and cost implications may lead to novel solutions using supercritical fluid technology. It is important to note that not a single one of the numerous applications listed below are specifically gold extraction related, since only limited exploration of this topic has been done to date. This, once again, emphasises the actuality of the research reported in this thesis.

Separation technology

Supercritical fluid extraction (SFE) simplifies certain separations which cannot normally be done by other methods. Extraction and separation of thermolabile compounds can generally be performed at favourable temperatures, depending on the supercritical fluid used. SFE may be used to replace traditional extraction techniques, like steam distillation and solvent extraction, to yield superior extracts suitable for the food industry. The extraction of caffeine from coffee beans is a classic example of SFE with *sc*-CO_2 as solvent. The process was commissioned by HAG in Germany after the prohibition of dichloromethane as extractant. The capacity of this plant exceeds 50 million tons per annum. The extraction of flavourants from hops and spices, of oils from seed, of unwanted fragrances from cosmetics and of pharmaceutical compounds from plant material represents only a few of the separation technology related industrial applications of SFE.[8,9] Laboratory based applications include extraction of fat from meat,[21] separation of milk fats,[22] and removal of cholesterol from meat[23] and milk.[24] Thermolabile and non-volatile compounds can be separated with high resolution using supercritical fluid chromatography (SFC), in which a supercritical fluid is used as mobile phase. SFC and combined SFE/SFC are increasingly used in analytical laboratories,[16,17] emphasising the versatility of supercritical fluids as unique solvents, extractants and carrier agents.

Process technology

Supercritical fluids can be used as solvents/reaction media for chemical reactions and even as a starting material or a building block in chemical synthesis.[25] Organic, catalytic, organometallic, polymer and biological reactions can all be conducted in supercritical fluids.[26]

The advantages are that

- temperature and pressure variations may be used to optimise reaction rate and selectivity;
- solvent characteristics can readily be adjusted;
- products can be recovered easily after relaxation to ambient conditions;
- heat and mass transfer may be more effective in the fluid phase.

Fossil fuel, petroleum and hydrocarbon processing

The petroleum and crude oil industries can selectively extract a desired hydrocarbon from a multi-component mixture by utilising CO_2, CH_4, C_2H_6 or C_3H_8 in the supercritical state. Light petroleum fractions can be separated from higher boiling fractions at the same time. The pure fluid is used to extract components with saturated structures, while a co-solvent is added to the fluid to isolate unsaturated, aromatic and heteroatomic structures from this extract.

Metal processing

An exciting environmental application of *sc*-CO_2 is the extraction of metals from solutions,[27] soil samples and other matrices. SFE of metals requires metal ions to be converted into neutral moieties soluble in the supercritical fluid. This can be accomplished via *in situ* chelation with suitable ligands.[28] The process is useful for environmental sampling, for remediating contaminated soil, for separation of metal mixtures and for processing of mineral ores. The topic of metal extraction is dealt with more specifically in **Section 2.6** since it was the main focus of the research work done in this investigation.

Material science

The manufacture of pure, solvent-free substances with unique physical and morphological properties is possible with processes such as RESS (Rapid Expansion of Supercritical Solution) and SAS (Supercritical Anti-Solvent).[7]

RESS is used to precipitate particles of uniform size distribution from a supercritical solution by either a rapid decrease in pressure or injection of a highly soluble gas/fluid as a cosolvent to cause rapid expansion of the solution and thereby a decrease in solvent strength of the supercritical fluid. As a result, the dissolved substance precipitates as small particles from the supersaturated solution. The size/morphology of the particles can be controlled to some extent and depends on concentration of the initial solution, the duration of injection, the extent of expansion of the initial solution and the temperature.

SAS is used when a substance is sparingly soluble or insoluble in a supercritical fluid. The substance is dissolved in an appropriate solvent, and a supercritical fluid, acting as an antisolvent, is introduced to decrease the solubility of the substance by diluting the solvent and thereby causes precipitation.

Environmental applications

Supercritical water oxidation (SCWO) is a technology of particular importance to the environment. It was developed specifically for the destruction of hazardous material,[29,30] and is commercially used to destroy, among others, industrial effluent, redundant explosives and ammunition, toxic organic compounds, potential pollutants and other environmentally undesirable substances. Combination of SFE and SCWO renders a two-step process which can be used to remediate contaminated soil. Oil, polychlorinated biphenyls (PCB's) and polyaromatic hydrocarbons (PAH's) are extracted from soil matrix by *sc*-CO_2 in a first step and destroyed by SCWO in a second step. The conditions for SCWO are extreme (374 ^{0}C, 221 atm), and corrosion of the reaction vessel is therefore a problem. This problem has been largely solved by utilising special reactor materials.

Other industrial applications

SFE does not only yield an extract but also regenerates an adsorbent or matrix exhausted in an environmental or industrial application. *sc*-CO_2 is increasingly used to degrease complex surfaces like electronic circuit boards, optical systems and machined objects.[9]

The process of extraction can be reversed to effect impregnation of materials. The use of supercritical fluids as impregnating agents has found application in a number of industrial sectors, including the wood industry (wood with antioxidants), food industry (tea/sugar with lemon fragrance), agricultural industry (seed with growth enhancing agents), textile industry (fibres with dye) and chemical industry (polymers with catalysts).

SFCD (Supercritical Fluid Chemical Deposition) is an alternative approach to deposit chemicals in thin layers onto surfaces.[31] The chemical is dissolved in a supercritical fluid, deposited onto the surface of the substrate and fixed by heating with an element or a laser beam.

The replacement of spray paint solvents with *sc*-CO_2 yields a less expensive product from which 70 % of the harmful organic solvent is removed.[32] The use of cosolvent modified *sc*-CO_2 is most recognised in a spray-coating process commercialised by Unicarb in the early 1990's. In this process, which has been implemented in the automotive and furniture industries, the majority of traditional solvents used in spray-coating has been replaced by *sc*-CO_2.[33]

2.6 Extraction of Metals with *sc*-CO_2

There is much interest in using *sc*-CO_2 for the extraction of metals because of its favourable solvating and transport properties. The high diffusivity and low viscosity of *sc*-CO_2 also allows direct extraction from solid matrices.

Metals in their elemental states do not dissolve in *sc*-CO_2. They must be oxidised first and then subjected to complex formation with a suitable chelating agent to make them soluble in CO_2.[27, 28, 34] Direct extraction of metal ions is inefficient and neutralisation of the charge of the ion is required.[35, 36]. This can be accomplished by modifying *sc*-CO_2 with chelating agents or by spiking the sample matrix with chelating agents and leaching the complexes formed with *sc*-CO_2.[37-40]

Chelation combined with solvent extraction is a known technique for preconcentration and separation of metal ions from aqueous samples. Solvent extraction is usually time consuming, especially where leaching is needed to release the metal ion before complexation and solvent extraction. In many cases, solvent extraction requires the use of toxic organic liquids, generating environmental problems for handling and disposal of used solvents.[28] A major advantage of utilising *sc*-CO_2 for the extraction of metal species is the minimisation of organic solvent waste generation.

2.6.1 Recent research

The metal recovery capability of supercritical fluids was first demonstrated by cobalt and iron chlorides in supercritical ethanol in 1879.[41] Until recently, little information was available in the literature regarding SFE of metal species. Quantitative measurements of metal complex solubilities in *sc*-CO_2 were first performed in 1991 using a high-pressure view cell and uv-visible spectrometry.[42] The authors showed that coordination to dithiocarbamates and fluorine substitution can largely enhance solubility in *sc*-CO_2. In 1992 copper extraction from solid and liquid materials by *sc*-CO_2 containing bis(trifluoroethyl)dithiocarbamate (FDDC) was demonstrated.[27] A variety of chelating agents, including dithiocarbamates, β-diketones, organophosphorus reagents, macrocyclic compounds and fluorinated surfactants, have been utilised for SFE of metals.[37-42] The feasibility of extracting organometallic compounds, heavy metals, lanthanides and actinides from solid and liquid materials using the *in situ* chelation-SFE method has been evaluated by research groups in various countries.

2.6.2 Parameters controlling SFE of metals

According to the literature, important parameters controlling SFE of metal species include (1) solubility and stability of chelating agents and metal chelates, (2) effect of water and pH, (3) temperature and pressure, (4) chemical nature of metal species, and (5) nature of matrix.[28] These parameters are discussed in more detail below.

Solubility and stability of chelating agents and metal chelates in sc-CO_2

The solubility of free ligands in *sc*-CO_2 depends on the chemical nature of the ligand. A variety of ligands mentioned in the previous section can be utilised for SFE of metal species. A few of these are general complexing agents and others are selective for certain metals. Experimental data indicate that fluorinated ligands usually form highly soluble metal complexes in *sc*-CO_2 and are thus very effective for SFE applications.[28,42] Alkyl substitution in ligands, especially tert-butyl substitution, can also enhance the solubility of metal complexes in *sc*-CO_2.[43] In some cases, SFE efficiencies for metal species can be enhanced using a mixture of ligands. [38,44]

Effect of water and pH

The efficiency of metal extraction using *in situ* chelation-SFE generally increases significantly when a small amount of water is added to a solid matrix such as filter paper, sand, soil or wood. The presence of water probably supports metal chelation.[28] The water may also serve as a modifier for the solute/matrix interactions by blocking the active sites of the matrix, thus reducing the adsorption of the solute by the active sites of the polar matrix.[45]

Another factor that should be considered in the SFE of metals is pH. Metal chelate formation generally depends on pH. When water is in equilibrium with CO_2 under normal SFE conditions, the pH of the water is around 2.9 due to the formation and dissociation of carbonic acid.[12]

$$CO_2 + H_2O \rightleftharpoons H_2CO_3 \rightleftharpoons H^+ + HCO_3^- \qquad (2.1)$$

The majority of ligands capable of successfully removing metals from matrices and solutes form complexes under these acidic conditions.

Temperature and pressure

The pressure of the supercritical fluid in the extraction cell has a decisive effect on the efficiency of extraction. With increase in pressure, the density of *sc*-CO_2 increases, thus enhancing the solubilities of ligands and metal chelates and, consequently, the extraction efficiency of metals.[42,46,47] Changing the temperature of the extraction cell also has an effect as it alters the analyte volatility, extraction kinetics and supercritical fluid density. These effects can be mutually opposing since, while the analyte volatility and extraction kinetics are usually favoured by increased temperatures, the resulting decrease in density has a detrimental effect on the extraction efficiency.[28]

Chemical nature of metal species

Metals can exist as organometallic compounds, ionic species and inorganic compounds (oxides, sulfides) in natural environments. SFE of metals is therefore more complicated than that of organic compounds. Some forms of metal species or compounds may not be extractable by the ligands utilised in SFE. Therefore, with proper selection of ligands, SFE may provide a means of metal speciation in natural samples. Organometallic compounds are usually more readily soluble in supercritical fluids and can be extracted without a ligand.[47] The oxidation state of the metal is also a major role-player in the extraction of metal species.

Nature of matrix

The nature of the solid matrix plays an important role in the efficiency of metal complex extraction by *sc*-CO_2. When metal ions are spiked onto solid supports such as filter paper or sand, high extraction efficiencies are observed. This may not be true for metal ions in real-world samples. The active sites and natural ligands present in real-world samples may bind strongly to certain metal ions and thus prevent their complexation with added ligands.[28] Dissolution and extraction from real-world matrices depend on the chelation ability and accessibility of the metal sites.[48]

2.6.3 SFE of gold

There are very few reports on gold extraction with supercritical fluids available in the literature. The extraction of Au(III) from cellulose paper using bis-triazolo-crowns in *sc*-CO_2 has been reported.[43] In the presence of 5% methanol as a modifier and the addition of microlitres of water quantities, up to 80% of the spiked gold was extracted. In the absence of modifier and spiked water, the extraction efficiency was insignificant.

Other papers recently reported on the desorption of gold from activated carbon using *sc*-CO_2.[36,49] Ion-pair solvation of sodium dicyanoaurate, $[Na^+ \ldots (AuCN)_2^-)]$, by tributyl phosphate (TBP) increased hydrophobicity and facilitated the charge neutralisation necessary for the elution of ionic $Au(CN)_2^-$ by non-polar *sc*-CO_2. Wet carbon loaded with gold cyanide was used and all the extractions were conducted in the presence of NaCN. Gold recovery of up to 60 % was claimed.

The extraction of gold(III) by complexated fluorinated calyx[4]arene thiourea derivative using *sc*-CO_2 was demonstrated by authors[41] whose main objective was to achieve gold extraction without the use of organic solvents. They obtained high extraction yields (~80%) compared to what other researchers in the field achieved.

The extraction of metallic gold from connector pins on a CPU processor board using HNO_3 as an oxidising agent and a fluorinated β-diketone as chelating agent was recently reported.[34]

References

1 Atkins, P.W., *Physical Chemistry 8th edition*, Oxford University Press: Oxford, **2006**.

2 Kiran, E.; Levelt, J.M.H., *Supercritical Fluids: Fundamentals for Application*, Kluwer Academic Publishers: Dordrecht, **1994**.

3 Hannay, J.B.; Hogarth, J., *Proceedings of the Royal Society*, **1879**, *29*, 324.

4 http://dwb.unl.edu/Teacher/NSF/C09/C09Links/www.phasex4scf.com/scf.htm

5. Schmieder, H.; Dahmen, N.; Schön, J.; Wiegand, G., *Industrial and Environmental Applications of Supercritical Fluids*, In: Van Eldik, R.; Hubbard, C.D., *Chemistry under Extreme or Non-Classical Conditions*, Wiley: New York, **1997**, 273.

6 Schneider, G.M., *Applications of Fluid Mixtures and Supercritical Solvents: A Survey*, In: *Supercritical Fluids: Fundamentals for Application*, Kluwer Academic Publishers: Dordrecht, **1994**.

7 Van Eldik, R.; Hubbard, C.D., *Chemistry Under Extreme or Non-Classical Conditions*, John Wiley & Sons, Inc: New York, Spektrum Akademischer Verlag: Heidelberg, **1996**.

8 McHugh, M.; Krukonis, V., *Supercritical Fluid Extraction*, Butterworth-Heinemann: Boston, **1994**.

9 Phelps, C.L.; Smart, N.G.; Wai, C.M., *Journal of Chemical Education*, **1996**, *73*, 1163.

10 Lira, C.T., *Fluid Phase Equilibria*, **1992**, *8*, 269.

11 Yonker, C.R.; Frye, S.L.; Kaldorf, D.R.; Smith, R.D., *Journal of Physical Chemistry*, **1986**, *90*, 3022.

12 Toews, K.; Schroll, R.; Wai, C.M.; Smart, N.G., *Analytical Chemistry*, **1995**, *67*, 4040.

13 Wiebe, R.; Gaddy, V.L., *Journal of the American Chemical Society*, **1941**, *63*, 475.

14 McClain, J.B., *Science*, **1996**, *274*, 2049.

15 Cooper, A.I.; Londono, J.D.; Wignall, G.; McClain, J.B.; Samulski, E.T.; Lin, J.S.; Dobrynin, A.; Rubinstein, M.; Burke, A.L.C.; Frechet, J.M.J.; Desimone, J.M., *Nature*, **1997**, *389*, 368.

16 Chester, T.L.; Pinkston, J.D.; Raynie, D.E., *Analytical Chemistry*, **1992,** *64*, 153.

17 Chester, T.L.; Pinkston, J.D.; Raynie, D.E., *Analytical Chemistry*, **1994,** *66*, 106.

18 Kirschner, C.H.; Taylor, L.T., *Analytical Chemistry*, **1993**, *65*, 78.

19 Yang, Y.; Hawthorne, S.B.; Miller, D.J., *Journal of Chromatography A*, **1995,** *699*, 265.

20 Langenfeld, J.J.; Burford, M.D.; Hawthorne, S.B.; Miller, D.J., *Journal of Chromatography,* **1992**, *594*, 297.

21 King, J.W.; Johnson, J.H.; Friedrich, J.P., *Journal of Agricultural and Food Chemistry*, **1989**, *37*, 951.

22 Arul,J.; Boudreau, A.; Makhlouf, J.; Tardiff, R.; Sahasrabudhe, M., *Journal of Food Science*, **1987**, *52*, 1231.

23 Bradley, R.L., *Journal of Dairy Science*, **1989**, *72*, 2834.

24 Wehling, R., *Advances in Applied Biotechnology*, **1991**, *12*, 133.

25 http://www.scs.uiuc.edu/chem/gradprogram/chem435/witmer.pdf

26 Savage, P.E.; Gopalan, S.; Mizan, T.I.; Martino, C.J.; Brock, E.E., *AIChe Journal*, **1995**, *41*, 1723.

27 Laintz, K.E.; Wai, C.M.; Yonker, C.R.; Smith, R.D., *Analytical Chemistry*, **1992**, *64*, 2875.

28 Wai, C.M.; Wang, S., *Journal of Chromatography A*, **1997,** *785*, 369.

29 Smart, N.G.; Carlson, T.; Kast, T., Clifford, A.A.; Burford, M.D.; Wai, C.M., *Talanta*, **1997**, *44*, 137.

30 Johnston, K.P., *Nature*, **1994**, *368*, 187.

31 Caruana, C.M., *Chemical Engineering Progress*, **1995**, *91*, 10.

32 Matson, D.W.; Futton, J.L.; Petersen, R.S.: Smith, R.D., *Industrial Engineering Chemical Research*, **1987**, *26*, 2298.

33 Brennecke, J.F., *Chemistry and Industry*, 4 November **1996**, 831.

34 Wang, J.S.; Wai, C.M., *Industrial and Engineering Chemistry Research*, **2005**, *44*, 922.

35 Fuoss, R.M.; Kraus, C.A., *Journal of the American Chemical Society*, **1933**, *55*, 1019, 2387.

36 Otu, E.O., *Separation Science and Technology*, **1997**, *32(6)*, 1107.

37 Laintz, K.E.; Tachikawa, E., *Analytical Chemistry*, **1994**, *66*, 2190.

38 Lin, Y.; Wai, C.M., *Analytical Chemistry*, **1994**, *66*, 1971.

39 Lin, Y.; Smart, N.G.; Wai, C.M., *Environmental Science and Technology*, **1995**, *29*, 2706.

40 Van Wyk, F., *Superkritiese Fluïedekstraksie van Kompleksverbindinge van Omgewingskadelike Metale*, M.Sc. Thesis, PU for CHE, **1998**.

41 Glennon, J.D.; Harris, S.J.; Walker, A.; McSweeney, C.C.; O'Connel, M., *Gold Bulletin*, **1999**, *32(2)*, 52.

42 Laintz, K.E.; Wai, C.M.; Yonker, C.R.; Smith, R.D., *Journal of Supercritical Fluids*, **1991**, *4*, 194.

43 Wang, S.F.; Elshani, S.; Wai, C.M., *Analytical Chemistry*, **1995**, *67*, 919.

44 Lin, Y.; Wai, C.M.; Jean, F.M.; Brauer, R.D., *Environmental Science and Technology*, **1994**, *28*, 1190.

45 Knipe, C.R.; Gere, D.R.; McNally, M.E., In: Bright, F.V.; McNally, M.E., (Eds), *Supercritical Fluid Technology - Theoretical and Applied Approaches to Analytical Chemistry, ACS Symposium Series 488*, American Chemical Society, Washington D.C., **1991**, 251.

46 Wai, C.M.; Wang, S.F.; Yu, J.J., *Analytical Chemistry*, **1996**, *68*, 3516.

47 Wai, C.M.; Lin, Y.; Brauer, R.; Wang, S.F.; Beckert, W.F.; *Talanta*, **1993**, *40*, 1325.

48 Smart, N.G.; Carleson, T.E.; Elshani, S.; Wang, S.F.; Wai, C.M., *Industrial and Engineering Chemistry Research*, **1997**, *36*, 1819.

49 Otu, E.O.; Wilson, J.J., *Separation Science and Technology*, **2000**, *35(12)*, 1879.

CHAPTER 3

TECHNICAL ASPECTS

This chapter describes the chemicals and materials, the supercritical extractor, the analytical techniques and the theoretical principles/approaches by virtue of which the different objectives stated in Chapter 0 could be achieved. The detailed procedures adopted for different aspects of the investigation (synthesis and characterisation of complexes, spectral data determination, monitoring of elemental composition of carbon surface before and after *sc*-CO_2 exposure, solubility measurement in *sc*-CO_2 by static mode of extraction, recovery by exhaustive extraction in dynamic mode, parameter optimisation, cosolvent entrainment) and the results obtained for the many experiments performed are discussed in appropriate chapters later in the thesis.

3.1 Reagents and Materials

Metallic gold with a purity of 99.9999% was donated by Rand Refinery in Germiston, South Africa. An MD 1076 permit for the legal transportation and handling of precious metals was obtained from the Gold and Diamond Division of the South African Police Service (SAPS) at Klerksdorp.

The activated carbon onto which $KAu(CN)_2$ was loaded was a coconut shell type (PJ816-CQ600) with high gold adsorption capability and outstanding abrasion resistance properties, specifically designed for use in Carbon-In-Pulp (CIP) and Carbon-In-Leach (CIL) gold recovery plants. Its specifications are listed in **Table 3.1**. It was obtained from ChemQuest, a company supplying a vast range of activated carbon products to Southern African industries.

Table 3.1 Specifications of activated carbon used in this investigation (product and specifications supplied by ChemQuest)

PHYSICAL PROPERTIES	STANDARD	TYPICAL
Bulk Density (g/L)	460-510	490
Pore Volume (mL/g)	0.70-0.85	0.77
Ash Content (%)	2.5% max	2%
Abrasion Resistance (24 h)	2% max	0.5%
Moisture (as packed)	4% max	3%
CHEMICAL PROPERTIES	**STANDARD**	**TYPICAL**
Gold Adsorption Rate (R-Value) (min)	55	55 - 62
Gold Adsorption Capacity (K-Value) (kg/MT min)	24	25
PARTICLE SIZE DISTRIBUTION	**STANDARD**	**TYPICAL**
Oversize (+2.38 mm)	2.0% max	0.5%
Undersize (-1.19 mm)	0.5% max	0.1%
Size (> 1.41 mm)	95% min	96%
d50 mm	1.8-2.1	1.95
Platelets	5% max	3.0%

The following analytical grade chemical reagents were used in the preparation of gold compounds from metallic gold: hydrochloric acid (30-33 % HCl) (Associated Chemicals Enterprises); nitric acid (55 % HNO_3) (Saarchem); 1.10-phenanthroline monohydrate ($C_{12}H_8N_2.H_2O$) (Saarchem); ethylenediamine ($C_4H_{16}N_4$) (Merck Chemicals); diethylether ($(C_2H_5)_2O$) (Labchem); ethanol (C_2H_5OH) (Labchem); thiourea ($CS(NH_2)_2$) (Labchem); perchloric acid (70 % $HClO_4$) (Analyticals Carlo Erba); potassium cyanide (KCN) (Associated Chemicals Enterprises); ammonium hydroxide (35 % NH_4OH) (Koch-Light Laboratories), tributyl phosphate (TBP) ($(C_4H_9)_3PO_4$) (Riedel-de Haën), hexafluoroacetylacetone, (HFA) ($C_5H_2F_6O_2$) (Fluka).

Technical grade liquid CO_2 with a purity of 99.0 % in a siphon-tube cylinder was used for all experiments performed with the supercritical fluid extractor (**Section 3.2**). Compressed air dry (moisture < 5 v/m) was used for the pneumatic operated mechanical section of the supercritical extractor, and UHP helium (99.999 %) was utilised to add a cosolvent to the extraction thimbles. All gases were supplied by Afrox.

Analytical grade (AR) organic solvents supplied by Merck Chemicals were used as modifiers and rinsing agents. Deionised water needed for rinsing, collection of extracts, spectrometric analysis (uv/visible, AA and ICP) and ultrasonic cleaning was prepared by a Millipore MilliQ$^+$ Ultrapure water system (conductivity < 2 x 10^{-6} S cm^{-1}).

UV/visible and AA spectrophotometric analysis of gold complexes were carried out in HPLC grade methanol (CH_3OH) (Associated Chemicals Enterprises) or deionised water. Reagents used for ICP analysis included suprapure nitric acid (65 % HNO_3) and suprapure hydrochloric acid (35 % HCl), both supplied by Merck Chemicals, and deionised water. Standards for ICP and AA analysis were prepared from a 1 000 ppm standard gold solution supplied by Set Point Instruments.

3.2 Supercritical Fluid Extractor

Figure 3.1 *Leco TFE 2000*™ supercritical fluid extractor

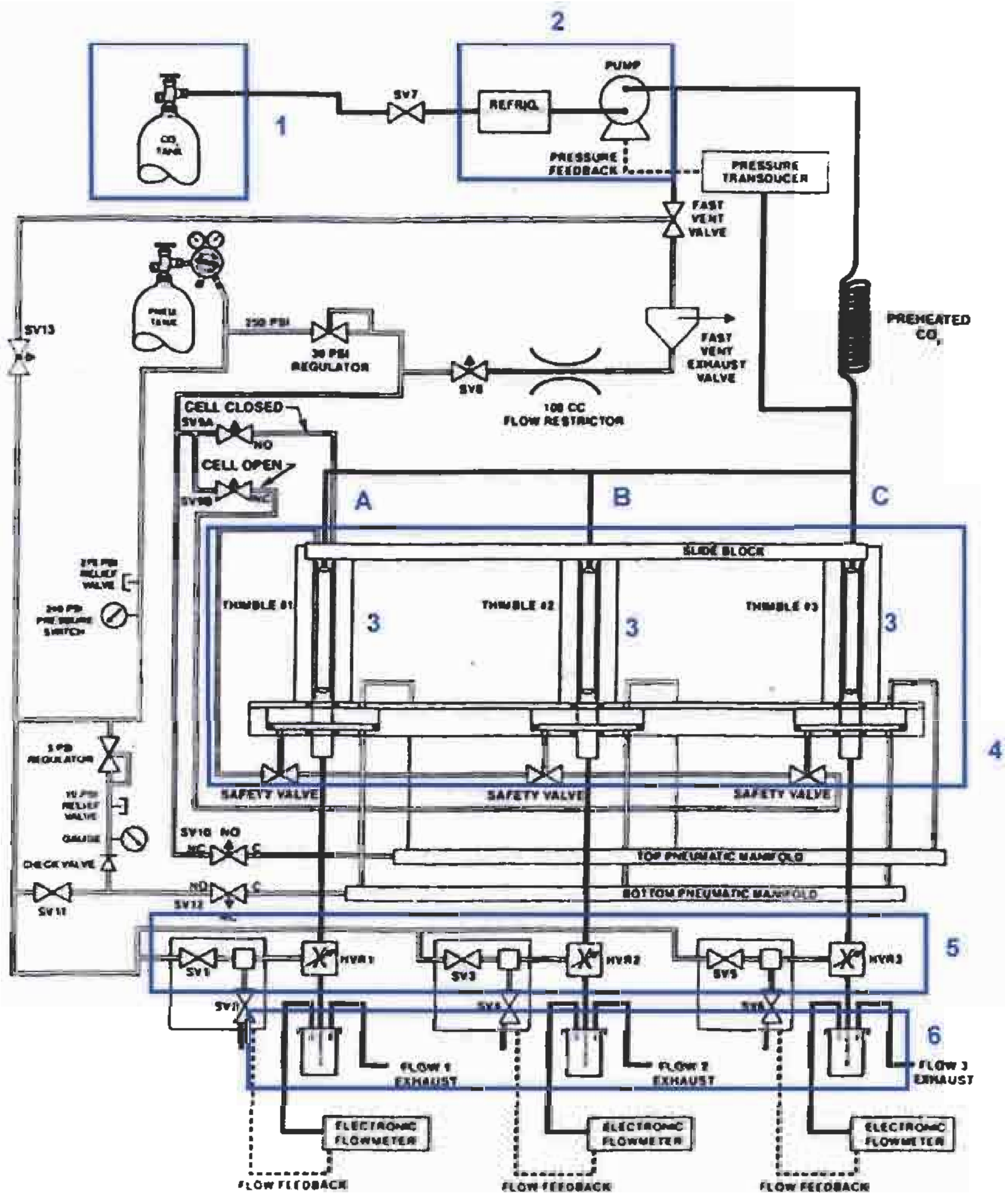

Figure 3.2 Schematic flow diagram of Leco TFE 2000 supercritical fluid extractor

A *Leco TFE 2000*™ supercritical fluid extractor (**Figure 3.1**) was used for laboratory scale recovery experiments and solubility measurements. A schematic representation of the different components of the apparatus, which largely correspond with those generally found in SFE equipment as outlined earlier (**Paragraph 2.4**) is given in **Figure 3.2**. The extractor features a three-channel system where a single flow line is split into three separate flow lines (A, B, C), each with its own sample thimble, control valves and restrictor to allow three extractions to be performed simultaneously.[1] This feature is advantageous where three totally different samples are exposed to *sc*-CO_2 in a single run or where results in triplicate for identical samples are required.

The execution of an extraction run or solubility measurement with the instrument can be described as follows: CO_2 from the supply cylinder (1) is premixed (if desired) with an amount of cosolvent (0-15%) from an optional M2000™ modifier pump and pressurised with a glass piston pump (2) to the desired level in the sample containing stainless steel thimbles (3) inserted into the thimble chamber (4) where the temperature is controlled up to 150 °C. The thimbles (10 mL internal volume) are sealed prior to insertion into the chamber by end-caps consisting of a porous frit and teflon seal assembly (**Figure 3.3**). Each of the three flow channels has an automated heated variable flow restrictor (HVR) (5) which facilitates recovery of extracted material having different heat sensitivities and/or viscosities. At the HVR's (**Figure 3.4**) ambient conditions are restored at a default flow rate of 2 L/min in order to recover the extract, but the flow rate can be varied (0 - 3 L/min) by entering the appropriate value into the microprocessor of the instrument. The extracted material is trapped in collection vials (6) (**Figure 3.4**).

Figure 3.3 Stainless steel thimbles

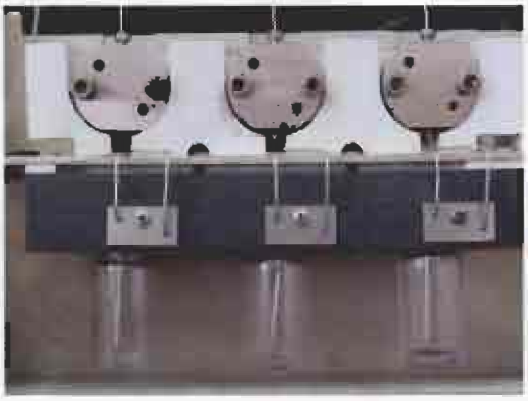

Figure 3.4 Heated variable restrictors (HVR's) and collection vials

Solid samples were mixed with Leco Dry® (an inert dehydrating agent preventing clogging of the sample by the high-pressure fluid) and loaded into thimbles for direct solubility measurement or extraction/recovery from a matrix using *sc*-CO_2. For liquid samples, however, precautions needed to be taken to ensure that the liquid was not instantaneously flushed from the thimble by the entering *sc*-CO_2. Initially glass wool was used to retain the liquid sample in the extraction thimble, but much better results were obtained by a method demonstrated in **Figure 3.5**. The liquid sample was placed in a small glass tube at the bottom of the extraction thimble. High density pulp tablets were then used to stabilise the glass tube and to prevent the high-pressure *sc*-CO_2 from flushing the liquid sample from the thimble.

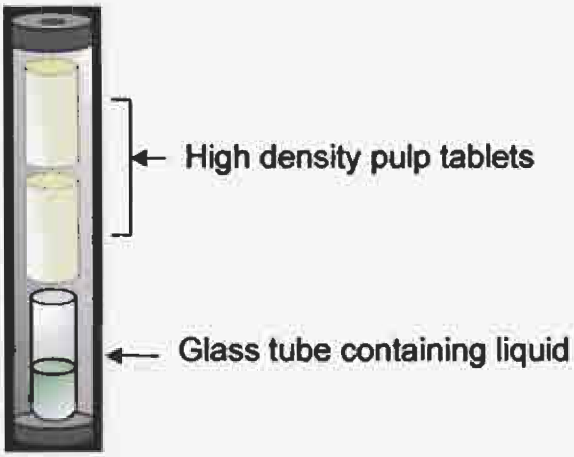

Figure 3.5 Handling of liquid samples during *sc*-CO_2 extraction

Two different modes of extraction can be selected with the supercritical extractor employed in this study. The static mode is used to extract a substance with a fixed amount of *sc*-CO_2 at selected conditions. The solubility of a substance in *sc*-CO_2 can be measured from the plateau of a concentration-time graph obtained by performing several static extraction runs of different duration at the same conditions. The plateau occurs when equilibrium is established between the solid and the solution phases. In the dynamic mode of extraction fresh fluid constantly flows through the sample, resulting in an exhaustive extraction of a substance or complete recovery of a material from a matrix. This is signified by a plateau occurring in a concentration-time graph when a dynamic mode run of infinite duration is performed at a given set of conditions.

3.3 Analytical Techniques

A variety of analytical techniques were used to monitor the outcomes of the experiments (synthesis, characterisation, dissolution, recovery) performed during this study.

3.3.1 Scanning Electron Microscopy with Electron Dispersion Spectrometry (SEM-EDS)

Surface analysis of activated carbon loaded with gold was performed with an FEI Quanta 200 scanning electron microscope (SEM) with an integrated Oxford Instruments INCA 200 EDS microanalysis system. An electron beam is passed over the surface of a sample to cause energy changes in the surface layer. These changes are detected and analysed to give information which can be displayed in a variety of ways. One of these is an image of the sample produced by several signals resulting from the interaction and detected by appropriate detectors. The signals include low-energy secondary emission, Auger-electron generation, characteristic X-ray emission, *bremmstrahlung*, backscattered electron emission and cathode luminescence.[2]

X-ray microanalysis yields information about the elemental composition of a sample. The interaction of a high-energy electron with an atom results in ejection of an electron from an inner shell. When an electron from an outer shell fills the vacancy, a change in energy in the form of an emitted X-ray and characteristic of the electronic structure of the atom of the element occurs. A spectrometer collects the characteristic X-rays and counts and sorts these on the basis of energy, a technique known as energy dispersive spectrometry (EDS). The resulting spectrum displays the number of X-rays on the vertical axis as a result of the input energy on the horizontal axis.[2,3]

SEM-EDS analysis gives the mass percentage of the component being analysed in relation to other components present. For carbon loaded with a gold complex the mass percentage of gold relative to carbon, oxygen and other elements present in the species is determined. An average value for gold present on the surface of the carbon is obtained by measuring the mass percentage of gold at different locations on the surface.

3.3.2 Atomic Absorption Spectrophotometry (AA)

A *Varian SpectrAA 250 Plus* AA spectrophotometer was used to determine gold present in extracts. A hollow cathode lamp for gold analysis was purchased from Set Point Instruments. Gold analysis was conducted at wavelengths of 242.8 nm and 267.6 nm depending on the concentration range of the samples measured. Calibration of the spectrophotometer was performed by using a 1 000 ppm gold standard. A reliable five point calibration line was compiled utilising solutions prepared by dilution of the standard stock solution. All gold concentrations were in the parts per million (ppm) range. The gold content of complexes synthesised in this study was determined in a similar way.

3.3.3 Induced Coupled Plasma Mass Spectrometry (ICP-MS)

Induced coupled plasma mass spectrometry was employed to determine very low concentrations (parts per billion) of gold. An *Agilent 7500c* ICP-MS system was used. Samples were introduced into the instrument's shield torch system by means of a Cetac ASX-510 auto sampler and a peristaltic pump. The total run time was less than 4 min per sample. A 1 % HNO_3 blank as well as five diluted gold standard solutions in 1 % HNO_3 was used as external standard. The isotope measured was ^{197}Au.

3.3.4 UV/Visible Spectrophotometry

A *Cary 50* spectrophotometer was used to record uv/visible spectra of synthesised gold complexes as a means of verifying these compounds by comparison to existing literature data (if available), and to monitor the solubility of these complexes in *sc*-CO_2 by matching the uv/visible spectra of extracts of these complexes to the original spectra. In most instances spectral data (λ_{max}, ε_{max}) for the different complexes could be determined by applying the Beer-Lambert law.[4]

3.3.5 Mercury Porosimetry

A *Micromeritics Autopore III* porosimeter was used to determine the pore size distribution and porosity of the activated carbon used in this investigation. A penetrometer with a total stem volume of 0.392 mL was used. The samples were loaded to obtain a stem volume of between 60 and 90 % under high-pressure intrusion. The density of the activated carbon was calculated by obtaining the bulk density at a given pressure as a percentage of the apparent (skeletal) density. The porosity is then acquired by subtracting the density from 100 %. The Washburn equation

$$p = \frac{4\gamma\cos\theta}{d} \qquad (3.1)$$

was used to determine the pore size distribution. Here γ is the surface tension of mercury (0.48 N/m), θ is the contact angle of mercury on the material being intruded (141.3°), p is the pressure required to force non-wetting liquid into the pores (Pa) and d is the diameter of the pores (m). Mercury is forced into pores at various pressures with the volume of mercury intruded determined at each pressure.[5]

3.4 Theoretical Principles

3.4.1 Surface Response Analysis

Statistical methods are used in experimentation to obtain the impact of a number of factors on a process from a minimum amount of data. The influence of independent variables on a given dependent is investigated and optimised for a range of conditions. The characteristics of *sc*-CO_2 largely depend on temperature and pressure. In order to resolve the influence of these parameters on the yield and properties of a product extracted, dissolved or recovered by *sc*-CO_2, a statistical central composite design included in the computer software Statistica for Windows® was employed.

In order to detect a curvature in the relationship between a dependent and an independent variable, at least 3 levels of an independent variable must be known. It is then possible to determine whether the change from -1 to 0 or from 0 to +1, for example, results in a linear (or proportional) or curvilinear (or disproportional) change in the outcome variable. This principle can be extended to multiple factors, though the dependent variable then constitutes a response surface over the levels of the independent variables of the design.[6]

A typical central composite design for two independent variables is shown in **Figure 3.6**. The design points are of a $2^{(k-p)}$ type derived from a cube. These do not reflect a curvature and therefore center points need to be added in a second-order central composite design (cube enhanced by a star) to estimate the second degree polynomial or quadratic components of the relationship between the independent and dependent variables.[6]

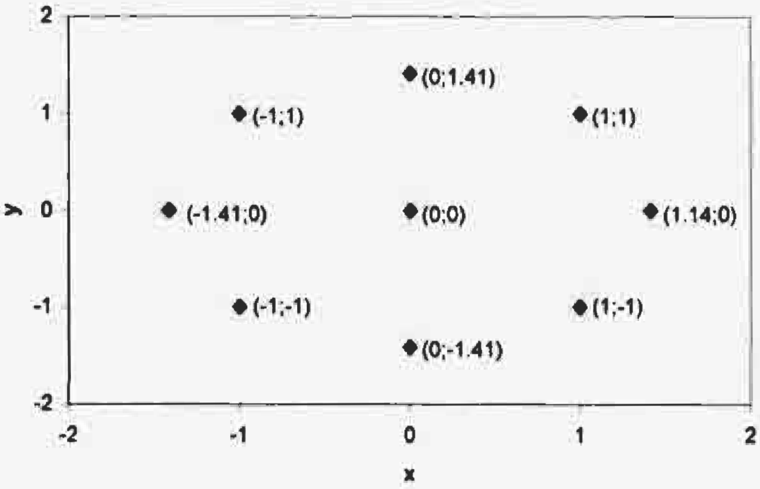

Figure 3.6 A rotatable central composite design for two independent variables

The values for the star points are chosen to make the design rotatable. The star points are arranged to form a circle together with the cube points around the center point.[7] In **Figure 3.7** an example of a surface response graph based upon the experimental design in **Figure 3.6** is shown.

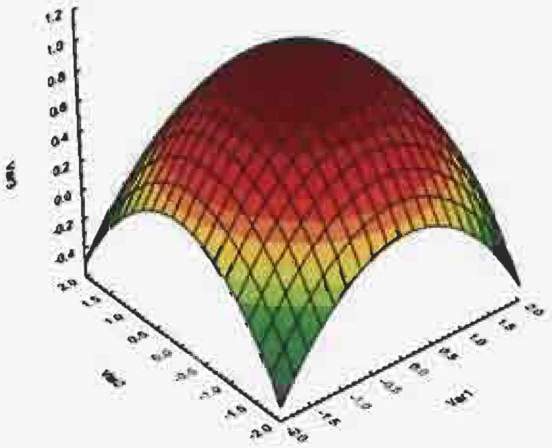

Figure 3.7 Surface response graph based upon an experimental design

3.4.2 Surface Processes

The attachment of materials to a surface is called adsorption. The substance that adsorbs is the adsorbate, and the underlying material onto which adsorption takes place, is the adsorbent or substrate. The process on the surface can be either physisorption (physical adsorption) or chemisorption (chemical adsorption), with the enthalpy of adsorption being the principal test to distinguish between the two since typical values are in the region of 20 and 200 kJ mol^{-1}, respectively.[4]

Adsorption can be presented as a dynamic process

$$A + M \underset{k_d}{\overset{k_a}{\rightleftharpoons}} AM \tag{3.2}$$

with k_a and k_d the rate constants for adsorption and desorption, respectively. At equilibrium, there is no nett change (two rates are equal or sum of rates is zero), so that the extent of surface coverage can be expressed by the fractional coverage

$$\Theta = \text{number of sites occupied/number of sites available} = \frac{K}{1+K} \tag{3.3}$$

with $K = k_a/k_d$. The temperature dependence of K can be used to determine the isosteric enthalpy of adsorption $\Delta_{ad}H^0$ at a fixed surface coverage. K is essentially an equilibrium constant, so that the van't Hoff equation can be written

$$\left(\frac{\partial \ln K}{\partial T}\right) = \frac{\Delta_{ad}H^0}{RT^2}. \tag{3.4}$$

Therefore, a plot of ln K (or ln p for that matter) against 1/T should be a straight line of slope $\Delta_{ad}H^0/R$, from which $\Delta_{ad}H^0$ can be calculated.

The loading of a gold complex species onto activated carbon is an example of adsorption. The adsorbed gold can be removed/recovered from the carbon surface in more than one way. In this investigation it was attempted to recover it either by pure *sc*-CO_2 or by cosolvent entrained *sc*-CO_2. The recovery might proceed by either chemical dissolution or by physical desorption, and the distinction should be made, as with adsorption, on the basis of the magnitude of the enthalpy of desorption. Desorption is always activated because the substance (adsorbed gold in this case) needs to be lifted from the foot of a potential well. The temperature dependence of the rate of departure from the surface is expected to be Arrhenius-like, with an activation of desorption E_d comparable to the enthalpy of adsorption, but opposite in sign. Its magnitude could serve the purpose of determining whether the desorption process is of a chemical or physical nature.

References

1 LECO TFE 2000^{TM} Instruction Manual, Copyright LECO® Corporation, **2002**.

2 Tiedt, L.R.; Pretorius, W.E., *An introduction to electron microscopy and X-ray analysis*, Laboratory for Electron Microscopy, Potchefstroom University for CHE.

http://www.puk.ac.za/fakulteite/natuur/lem/LEM_diktaat.pdf

3 Oxford Instruments, The Oxford Guide to X-ray Microanalysis, CD-ROM Tutorial, England, **1997**.

4 Atkins, P.W., *Physical Chemistry 8th Edition*, Oxford University Press: Oxford, **2006**.

5 Bissett, H., *Manufacture and optimization of tubular ceramic membrane supports*, M.Sc. Thesis, North-West University: Potchefstroom Campus, **2005**.

6 *CSS: Experimental Design*, In: CSS Statistica User Manual (Volume II), Copyright© Statsoft, Inc., United States of America, **1991**.

7 Box, G.E.P.; Draper, N.R., *Empirical Model-Building and Response Surfaces*, Wiley: New York, **1988**.

CHAPTER 4

Solubility in *sc*-CO_2 of Selected Gold Complexes

This chapter deals with the synthesis, characterisation and solubility measurement in *sc*-CO_2 of various gold complexes. The solubility was measured since chemical dissolution in *sc*-CO_2 of these complexes was considered to be a possible route for the recovery of gold from a matrix such as activated carbon. The uv/visible spectra of the different complexes were recorded as a means of verifying the synthesised compounds by comparison to existing literature data (if available), and of monitoring the solubility of the complexes in *sc*-CO_2 by matching the uv/visible spectra of the extracts to them. In cases where no existing spectral data were available, the recorded spectra and associated data in this chapter represent new information regarding the complexes under consideration.

4.1 Synthesis and Characterisation of Gold Complexes

4.1.1 $HAuCl_4$

Metallic gold, Au(0), was dissolved in a mixture of 1 part HNO_3 and 3 parts HCl (aqua regia). The solution was heated slowly to evaporate most of the HNO_3, and HCl was then added to further decrease HNO_3 and to yield an oleaginous solution from which yellow crystals of $HAuCl_4.3H_2O$ crystallise upon cooling.[1,2] The complex so obtained was utilised in the preparation of different gold compounds as described later (**Section 4.1.2 - 4.1.5**).

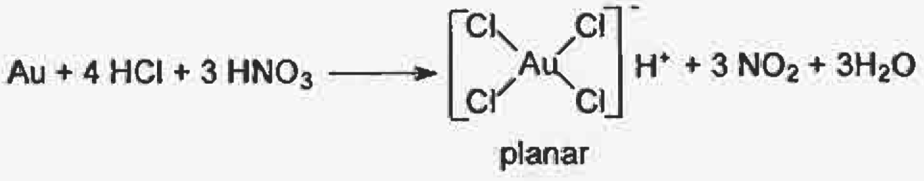

(4.1)

$HAuCl_4$ is a four-coordinated $5d^8$ Au(III) complex with square-planar geometry. The uv/visible spectrum of the complex is shown in **Figure 4.1 (a)**. The high-intensity absorbance in the region of λ = 220 nm is consistent with a ligand to metal charge transfer (LMCT) transition resulting from the migration of electrons from the four Cl atoms to the central Au(III) atom.[3] The absorbance at λ = 290 nm arises from the excitation $(t_{2g})^5(e_g)^3 \leftarrow (t_{2g})^6(e_g)^2$ since the particular wavelength is typical of ligand-field splittings (d-d transitions) in complexes of elements in the second and third rows of the d-block ($4d^8$ and $5d^8$).[4] The broad, essentially featureless band with its weakly defined maximum around 280 < λ < 300 nm as is more clearly shown in **Figure 4.1 (b)** can be attributed to unresolved vibrational structure typical of electronic transitions of liquid samples.[5] It conforms to the Beer-Lambert law over the range 0 < [Au(III)] < 100 ppm, leading to a molar absorption coefficient ε_{max} = 203 m^2 mol^{-1} at λ_{max} = 290 nm.

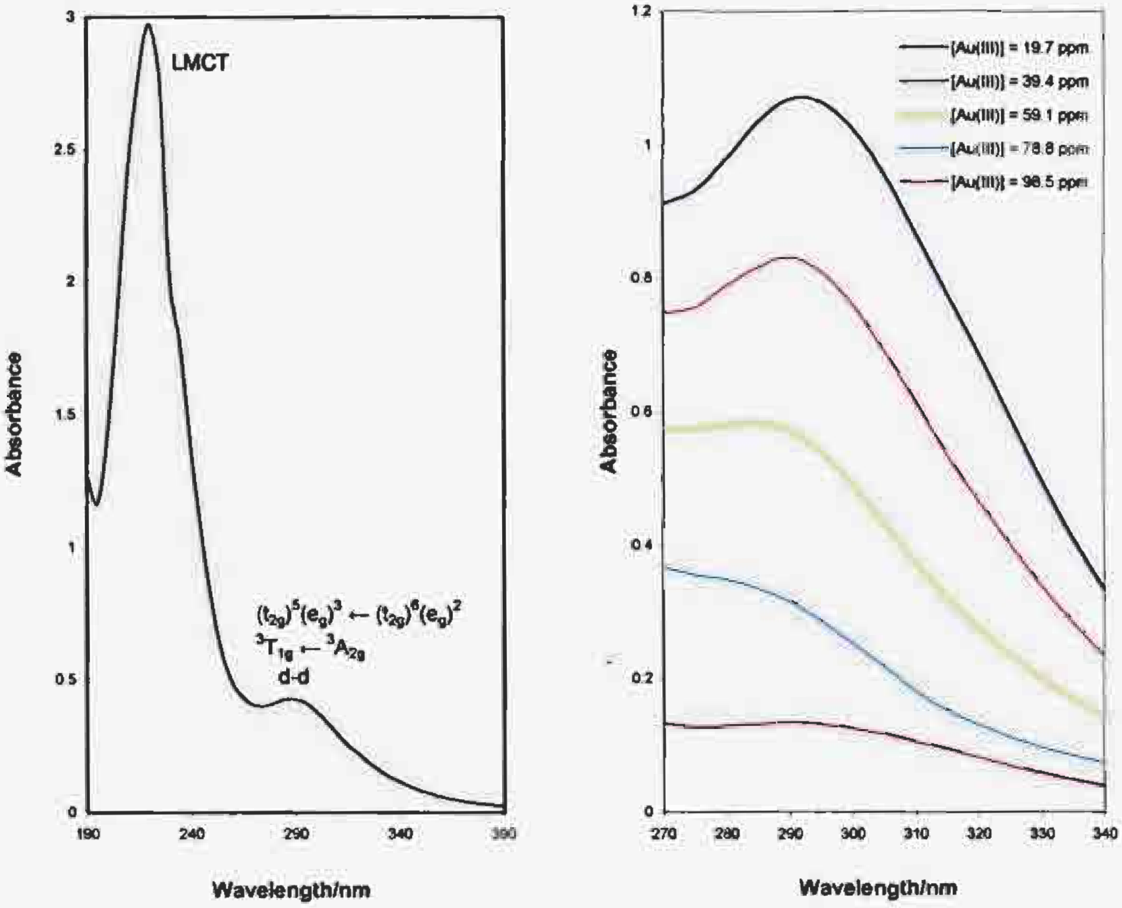

(a) (b)

Figure 4.1 UV/visible spectrum of $HAuCl_4$

4.1.2 $KAu(CN)_2$

Concentrated ammonia was added to a solution of $HAuCl_4$ to form fulminating gold which was isolated by filtration. The fulminating gold was dissolved in a concentrated solution of KCN, which was then diluted in a volumetric flask to yield a (1 000 ± 10) ppm gold containing solution.[6] The concentration of the solution was determined by ICP-MS.

$$\mathrm{Au} + 2\,\mathrm{KCN} + \mathrm{OH^-} \longrightarrow \underset{\text{linear}}{\left[\mathrm{N{\equiv}C{-}Au{-}C{\equiv}N}\right]^-}\ \mathrm{K^+} + \mathrm{KOH} \qquad (4.2)$$

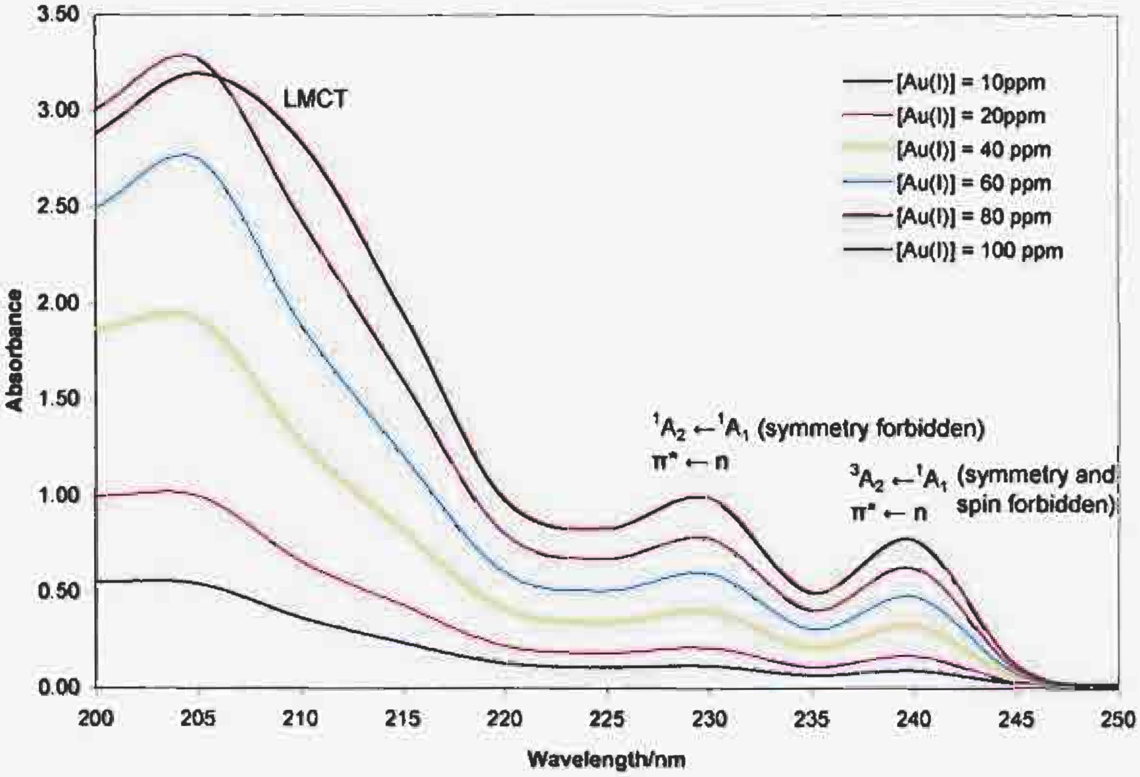

Figure 4.2 UV/visible spectrum of $KAu(CN)_2$

Figure 4.2 shows the uv/visible spectrum of the gold(I) complex synthesised. It exhibits two clearly defined absorption bands at λ_{max} = 229 nm and 239 nm and the typical ligand to metal charge transfer (LMCT) absorption band in the uv region (λ = 205 nm). The ligand C≡N acts as a chromophore. An important transition is a $\pi^* \leftarrow \pi$ transition in which an electron is promoted from a π-orbital to the corresponding π*-orbital within the ligand. A $\pi^* \leftarrow n$ transition occurs as a result of the excitation of a non-bonding lone-pair electron on the N atom to an antibonding π-orbital of the C≡N ligand. The two observed peaks in the spectrum probably both result from $\pi^* \leftarrow n$ transitions with different selection rules, since $\pi^* \leftarrow \pi$ transitions are expected to occur at $\lambda < 200$ nm (typical $160 < \lambda < 180$ nm).[5] The Beer-Lambert law is obeyed over the specified concentration range by both peaks, and the corresponding molar absorption coefficients were determined as $\varepsilon = 194\ m^2\ mol^{-1}$ and $154\ m^2\ mol^{-1}$, respectively. These values are in good agreement with typical values ($100 < \varepsilon < 200\ m^2\ mol^{-1}$ for a variety of chromophores (C=O, -N=N-, $-NO_2$) reported in the literature.[5]

4.1.3 $[Au\{CS(NH_2)_2\}_2]ClO_4$

A gold(I) thiourea complex was prepared by adding a solution of $HAuCl_4$ dropwise to a concentrated solution of thiourea. Concentrated $HClO_4$ was added, resulting in the formation of white crystals of the complex.[7] It was recrystallised twice from water and analysed by atomic absorption (AA) spectrophotometry. According to the stoichiometry of the compound, it theoretically has a 43.9 % gold content. The gold percentage established from the analysis of the synthesised complex was (42.1 ± 0.3) %.

$$HAuCl_4 + 2\ S{=}C(NH_2)_2 \xrightarrow{HClO_4} \underset{\text{linear}}{\left[(NH_2)_2C{=}S{-}Au{-}S{=}C(NH_2)_2\right]^+}\ ClO_4^- \qquad (4.3)$$

In **Figure 4.3** the uv/visible spectrum of the gold thiourea complex at different concentrations is shown. In addition to the high-intensity LMCT band at $\lambda = 205$ nm an absorption band with a clearly defined maximum at $\lambda_{max} = 252$ nm is observed. It complies with the Beer-Lambert law and the molar absorption coefficient turned out to be $\varepsilon_{max} = 154\ m^2\ mol^{-1}$. The wavelength at which it occurs and the value of the corresponding molar absorption coefficient suggest that its occurrence can be ascribed to a $\pi^* \leftarrow n$ transition involving an electron of the lone-pair on the N atom excited to an antibonding NH_2 π-orbital. Since a gold(I) complex is a d^{10} system, no transitions can result from ligand-field splitting and an $\pi^* \leftarrow n$ transition is thus the only option.

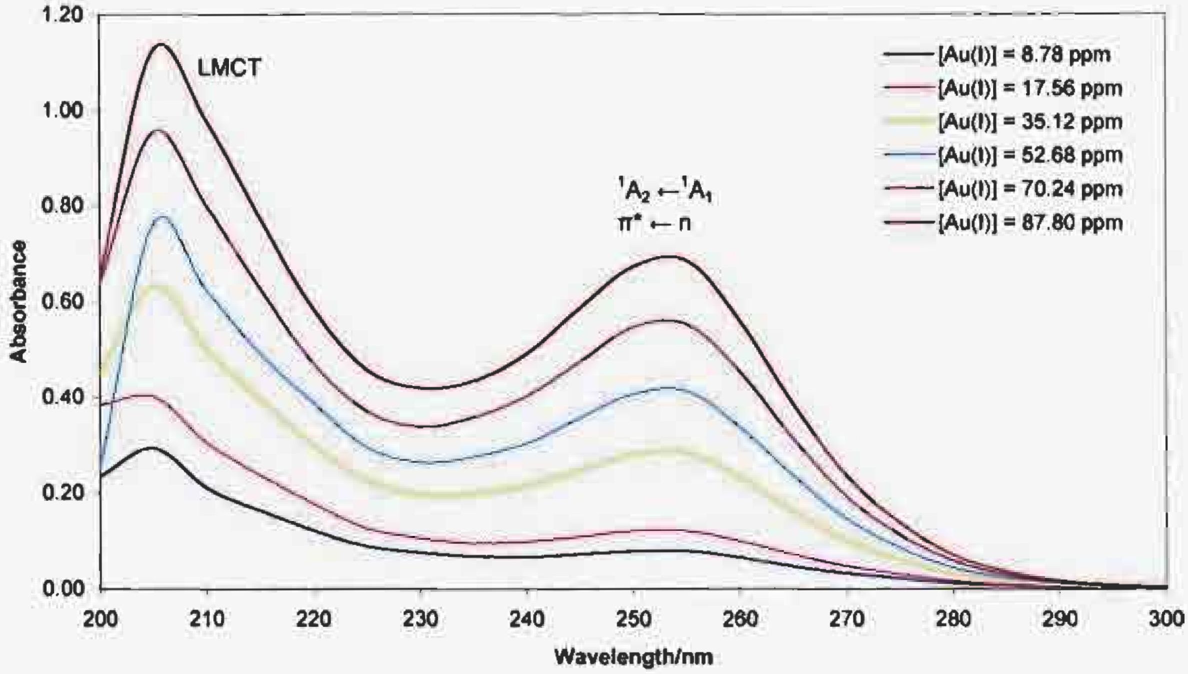

Figure 4.3 UV/visible spectrum of $[Au\{CS(NH_2)_2\}_2]ClO_4$

The uv/visible spectrum and spectral data for $KAu(CN)_2$ and $[Au\{CS(NH_2)_2\}_2]ClO_4$ are reported here for the first time, and represent a valuable contribution to existing knowledge.

4.1.4 $[Au(phen)Cl_2]Cl$

The addition of 1.10-phenanthroline monohydrate dissolved in ethanol to a solution of $HAuCl_4$ in ethanol gave a yellow precipitate which turned orange after heating the mixture for 2 hours.[8] The isolated mixed ligand gold(III) complex was analysed by AA, and the real Au content turned out to be (39.2 ± 0.3) % as opposed to the theoretical value of 40.7 %. It will be shown later (**Paragraph**

4.2.1) that the real gold content could be improved upon and brought closer to the theoretical value by purifying the complex by *sc*-CO_2.

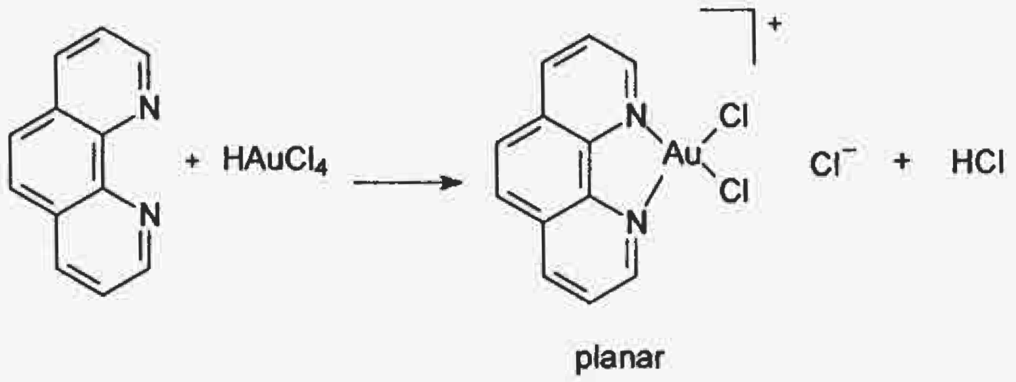

(4.4)

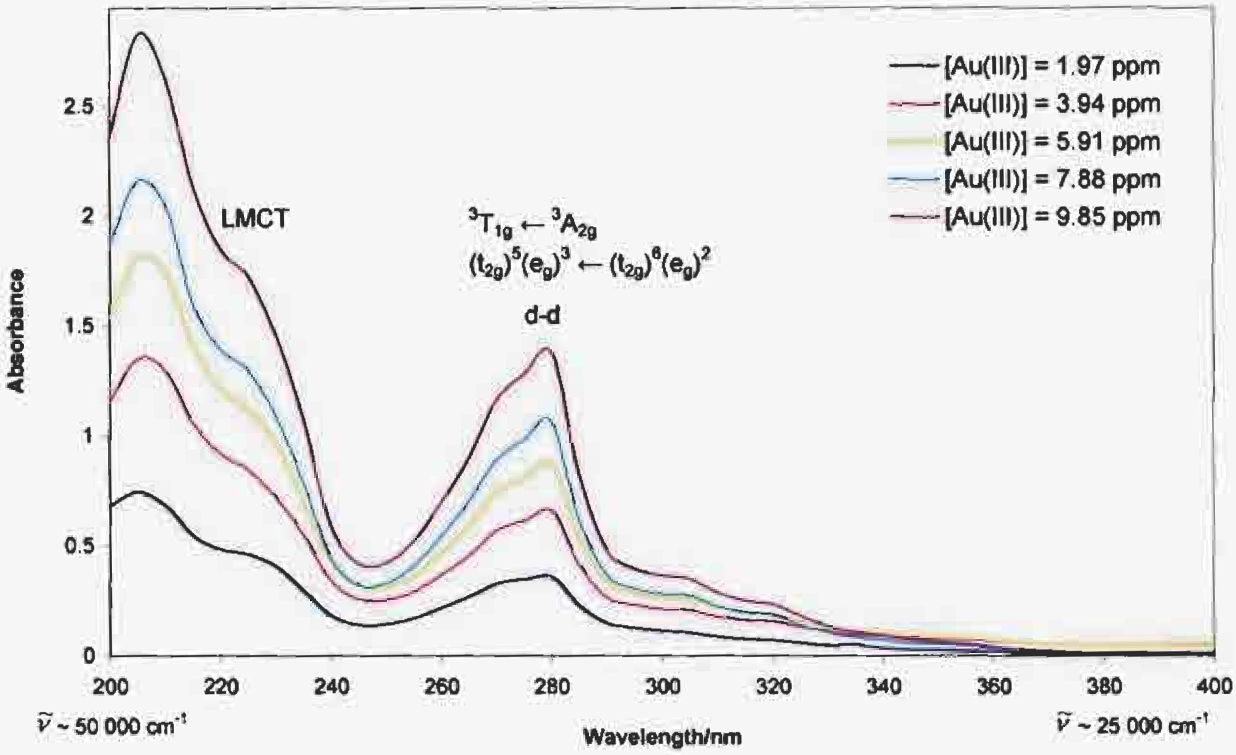

Figure 4.4 UV/visible spectrum of $[Au(phen)Cl_2]Cl$

Figure 4.4 shows the uv/visible spectrum of $[Au(phen)Cl_2]Cl$ recorded for different concentrations. Since two ligands (1.10-phenanthroline, Cl) are involved, both with strong electron-donor capability, a high-intensity ligand to metal charge transfer (LMCT) band with maxima at λ = 205 and 220 nm is observed. The d-d transition observed at λ = 290 nm in the spectrum of $HAuCl_4$ (**Figure 4.1 (b)**) is also observed here, though the wavelength slightly shifted by ca. 10 nm (now λ = 280 nm) due to the shoulder appearing on the high-energy side of the particular d-d band as a result of the decrease in symmetry on going from the symmetrical $AuCl_4^-$ to the less symmetrical $Au(phen)Cl_2^+$ mixed-ligand complex.[3] The observed maxima at λ_{max} = 205 nm and 280 nm correspond with those reported in the literature.[9] The absorbances conform to Beer's law and the molar absorption coefficients were determined as ε_{max} (205 nm) = 5 760 $m^2\ mol^{-1}$ and ε_{max} (280 nm) = 2 820 $m^2\ mol^{-1}$. The much higher molar absorption coefficient at λ_{max} = 280 nm for $[Au(phen)Cl_2]Cl$ (**Figure 4.4**) as compared to that at λ_{max} = 290 nm for $HAuCl_4$ (**Figure 4.1**) is attributed to the superimposed ligand-field splitting contributions of the two ligands. Moreover, it was discovered later (**Section 4.2.1**) that a sample of the complex contained some unreacted ligand as an impurity, and that the free ligand also exhibited strong absorbances in the same wavelength region. Likewise, the high molar absorption coefficient of the intense LMCT band probably resulted from the superposition of the absorbances of both ligands in the wavelength region concerned.

4.1.5 $[Au(en)_2]Cl_3$

A solution of 1.2-ethylenediamine in diethyl ether was added to a solution of $HAuCl_4$ dissolved in diethyl ether. It resulted in the formation of a gummy yellow precipitate which was dissolved in water. The addition of ethanol to the yellow solution led to the formation of a white precipitate. The product was recrystallised by dissolving it in water and adding ethanol to the solution.[8] AA analysis gave a gold content of (40.1 ± 0.3) % compared to the theoretically expected value of 46.5 %. The difference between the theoretically expected and experimentally measured gold content could possibly be ascribed to incomplete removal of unreacted ethylenediamine (ligand) which, as a result of its oily nature, could not be fully removed by recrystallising the product obtained.

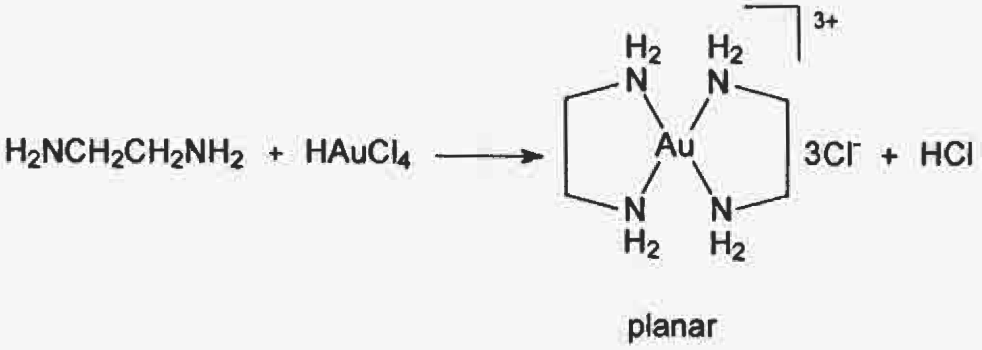

(4.5)

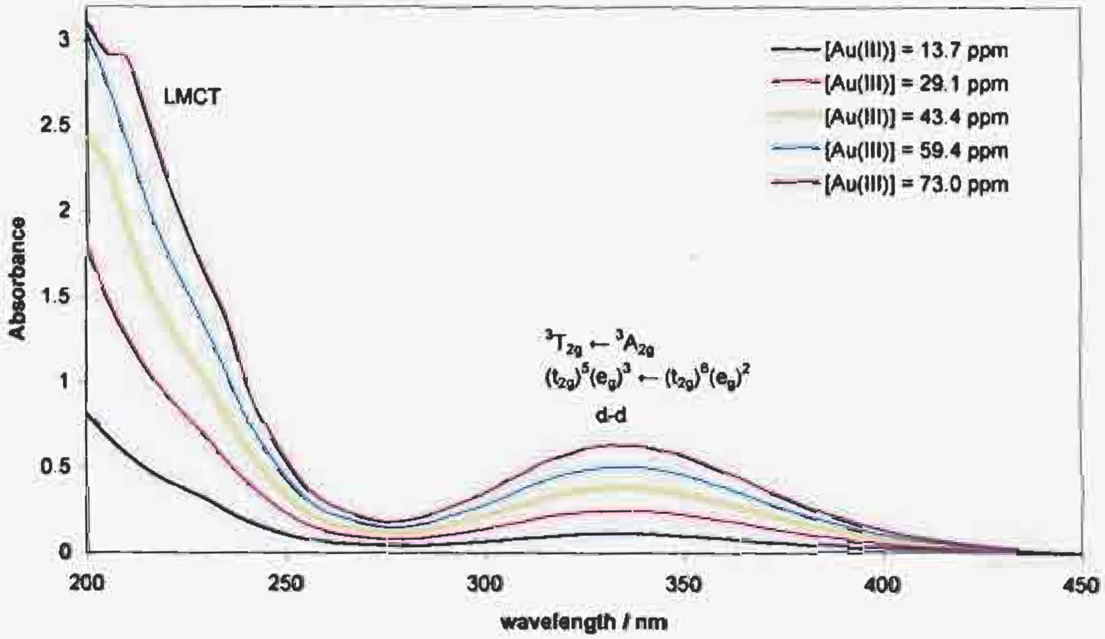

Figure 4.5 UV/visible spectrum of $[Au(en)_2]Cl_3$

In **Figure 4.5** the uv/visible spectrum of the complex at various concentrations is shown. An absorption band with a maximum at λ_{max} = 335 nm is observed, which corresponds to that reported in the literature[9]. It is ascribed to a d-d or ligand-field transition caused by splitting of the 5d orbitals by the ethylenediamine ligand. The strong electron-donating character of the four nitrogen atoms of the ligand causes a high-intensity LMCT band to occur in the uv region. The molar absorption coefficient at λ_{max} = 335 nm was calculated as $\varepsilon = 125\ m^2\ mol^{-1}$.

In **Figure 4.6** the calibration lines obtained for $KAu(CN)_2$ (λ_{max} = 239 nm) and $[Au(phen)Cl_2]Cl$ (λ_{max} = 280 nm) are shown as representative examples of the conformation of the absorbance maxima to the Beer-Lambert law. The molar absorption coefficients at λ_{max} of each of the complexes were determined from the slopes of the calibration lines. The vast difference between the molar absorption coefficients of the two complexes at the specified wavelengths relates to the difference in origin of the two absorbance maxima, the one in the case of $KAu(CN)_2$ being the result of a $\pi^* \leftarrow n$ transition within the ligand and the one in the case of $[Au(phen)Cl_2]Cl$ a d-d transition within the splitted d-orbitals of the central metal atom.

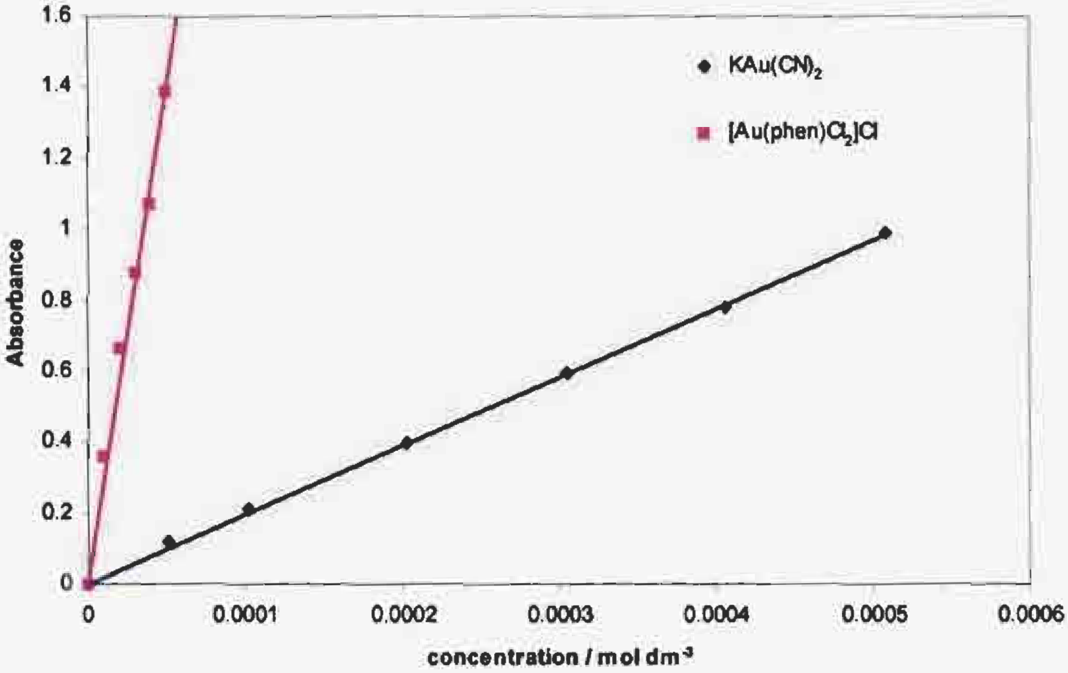

Figure 4.6 Calibration lines for $[Au(phen)Cl_2]Cl$ (λ_{max} = 280 nm) and $KAu(CN)_2$ (λ_{max} = 239 nm)

In **Table 4.1** the spectral data observed for all the gold complexes under consideration is summarised and compared to literature values.

Table 4.1 Spectral data acquired for synthesised gold complexes

Complex	λ_{max} / nm	ε_{max} / $m^2\ mol^{-1}$	Reference
$HAuCl_4$	290	203	this work
$KAu(CN)_2$	230; 240	194; 154	this work
$[Au\{CS(NH_2)_2\}]ClO_4$	252	154	this work
$[Au(phen)Cl_2]Cl$	205; 280	5 760; 2 820	this work
	205; 280		9
$[Au(en)_2]Cl_3$	335	125	this work
	335		9

4.2 Solubility of Synthesised Complexes in *sc*-CO_2

In order to investigate the viability of *sc*-CO_2 recovery of gold, the solubility in *sc*-CO_2 of the different gold complexes covered in **Section 4.1** was studied. A range of conditions was selected at which dissolution of the complexes was attempted. These conditions are listed in **Table 4.2**. Temperature and pressure were varied to yield fluid densities which would guarantee good solvent strength ($0.85 < \rho < 1.00$ g/mL). The mode of *sc*-CO_2 extraction was strictly kept static as required for solubility measurement under equilibrium conditions, but a dynamic mode of extraction was employed in a few cases to increase the chance of dissolving some material by continuously introducing fresh *sc*-CO_2. The polarity of sc-CO_2 was adjusted in a few cases by small amounts of methanol added as a cosolvent/modifier.

4.2.1 [Au(phen)Cl$_2$]Cl

A typical uv/visible spectrum of an extract obtained from static runs conducted on $[Au(phen)Cl_2]Cl$ according to **Table 4.2** is shown in **Figure 4.7**. It does not correspond to that of $[Au(phen)Cl_2]Cl$ in **Figure 4.4**, but does show that a species with distinct absorption bands was dissolved. It seemed that this species was the free ligand 1.10-phenanthroline as shown by superimposing its spectrum on that of the extract in **Figure 4.7**. The two spectra are so similar that it could be concluded that only free ligand was dissolved. This was supported by AA analysis of the extract, indicating that no gold was dissolved by *sc*-CO_2.

Table 4.2 Selected conditions for attempted dissolution of $[Au(phen)Cl_2]Cl$, $[Au(en)_2]Cl_3$ and $[Au\{CS(NH_2)_2\}_2]ClO_4$ in *sc*-CO_2. mass = (0.100 ± 0.005) g, flow rate for dynamic mode = 1 L min^{-1}

Temperature / °C	**Pressure / atm**	**Density / g mL^{-1}**	**Static time / min**	**Dynamic time / min**	**Modifier**
35	450	1.000	5		
35	450	1.000	15		
35	450	1.000	30		
35	450	1.000	45		
35	450	1.000	60		
35	450	1.000	60		methanol
70	450	0.887	60		
70	450	0.887	60		methanol
70	450	0.887	60		TBP/methanol
70	550	0.935	60		
35	260	0.916	60		
35	260	0.916	60		methanol
60	450	0.919	60		
60	450	0.919	60		methanol
60	550	0.965	60		
70	450	0.887		90	
35	260	0.916		90	
70	450	0.887		90	methanol
35	260	0.916		90	methanol

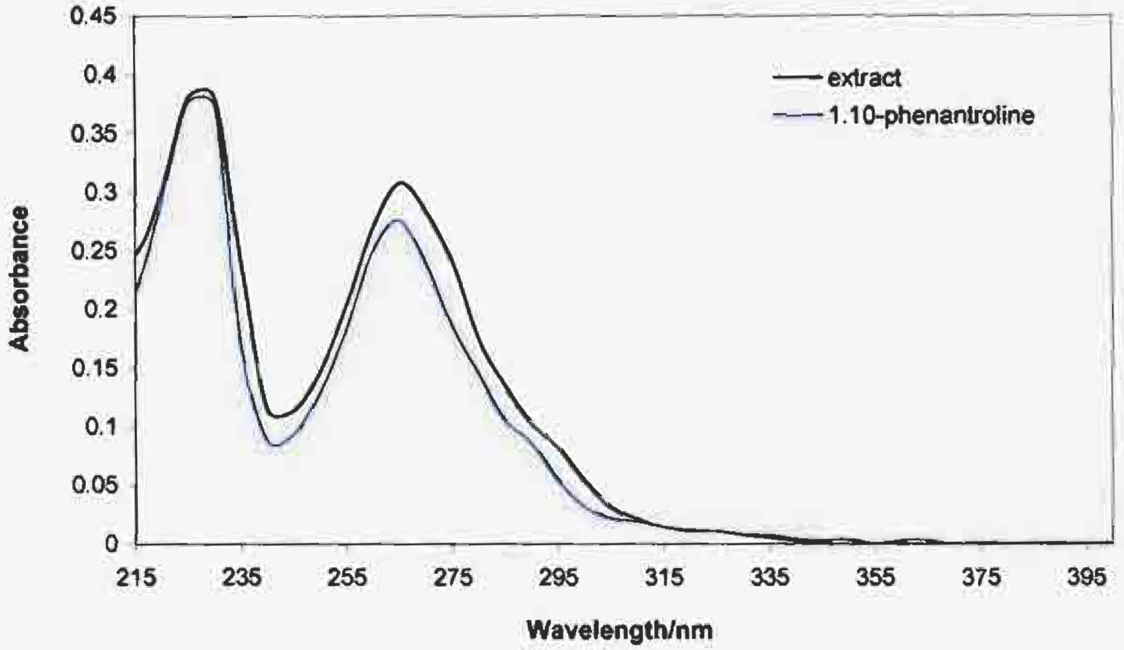

Figure 4.7 Typical uv/visible spectrum of extract obtained from dissolution of [Au(phen)Cl_2]Cl in *sc*-CO_2 compared to uv/visible spectrum of 1.10-phenanthroline (free ligand)

The question arose as to how free ligand could be dissolved by *sc*-CO_2 as the fluid was not considered capable of decomposing the complex. A possibility could be that some free ligand was present in the sample as a contaminant or impurity due to incomplete removal during crystallisation of the complex species, and that the unreacted ligand was removed from the sample by dissolution in *sc*-CO_2. If this were the case, the gold content of the sample after exposure to *sc*-CO_2 should be closer to the theoretically expected value than the gold content before *sc*-CO_2 treatment. As noted in **Section 4.1.4**, the theoretical value for the gold content of this complex was 40.7 %, and the experimental value determined for the synthesised complex was (39.2 ± 0.3) %. AA analysis of the complex after exposure to *sc*-CO_2 gave a gold content of (40.3 ± 0.3) %, which was much closer to the theoretical value and, in fact, quite close to the expected value. This supports the explanation that free ligand was present as an impurity in the sample, and that this was dissolved in *sc*-CO_2. Exposure to *sc*-CO_2 thus served as a means of purifying the synthesised complex by removal of unreacted free ligand by dissolution.

4.2.2 $[Au(en)_2]Cl_3$

Runs were also performed on $[Au(en)_2]Cl_3$ at the conditions listed in **Table 4.2**. The uv/visible spectrum of a typical extract obtained with *sc*-CO_2 did not correlate with the spectrum of $[Au(en)_2]Cl_3$ in **Figure 4.5**. AA analysis of the extract also indicated that no gold had been extracted from the sample in the thimble. It seemed as if this species was the free ligand 1,2-ethylenediamine on comparing its spectrum to that of the extract.

4.2.3 $[Au\{CS(NH_2)_2\}_2]ClO_4$

Runs were also conducted to investigate the solubility of $[Au\{CS(NH_2)_2\}_2]ClO_4$ in *sc*-CO_2. AA and uv/visible analyses indicated that the complex was insoluble in *sc*-CO_2 as no gold or gold thiourea could be detected in the extracts obtained.

4.3 Dissolution of 1.10-Phenanthroline in *sc*-CO_2

The result obtained in **Section 4.2.1** that $[Au(phen)Cl_2]Cl$ was insoluble in *sc*-CO_2 but that the free ligand present as an impurity could be dissolved and removed by *sc*-CO_2, opted us to investigate in more detail the solubility of 1.10-phenanthroline monohydrate in *sc*-CO_2. A more complete spectrum of 1.10-phenanthroline is presented in **Figure 4.8**. The observed maxima in the spectrum of the free ligand assisted us in interpreting the higher than expected molar absorption coefficients determined for $[Au(phen)Cl_2]Cl$ in **Figure 4.4** in terms of the superposition of absorbances of the two entities. **Figure 4.9** shows calibration lines based upon known concentrations of 1.10-phenanthroline monohydrate in methanol and the corresponding absorbances at two appropriate wavelengths (λ_{max} = 220 and 265 nm) derived from **Figure 4.8**. The molar absorption coefficients at these wavelengths were calculated as ε_{max} (220 nm) = 5 060 $m^2\ mol^{-1}$ and ε_{max} (265 nm) = 3 170 $m^2\ mol^{-1}$.

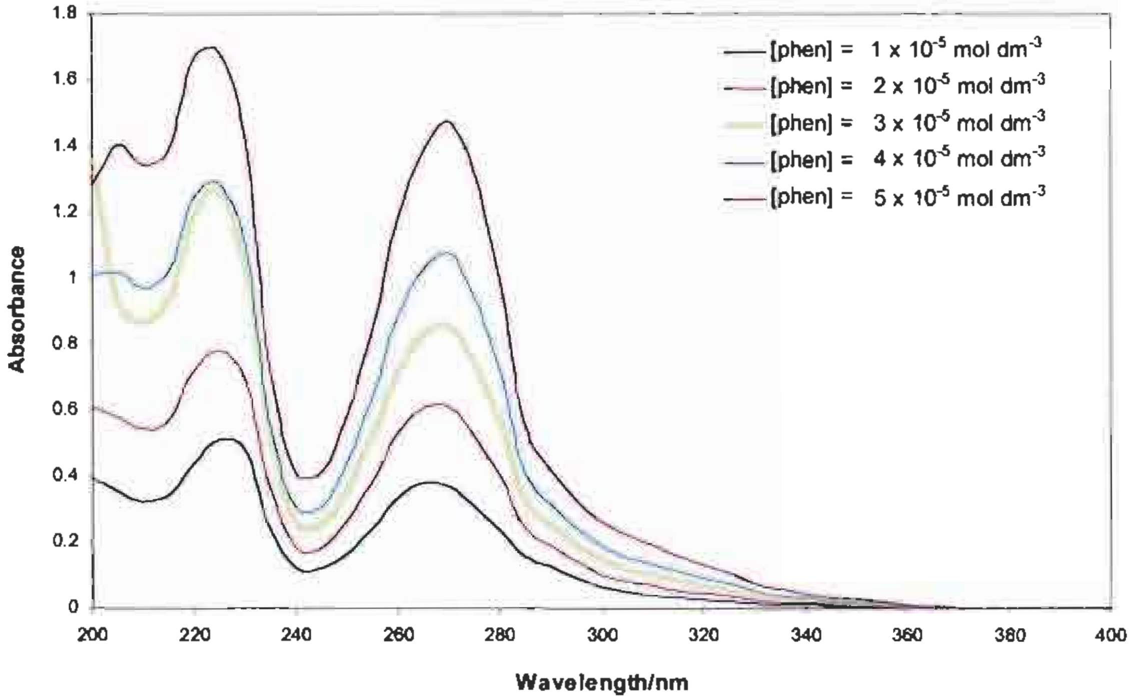

Figure 4.8 UV/visible spectrum of 1.10-phenanthroline monohydrate in water λ_{max} = 220 and 265 nm

In the static extraction mode employed the concentration of 1,10-phenanthroline monohydrate present in a fixed amount of *sc*-CO_2 after selected time intervals was determined. At sufficiently long time intervals, *sc*-CO_2 was saturated with the dissolved substance and no further dissolution occurred. The solubility could be read from the plateau of a concentration-time graph occurring when equilibrium was established between the solid and solution phases. To acquire a statistically acceptable average, four runs were performed for each time interval. The absorbance of each collected extract was measured at the two wavelengths concerned (**Figure 4.8**), and these values were converted to concentration by virtue of the calibration lines in **Figure 4.9**. The concentrations (mol/L) were finally expressed in grams per gram of *sc*-CO_2 using the volume of the extraction thimble and the density of the fluid at the conditions concerned to calculate the corresponding mass of CO_2.

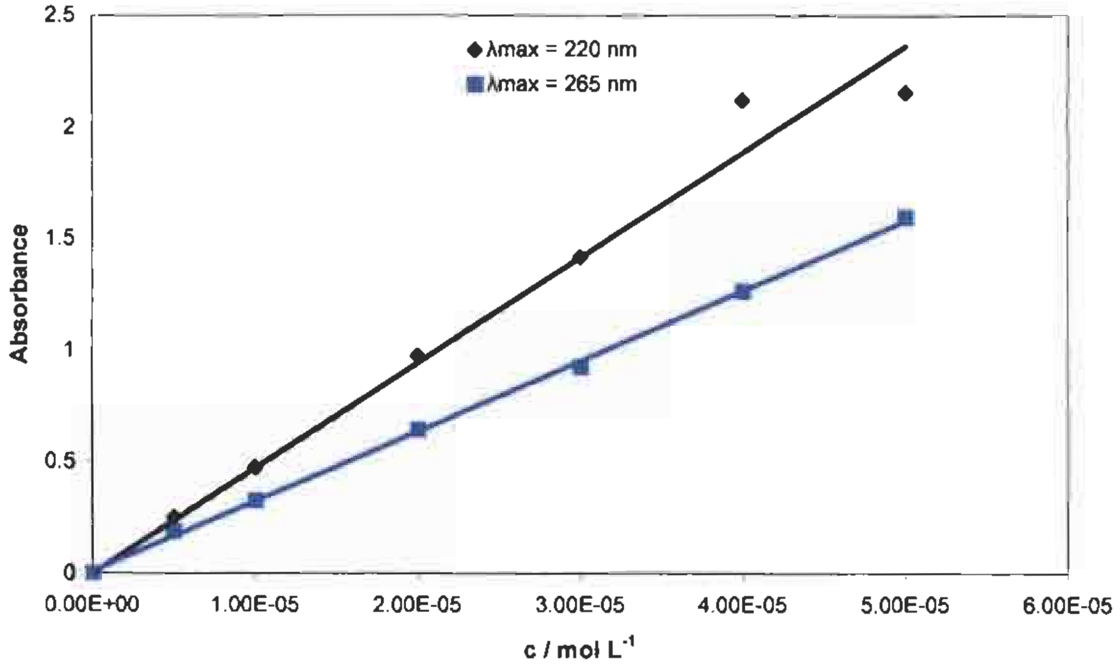

Figure 4.9 Calibration lines for 1.10-phenatroline in methanol

The resulting solubility curve (concentration-time graph) for 1,10-phenanthroline monohydrate in *sc*-CO_2 is presented in **Figure 4.10**. The solubility is given by the plateau of the curve, which turned out to be 6 x 10^{-4} g per gram of CO_2 (2.8 x 10^{-3} mol/L) at 40 °C and 300 atm (ρ = 0.92 g/mL) as indicated by the horizontal arrow. The time interval required to prepare a saturated solution of 1,10-phenanthroline in sc-CO_2 at the conditions under consideration is 60 minutes as shown by the vertical arrow in **Figure 4.10**.

Sodium diethyldithiocarbamate (NaDDC), tributylphosphine oxide (TBPO) and triazolocrown ethers are chelating agents that have been used by other authors to synthesise metal complexes. The solubilities measured for these ligands are listed in **Table 4.3** together with the solubility for 1.10-phenanthroline obtained in this investigation. The value corresponds well with the literature values in terms of magnitude and thus creates confidence in the experimental procedure followed for its determination.

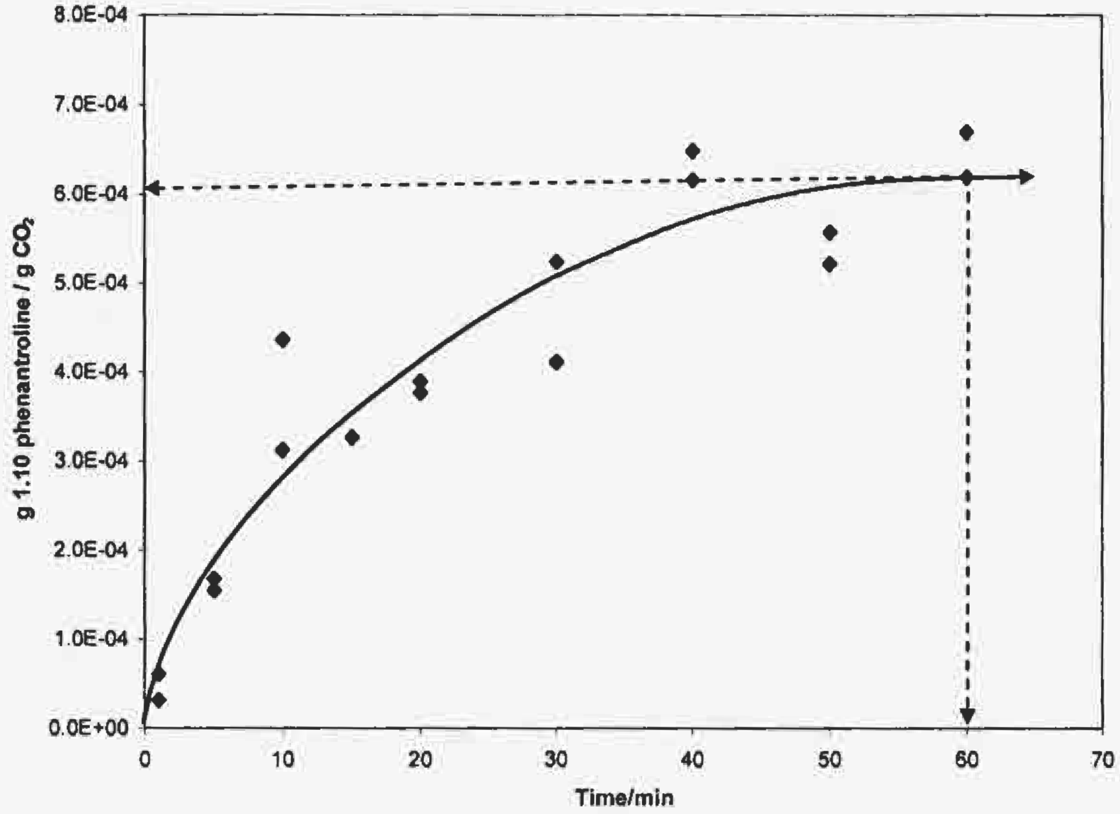

Figure 4.10 Concentration-time graph of 1,10 phenanthroline monohydrate in *sc*-CO_2. Temperature = 40 °C; Pressure = 300 atm; $\rho = 0.921$ g/mL

Table 4.3 Solubility of different ligands in *sc*-CO_2

Ligand	T / °C	P / atm	Solubility / mol L^{-1}	Ref.
NaDDC	60	200	1.5×10^{-3}	10
TBPO	60	200	0.85	11
Triazolocrown ethers	60	200	$1 - 1.3 \times 10^{-5}$	12
1.10 phenanthroline	40	300	4.6×10^{-3}	this work

References

1 Biltz, W.; Wein, W., *Zeitschrift für Anorganische und Allgemeine Chemie*, **1925**, *148*, 192.

2 Thomson, J., *Berichte der Deutschen Chemischen Gesellschaft*, **1883**, *16*, 1585.

3 Shriver, D.F.; Atkins, P.W., *Inorganic Chemistry 3rd Edition*, Oxford University Press: Oxford, **1999**.

4 Barrow, G.M., *Introduction to Molecular Spectroscopy*, McGraw-Hill Int. Book Company: London, **1984**.

5 Atkins, P.W., *Physical Chemistry 8th Edition*, Oxford University Press: Oxford, **2006**.

6 Rose, T.K., *The Metallurgy of Gold*, Charles Griffin & Company, Ltd: London, **1915**, 67.

7 Kazakov, V.P.; Lapshin, A.I.; Peschchevitskii, B.I., *Russian Journal of Inorganic Chemistry*, **1964**, 708.

8 Block, B.P.; Bailar, J.C., *Journal of the American Chemical Society*, **1951**, *73*, 4722.

9 Messori, L.; Abbate, F.; Marcon, G.; Orioli, P.; Fontani, M.; Mini, E.; Mazzei, T.; Carotti, S.; O'Connel, T.; Zanello, P., *Journal of Medicinal Chemistry*, **2000**, *43*, 3541.

10 Wai, C.M.; Wang, S.F.; Liu, Y.; Lopez-Avilla, V.; Beckert, W.F., *Talanta*, **1996**, *43*, 2083.

11 Lin, Y.; Smart, N.G.; Wai, C.M., *Environ Sci Technol*, **1995**, *29*, 2706.

12 Wang, S.F.; Elshani, S.; Wai, C.M., *Analytical Chemistry*, **1995**, **67**, 919.

CHAPTER 5

sc-CO_2 Recovery of $KAu(CN)_2$ from Granular Activated Carbon

The recovery of gold from industrial matrices by *sc*-CO_2 was mimicked in the laboratory by preloading a suitable complex species onto granular activated carbon and exposing the resulting material to extraction in a laboratory-size supercritical extractor. The gold compound that could be loaded successfully onto activated carbon for the purpose of this study was $KAu(CN)_2$. The mechanism of adsorption of the dicyanoaurate(I) complex ion $Au(CN)_2^-$ on activated carbon is based on ion-pair formation $[M^{n+}...(Au(CN)_2^-)_n]$ and has been studied extensively.[1,2] The detail of the mechanism is beyond the scope of interest of this study, though.

5.1 Loading $KAu(CN)_2$ onto Activated Carbon

The selected complex species was loaded onto activated carbon to such an amount that measurable concentrations of gold as monitored by SEM-EDS could be recovered by *sc*-CO_2 (if feasible) from the active carbon surface. 1 g of activated carbon was exposed to 100 mL of a 1 000 ppm gold(I) stock solution, implying that up to 100 mg of gold could be loaded onto 1 000 mg of carbon. In order to monitor the progress of gold(I) adsorption onto the carbon, the concentration of the bulk solution was determined at fixed intervals. It was found that $KAu(CN)_2$ was almost completely adsorbed after ca. 6 h. Longer times of exposure did not lead to the adsorption of more gold. AA analysis of the remaining gold in solution indicated a concentration of 0.6 ppm, which means that only 0.06 mg of gold (< 0.1 % of the initial amount) had not been adsorbed onto the activated carbon. It could be concluded that after 6 h practically all available gold had been adsorbed.

5.2 SEM-EDS Analysis of $KAu(CN)_2$ Loaded onto Activated Carbon

SEM-EDS was used to examine the surface of individual carbon granules and to determine the elemental composition of the surface of these granules prior to and after *sc*-CO_2 exposure. Preliminary measurements confirmed that a good representation of the composition of a batch of $KAu(CN)_2$ loaded activated carbon is obtained if the average of the surface composition of five carbon granules was determined. A batch of five granules was carefully selected by viewing them with a light microscope. The elemental composition of the surface of each granule was established by EDS analysis, and an average surface composition for the batch of five granules was calculated. The five granules were then inserted into the extraction thimble of the supercritical extractor and exposed to *sc*-CO_2 at a selected set of conditions. EDS analysis was used again to measure the average elemental composition of the same area of the five granules after *sc*-CO_2 exposure. A typical elemental composition of the surface of a batch of five activated carbon granules prior to and after *sc*-CO_2 exposure is shown in **Table 5.1** and **5.2**, respectively.

Table 5.1 Typical elemental composition of surface of five activated carbon granules prior to *sc*-CO_2 exposure

	C	O	K	Au	Total
1	74.18	11.37	3.02	11.43	100
2	78.53	12.85	2.14	6.48	100
3	69.27	11.51	5.27	13.95	100
4	75.44	12.32	2.70	9.55	100
5	76.03	12.52	2.92	8.54	100
Average	74.7 ± 3.4	12.1 ± 0.7	3.2 ± 1.2	10,0 ± 2.8	100

Table 5.2 Typical elemental composition of surface of five activated carbon granules after *sc*-CO_2 exposure

	C	O	K	Au	Total
1	78.36	14.87	2.42	4.35	100
2	80.36	14.10	1.48	4.07	100
3	77.98	14.82	2.38	4.82	100
4	76.55	16.27	3.46	3.71	100
5	77.04	16.66	2.77	3.53	100
Average	78.1 ± 1.5	15.3 ± 1.1	2.5 ± 0.7	4.1 ± 0.5	100

A shift in the elemental composition of the surface of each granule as a result of *sc*-CO_2 exposure was observed. The percentage of Au and K decreased, while the percentage of the remaining elements increased such that a total of 100 % was maintained throughout. This can be explained by removal of $KAu(CN)_2$ by *sc*-CO_2 from the surface of the granules.

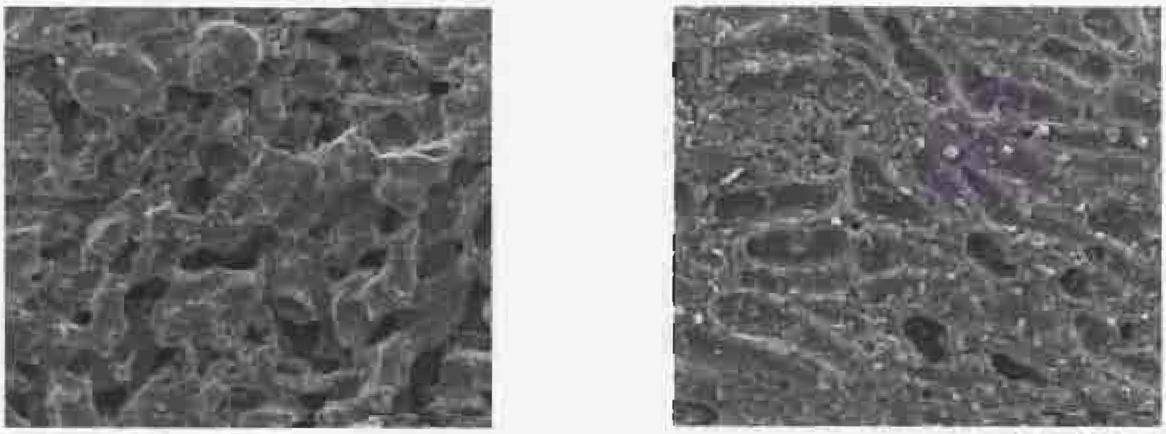

Before *sc*-CO_2 exposure

After *sc*-CO_2 exposure

Figure 5.1 Backscatter SEM micrographs of a $KAu(CN)_2$ loaded activated carbon granule

In **Figure 5.1** backscatter SEM micrographs of a single activated carbon granule before and after exposure to *sc*-CO_2 are shown. These micrographs illustrate that there were no changes in the structure of an activated carbon granule as a result of exposure to *sc*-CO_2, but they do reflect the shift in the elemental composition of the activated carbon surface since the gold compound was homogeneously spread over the entire surface area.

The observation of a shift in the average elemental composition of the surface of a batch of five granules of activated carbon loaded with $KAu(CN)_2$ was a positive sign of gold recovery by *sc*-CO_2 and served as motivation to more comprehensively investigate the effect of *sc*-CO_2 exposure. In the experiments performed for that purpose three batches consisting of five carbon granules each were used. The gold percentage of each granule was determined and an average for each batch was calculated prior to and after *sc*-CO_2 exposure of different duration. The statistical reliability of the method was warranted by measuring the composition at ten selected sites of each granule and obtaining an average for each granule before an average for the batch of five granules was calculated.

A dynamic mode of sc-CO_2 extraction was used since it offers the fastest way to recover adsorbed material because fresh solvent continuously interacts with the adsorbate and dissolves/displaces/desorps it from the surface. The results are shown as a graph of mass % of gold recovered versus extraction time in **Figure 5.2**. The plateau occurring in the graph while using a dynamic mode of extraction signifies a maximum amount of adsorbed gold which could be removed from the surface by *sc*-CO_2 as limited by a surface related factor, e.g. intermolecular forces preventing more of the adsorbate to be removed or incapability of *sc*-CO_2 to remove adsorbed gold from the inner pore structure of the adsorbent.

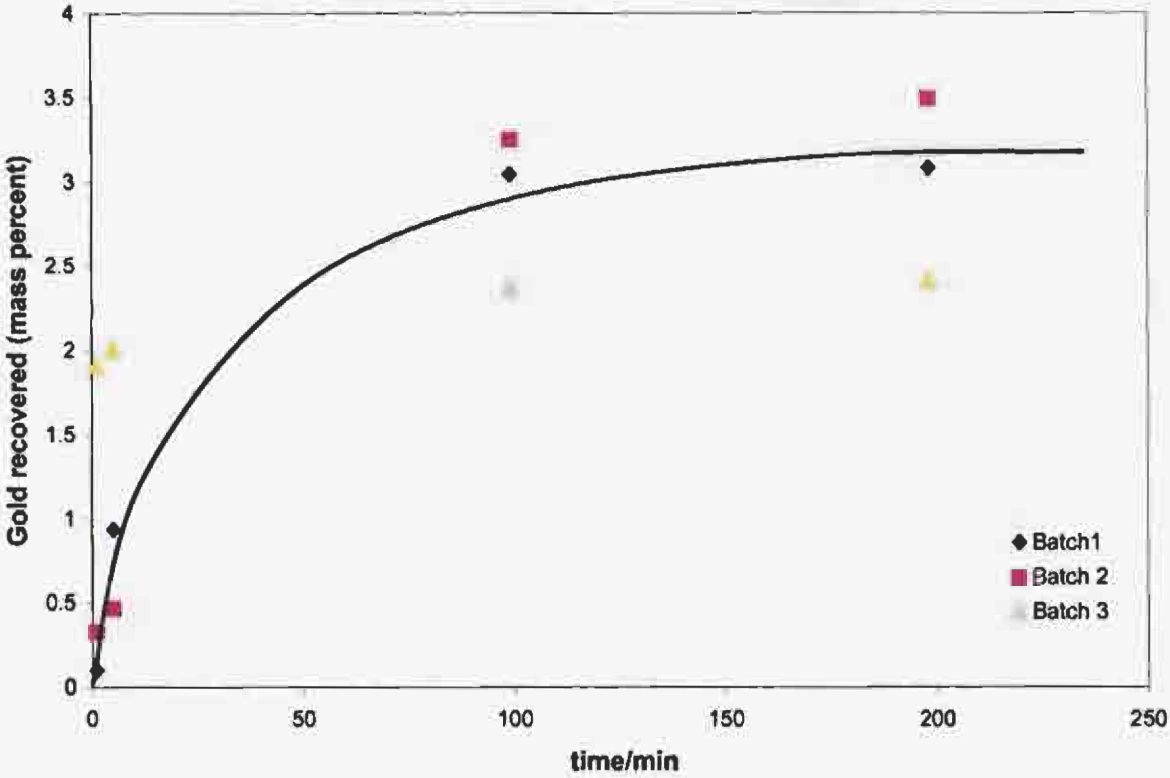

Figure 5.2 *sc*-CO_2 recovery of gold from surface of activated carbon granules as function of time using a dynamic mode of extraction. Temperature: 65 °C, Pressure: 300 atm, Flow rate: 2 L/min

ICP analysis of the extracts of the three batches of loaded activated carbon granules collected from the supercritical extractor after runs of 198 min (cf. **Figure 5.2**) showed the presence of gold and thus confirmed that gold had indeed been recovered from the surface as indicated by SEM-EDS. The amount of gold recovered from the three batches are listed below. The values mutually agree quite well, and demonstrate the good reproducibility obtained by ICP despite the very low concentrations of gold involved.

Batch 1: 306.2 ± 9.2 ppb

Batch 2: 374.7 ± 11.2 ppb

Batch 3: 331.1 ± 9.9 ppb

average = (337 ± 35) ppb

The percentage gold retrieved by *sc*-CO_2 according to the ICP results is smaller than 1 % of the gold initially loaded onto the activated carbon and cannot be directly compared to the 3 % of gold recovered according to SEM-EDS. The figure of 3 % relates to gold present on the surface of the activated carbon as detectable by SEM and not the total amount of gold loaded onto the activated carbon. An important perspective thus is that the percentage of gold recovered by *sc*-CO_2 as measured by SEM-EDS and by ICP will indeed be different since the two techniques do not deal with the same bulk of loaded gold. SEM-EDS is limited to detection of gold as a mass percentage of the elements present on the surface of the carbon granules, whereas ICP measures the amount of recovered gold as a mass percentage of the total amount of gold loaded onto the carbon granules. However, the presence of gold in the extracts proved the recovery of at least a small percentage of the loaded gold by *sc*-CO_2, and thus supports the evidence of *sc*-CO_2 removal of gold by SEM-EDS.

5.3 Mechanism of $KAu(CN)_2$ Recovery by *sc*-CO_2

The question was how $KAu(CN)_2$ had been recovered – by chemical dissolution, by physical displacement or by reversed adsorption?

In an effort to get an answer to this question a study was performed during which a static extraction mode was employed to measure the maximum concentration of $KAu(CN)_2$ which can prevail in a fixed amount of *sc*-CO_2 at a selected condition. Since the graph in **Figure 5.2** obtained in dynamic mode already approached a maximum after 60 minutes, and the maximum duration of a static run on the supercritical extractor was also 60 minutes, all runs to check the amount of $KAu(CN)_2$ recoverable by *sc*-CO_2 in this mode of extraction were performed with this duration. The different conditions at which these runs were performed, and the corresponding shifts in elemental surface composition measured, are listed in **Table 5.3**. The temperatures and pressures were selected to yield liquid-like densities and thus high solvent strengths for *sc*-CO_2 to make provision for removal of the gold compound from the activated carbon granules by dissolution.

Table 5.3 Shift in elemental composition of activated carbon granules on exposure to *sc*-CO_2 at different conditions. t = 60 min

Batch	T / °C	p / atm	ρ / g mL^{-1}	Modifier	Elemental Surface Composition					Shift
					C	O	K	Au	total	
1					77.79	11.12	4.44	6.65	100	
	100	500	0.823		81.99	13.32	2.02	2.67	100	3.98
2					75.89	12.01	3.57	8.53	100	
	100	300	0.667		75.38	16.37	2.82	5.43	100	3.10
3					72.67	13.23	3.35	10.75	100	
	60	500	0.943		75.51	15.72	2.72	6.05	100	4.70
4					71.98	14.12	3.92	9.98	100	
	60	300	0.839	5% methanol	73.13	17.15	2.9	6.82	100	3.16
5					76.40	12.78	3.77	7.05	100	
	100	500	0.823	5% methanol	78.43	15.04	2.94	3.59	100	3.46
6					71.61	13.76	4.58	10.05	100	
	100	300	0.667	5% methanol	74.18	16.92	2.1	6.8	100	3.15
7					73.92	13.66	3.69	8.73	100	
	60	500	0.943	5% methano	74.22	17.37	2.69	5.72	100	3.01

Batch	T / °C	ρ / atm	ρ / g mL^{-1}	Modifier	Elemental Surface Composition					Shift
					C	O	K	Au	total	
8					72.17	14.34	4.92	8.57	100	
	100	500	0.823	5% methanol	75.22	18.27	1.62	4.89	100	3.68
9					75.05	13.44	3.88	7.61	100	
	100	300	0.661	5% methanol	75.19	19.48	0.52	4.81	100	2.80
10					73.45	13.88	3.7	8.97	100	
	60	300	0.839		73.7	16.38	3.08	6.84	100	2.23
11					72.63	14.21	4.95	8.21	100	
	65	300	0.816		75.06	18.53	1.90	4.51	100	3.70
12					73.64	13.89	3.08	9.39	100	
	65	300	0.816		73.91	16.40	2.65	7.04	100	2.35
13					71.83	11.85	4.29	12.03	100	
	65	300	0.816		73.29	16.15	2.63	7.93	100	4.10
14					73.01	13.47	4.73	8.79	100	
	65	300	0.816		75.02	15.01	4.33	5.64	100	3.15
15					75.08	13.14	2.70	9.08	100	
	65	300	0.816		77.45	15.92	2.47	4.15	100	4.93

Batch	T / °C	p / atm	ρ / g mL^{-1}	Modifier	Elemental Surface Composition					Shift
					C	O	K	Au	total	
16					75.83	12.67	2.67	8.87	100	
	65	300	0.816		78.73	15.45	2.02	3.81	100	5.06
17					76.43	12.47	2.57	8.54	100	
	65	300	0.816		77.63	15.75	2.41	4.22	100	4.32
18					76.95	12.54	2.58	7.93	100	
	65	300	0.816		76.43	15.67	2.48	5.41	100	2.52
19					77.46	12.37	2.57	7.59	100	
	65	300	0.816		77.19	17.20	2.19	3.42	100	4.17
20					76.95	13.26	2.82	6.96	100	
	65	300	0.816		77.39	16.91	2.20	3.50	100	3.46
Average shift										**3.6 ± 0.8**

An average shift of (3.6 ± 0.8) mass % was obtained for the 20 runs performed under a variety of conditions while maintaining a static mode of extraction throughout. This value corresponds to the maximum amount of gold which could be removed by a dynamic mode of extraction as shown in **Figure 5.2**. The fact that the percentage shift is almost the same for measurements in both static and dynamic mode means that the maximum amount of gold complex that can be extracted by *sc*-CO_2 (yield of exhaustive extraction) is also the maximum amount of gold complex that can prevail in a fixed amount of *sc*-CO_2 (yield of partial extraction) at similar conditions. The logical conclusion is that the limiting factor for gold recovery from granular activated carbon is not the solubility in or desorption/displacement by the fluid, but the amount of removable gold on the outer surface of the adsorbent. Once this has been removed, there is no more gold to retrieve, resulting in comparable maxima for the concentration-time graphs obtained in static and dynamic modes of extraction.

The question as to whether the removal of gold by either static or dynamic mode of extraction could be attributed to chemical dissolution, reversed adsorption or physical displacement remained unanswered. It was realised that no confirmation as to which one of the mechanisms was operative could be reached without having more evidence of the nature of the process of gold removal by *sc*-CO_2. This matter will be dealt with at a later stage (**Paragraph 6.2**).

References

1 McDougall, G.J.; Hancock, R.D.; Nicol, M.J.; Wellington, O.L.; Copperthwaite, R.G., *Journal of the South African Institute of Mining and Metallurgy*, **1980**, *80*, 344.

2 Adams, M.D.; Fleming, C.A., *Metallurgical Transactions B*, **1989**, *20B*, 315.

CHAPTER 6

Recovery of $KAu(CN)_2$ from Activated Carbon by Tributyl Phosphate

The previous chapter showed that $KAu(CN)_2$ could be removed from activated carbon by *sc*-CO_2 only to a very limited extent. We therefore looked for an alternative substance which could possibly be used either as a stand-alone extractant or as a cosolvent to *sc*-CO_2 to more effectively recover adsorbed $KAu(CN)_2$ from granular activated carbon. Tributyl phosphate (TBP) had been used to extract $KAu(CN)_2$ from liquid solutions.[1,2] This opted us to investigate the possibility of extracting $KAu(CN)_2$ from granular activated carbon by either pure TBP or by TBP entrained *sc*-CO_2. A plausible mechanism for such extraction given in the literature is that it can solvate and quantitatively extract $K^+ ..... Au(CN)_2^-$ ion-pairs to form $KAu(CN)_2.pTBP$ where *p* is the number of TBP molecules solvating the ion-pair.

6.1 Recovery of $KAu(CN)_2$ from Activated Carbon by TBP

The extraction of $KAu(CN)_2$ with TBP was monitored by adding 2 mL TBP to 0.1 g activated carbon loaded with 10 mg Au as $KAu(CN)_2$ and measuring the % Au extracted after different time intervals by AA analysis of the filtrate obtained in each individual run. The results are shown in **Figure 6.1**. It can be concluded from the graph that after 600 min (10 h) a maximum of ca. 10 % of the adsorbed gold could be extracted with a 2 mL aliquot of TBP. Runs lasting 24 h, 48 h and 72 h were also conducted, but no more than 10 % of the loaded gold could be recovered from the activated carbon. The logical interpretation of this result would be that an aliquot of 2 mL of TBP was saturated with the recovered gold species after about 10 h and that no more gold could be retrieved from the carbon surface unless more TBP was used. It also seemed reasonable to argue that the limiting factor was the solubility of $KAu(CN)_2$ in TBP, which corresponds with the plateau of the concentration-time profile in **Figure 6.1**, as the experiment was performed in a given amount of TBP and no additional extractant was added in the course of the experiment.

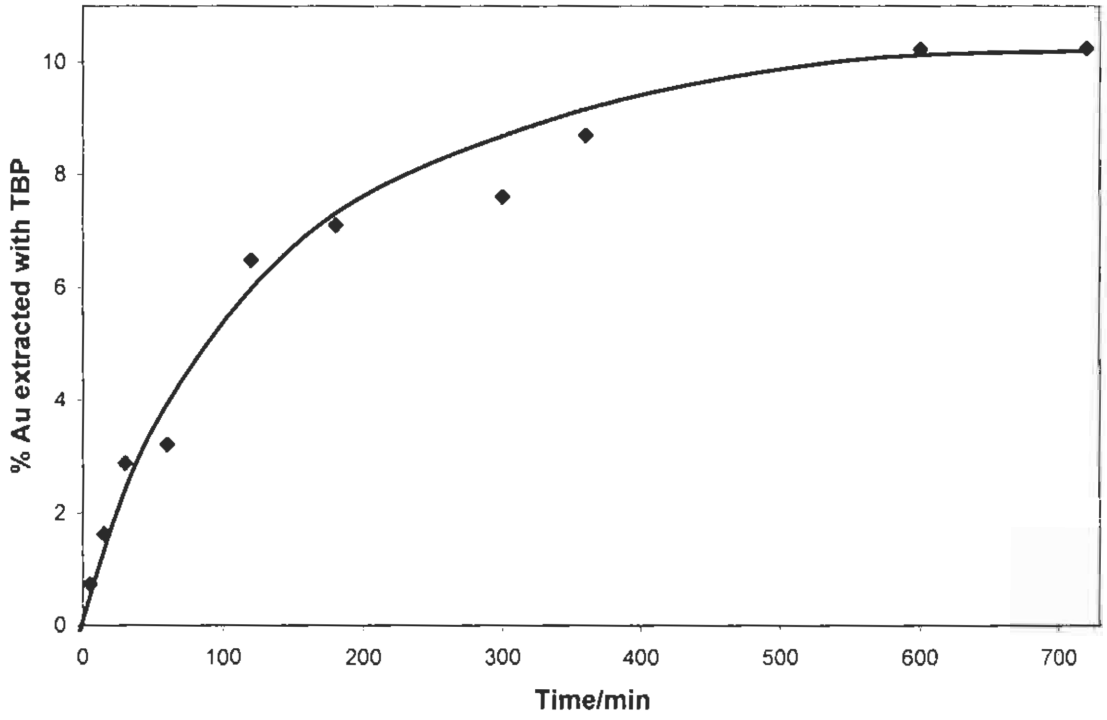

Figure 6.1 % Au recovered with TBP from 0.1 g of activated carbon containing 10 mg of Au. Temperature = 40°C, Pressure = 1 atm

In order to establish whether solubility was indeed the limiting factor, experiments were performed with double the amount of TBP (4 mL instead of 2 mL) added to 0.1 g of $KAu(CN)_2$ loaded carbon. One would expect that, by doubling the amount of TBP added to the sample, the amount of gold extracted by or dissolved in TBP would also double. These experiments, however, also resulted in a 10 % recovery of loaded gold after 10 h, implying that the limiting factor for the recovery of $KAu(CN)_2$ from activated carbon was not its solubility in TBP but a retrievable amount of this complex from the surface of the activated carbon. The recovery of gold in all experiments thus seemed to be limited by the amount of removable complex species on the carbon surface (i.e. a surface related limitation) and not by the solubility in TBP (i.e. a TBP related limitation).

The relative success achieved by extracting $KAu(CN)_2$ from activated carbon by TBP prompted us to investigate the possibility of using TBP entrained *sc*-CO_2 as a possible way to improve the yield of recovery. A first essential step towards this approach was to determine whether TBP was soluble in *sc*-CO_2, since that would allow TBP to be used as a modifier or cosolvent.

The solubility of TBP in *sc*-CO_2 was measured using the special procedure for handling a liquid sample outlined in Chapter 3. The liquid was put in a small vial at the bottom of the thimble underneath a protective packaging of high-density pulp (**Figure 3.5**). A static extraction mode was employed to measure the maximum concentration of TBP prevailing in a fixed amount of *sc*-CO_2 after selected time intervals. For each run an amount of (0.500 ± 0.005) g TBP was put into the vial, inserted into the extraction thimble and exposed to *sc*-CO_2 at selected conditions for a specific time interval. The amount of TBP dissolved in *sc*-CO_2 was determined gravimetrically and the solubility of TBP in *sc*-CO_2 was calculated to be $(1.5 \pm 0.32) \times 10^{-2}$ g per gram of CO_2 ($(5.1 \pm 1.1) \times 10^{-2}$ mol/L) at 200 atm and 40 °C. In **Table 6.1** this value is compared to the solubilities in *sc*-CO_2 of other organophosphorus compounds measured by other authors (references included in table).

Table 6.1 Solubility of organophosphorus compounds in *sc*-CO_2

Compound	T/°C	p/atm	Solubility/mol L^{-1}	Ref.
TOPO	45	200	6.6×10^{-2}	13
TBPO	60	200	0.85	13
TPPO	60	200	7.7×10^{-3}	13
TBP	40	200	5.1×10^{-2}	this work

The effort to improve the yield of gold recovery by TBP entrained *sc*-CO_2 instead of pure TBP was taken one step further by considering a TBP-HNO_3 adduct. It is generally believed that complexes with metals in higher oxidation states are more soluble in *sc*-CO_2. A good approach would therefore be to introduce an oxidising agent into the *sc*-CO_2 phase in order to oxidise the prevailing gold(I) species on the carbon surface to a gold(III) species. Nitric acid was considered to be a good oxidising agent, but it is insoluble in *sc*-CO_2 due to vast polarity differences between the two substances. A possible way of introducing HNO_3 into the *sc*-CO_2 flow was to allow it to bind to TBP to form a Lewis base - Lewis acid adduct as shown in **Figure 6.2**. A Lewis base has an electron pair to donate and a Lewis acid can accept an electron pair. In this particular case TBP (Lewis base) is CO_2-philic and thus acts as a carrier to introduce the acid into the *sc*-CO_2 phase, which in turn can lead to *in situ* oxidation of gold to possibly yield a more soluble complex species in TBP entrained *sc*-CO_2.

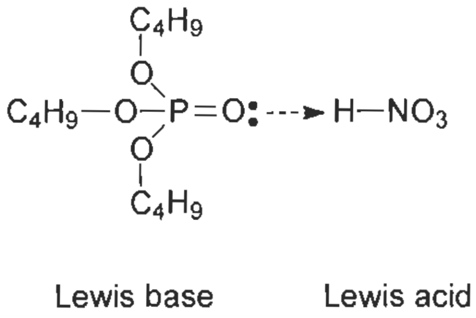

Figure 6.2 Lewis base-Lewis acid adduct of TBP-HNO_3

Recent literature^{3,4,5} reported on the use of a TBP-HNO_3 "complex" for the dissolution of UO_2 and of Au(0) on electronic circuit boards in *sc*-CO_2. HNO_3 linked to TBP was claimed to have oxidised the compounds and converted them into *sc*-CO_2 soluble species. This principle was applied in this investigation in an attempt to recover $KAu(CN)_2$ from activated carbon by either using a TBP-HNO_3 adduct as a stand-alone extractant or by using the TBP-HNO_3 adduct as an entrainer in a *sc*-CO_2 based recovery. The preparation of a suitable TBP-HNO_3

adduct and the results obtained by implementing it as either an extractant or a *sc*-CO_2 modifier are described in the next paragraph.

6.2 Recovery of $KAu(CN)_2$ from Activated Carbon by TBP-HNO_3 Adduct

A $TBP(HNO_3)_{0.7}(H_2O)_{0.7}$ adduct was prepared by mixing 5 mL of TBP with 0.815 mL of a 15.5 mol/L nitric acid solution. The mixture was shaken vigorously for 4 minutes with a Vortex-Genie 2 shaker, followed by centrifuging for 1 hour at 5 000 revolutions per minute.[4,5] The characterisation of the adduct was done by titration methods and proton NMR spectroscopy as described in the literature.[4]

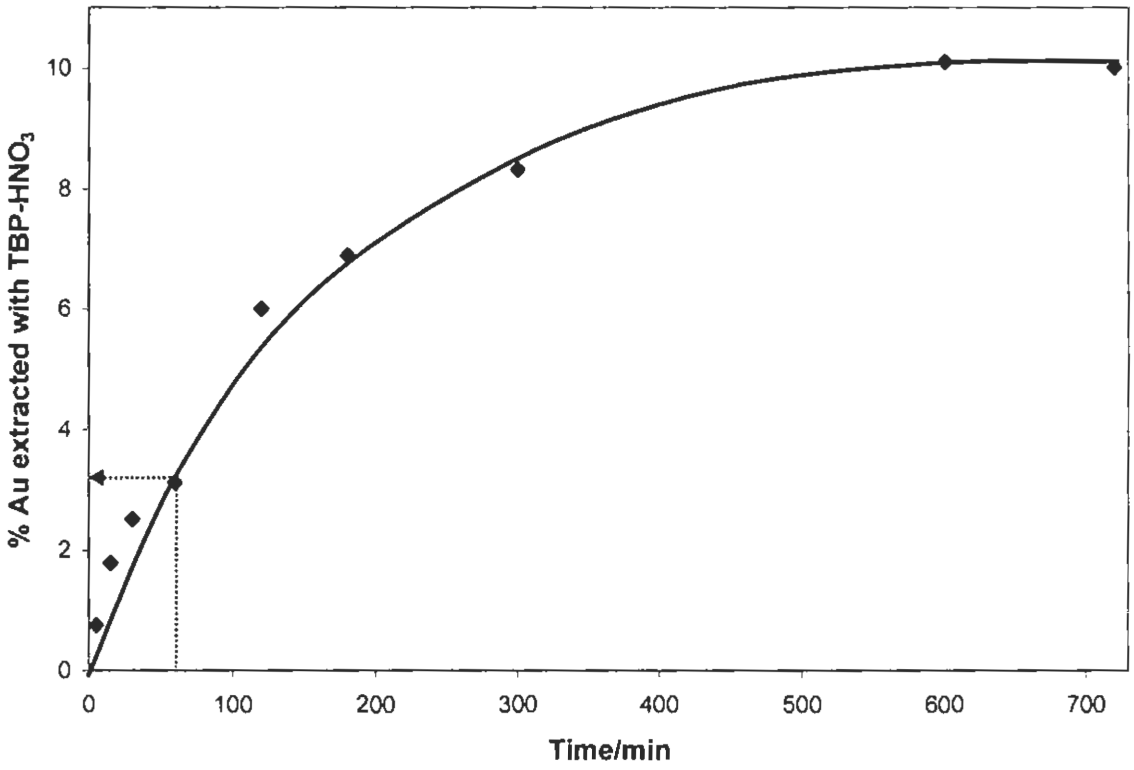

Figure 6.3 % Au gold recovered with TBP-HNO_3 adduct from 0.1 g of activated carbon containing 10 mg of Au. Temperature = 40°C, Pressure = 1 atm

The extraction of $KAu(CN)_2$ with TBP-HNO_3 adduct was studied by adding 2 mL of the adduct to 0.1 g of activated carbon loaded with 10 mg of gold as $KAu(CN)_2$ and measuring the % Au extracted after different time intervals in exactly the same way as with pure TBP in **Paragraph 6.1**. The resulting concentration-time graph in **Figure 6.3** resembles the one obtained with pure TBP in **Figure 6.1** and shows that introduction of HNO_3 as an oxidising agent to convert the complex species on the carbon surface to a higher oxidation state of gold did not improve its recovery by TBP. Runs lasting 24 h, 48 h and 72 h were also conducted as for TBP, but no more than 10 % of the loaded gold could be removed from the activated carbon.

It was checked again whether an increase in the amount of TBP-HNO_3 would have any effect on the yield of recovery. As in the case of pure TBP, 4 mL TBP-HNO_3 was added to 0.1 g carbon containing $KAu(CN)_2$, but this led to no improvement in the yield of 10 % m/m of recovered gold obtained with 2 mL of TBP-HNO_3 adduct. This indicated once more that the limiting factor for the recovery was surface related and not TBP-HNO_3 related.

In order to compare the recovery of $KAu(CN)_2$ from activated carbon by TBP-HNO_3 entrained *sc*-CO_2 with that achieved by TBP-HNO_3 as primary extractant in the preceding paragraphs, static extraction runs aimed at determining the maximum amount of $KAu(CN)_2$ prevailing in a fixed volume of TBP-HNO_3 modified *sc*-CO_2 were performed using the available supercritical extractor. In these experiments 2 mL of the TBP-HNO_3 adduct was added to 0.1 g activated carbon loaded with 10 mg of Au in exactly the same way as in the experiments above. The samples were handled according to the special procedure for liquid samples outlined in Chapter 3. The results of the extraction runs are shown in **Figure 6.4**. Since the duration of a static run is limited to 60 min with the available supercritical extractor, a maximum in the concentration-time graph was not reached as in **Figure 6.3**. However, by comparing gold retrieval after 60 min in **Figure 6.3** (ca. 3.12 %) and **6.4** (ca. 3.28 %), it does not seem that *sc*-CO_2 brought about any added advantage.

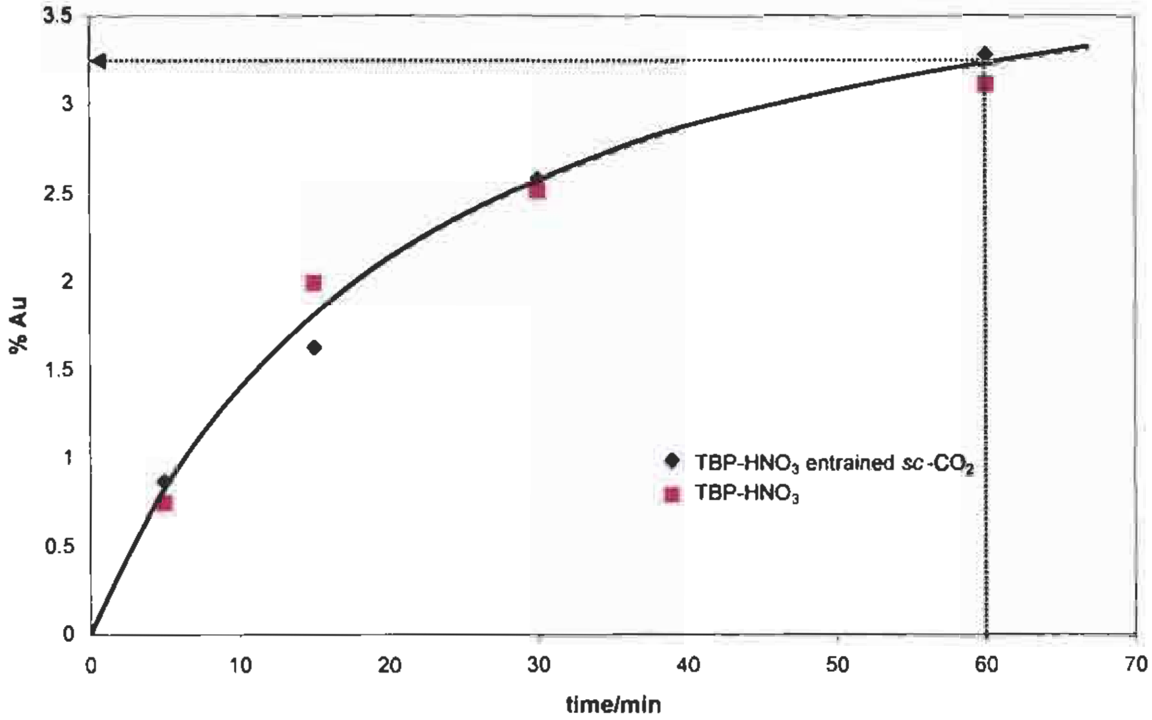

Figure 6.4 Recovery of $KAu(CN)_2$ from activated carbon with TBP-HNO_3 adduct (primary extractant) and TBP-HNO_3 entrained *sc*-CO_2 (cosolvent). Temperature = 40°C; pressure = 200 atm

A more complete comparative study was conducted to further investigate whether using TBP-HNO_3 in a *sc*-CO_2 environment would bring any advantage. Measurements were performed at different time durations and temperatures to obtain information regarding the effect of sc-CO_2 on the static recovery of gold from activated carbon with TBP-HNO_3. The pressure of *sc*-CO_2 was kept at p = 200 atm throughout. The results in **Table 6.2** show that there was essentially no difference in the % Au recovered from activated carbon by TBP-HNO_3 in the absence or presence of *sc*-CO_2.

Table 6.2 Comparison between gold recovery by TBP-HNO_3 in the absence or presence of *sc*-CO_2. Pressure = 200 atm

Time/ min	% Au recovered							
	32 °C		40 °C		50 °C		60 °C	
	without *sc*-CO_2	with *sc*-CO_2	without *sc*-CO_2	with *sc*-CO_2	without *sc*-CO_2	with *sc*-CO_2	without *sc*-CO_2	with *sc*-CO_2
5	1.57	1.26	0.75	0.87	1.56	1.25	2.09	2.04
15	2.28	2.13	2.00	1.63	2.41	2.00	2.75	2.50
30	2.75	2.81	2.52	2.59	2.88	2.78	3.28	3.13
60	3.13	3.05	3.12	3.28	4.17	3.54	4.68	4.50

The influence of temperature and pressure on the recovery of $KAu(CN)_2$ from activated carbon using TBP-HNO_3 entrained *sc*-CO_2 was also investigated. A statistical experimental design as described in **Paragraph 3.4.1** was used to determine the optimum conditions (temperature and pressure) for the recovery of gold from activated carbon containing $KAu(CN)_2$ in a fixed period of time (30 min). In **Table 6.3** the conditions and corresponding results are listed. A software package[6] was used to determine the density of *sc*-CO_2 at the different combinations of pressure and temperature. A surface response graph based on these results is shown in **Figure 6.5**. It displays two principal features of gold recovery from activated carbon by TBP-HNO_3 entrained *sc*-CO_2 as outlined below.

Table 6.3 Influence of temperature and pressure on the recovery of $KAu(CN)_2$ from granular activated carbon using $TBP-HNO_3$ entrained *sc*-CO_2. Time: 30 min.

Pressure / atm	**Temperature / °C**	**Density / g mL^{-1}**	**% Au**
500	40	1.003	2.01
200	60	0.732	2.16
500	60	0.943	2.05
100	60	0.300	2.49
600	60	0.981	2.50
350	60	0.872	2.19
200	80	0.593	2.00
500	80	0.881	2.47
350	100	0.718	3.13
350	32	0.961	1.48
200	40	0.849	2.27

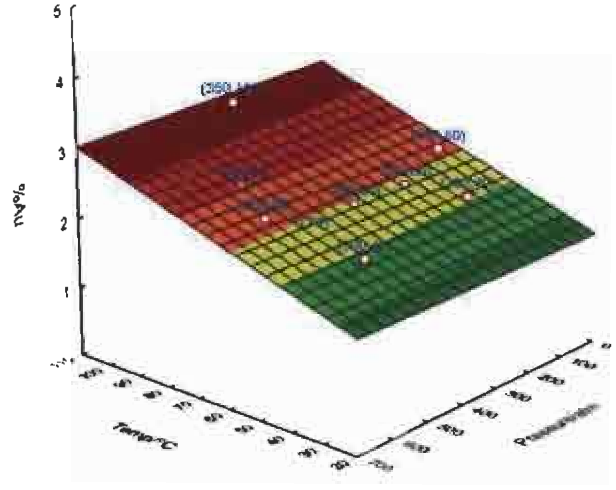

Figure 6.5 Surface response graph for the recovery of $KAu(CN)_2$ from activated carbon by $TBP-HNO_3$ entrained *sc*-CO_2. Time: 30 min.

Firstly, the recovery is independent of pressure at any given temperature, implying that the density and thus the solvent strength of *sc*-CO_2 has no effect on the process. This is also illustrated by the graph in **Figure 6.6**, which shows how % Au recovered relates to the density of the fluid. The independence of the density (and thus the solvent strength) of *sc*-CO_2 is understandable in view of the similar results obtained with TBP-HNO_3 in the absence or presence of *sc*-CO_2, indicating that the extractant is TBP-HNO_3 and not *sc*-CO_2.

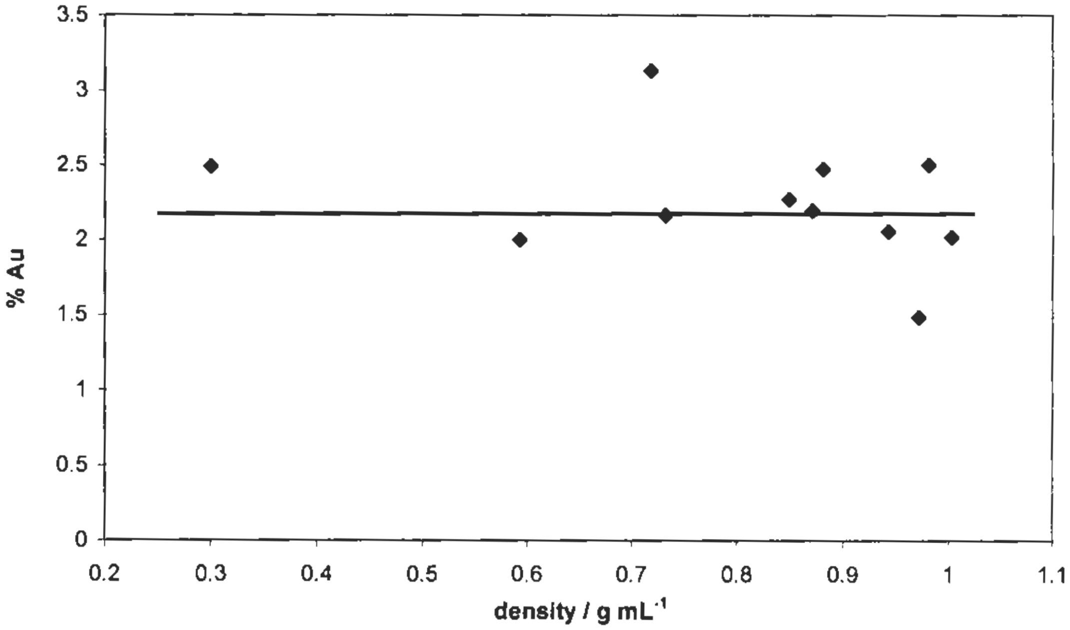

Figure 6.6 The influence of density of *sc*-CO_2 on the recovery of $KAu(CN)_2$ from activated carbon

Secondly, temperature seems to have a slightly positive effect on the recovery at any given pressure. By plotting the logarithm of the percentage of gold recovered against the inverse of the temperature as shown in **Figure 6.7**, the isosteric enthalpy of recovery (**Paragraph 3.4.2**) of $KAu(CN)_2$ by TBP-HNO_3 entrained *sc*-CO_2 could be calculated from the slope $m = -\Delta H^0/R$ of the resulting straight line[7]. The value turned out to be $AH^0 = 8.6$ kJ/mol, which is a small positive value suggesting that gold removal from the activated carbon surface by TBP-HNO_3 takes place by physical desorption.

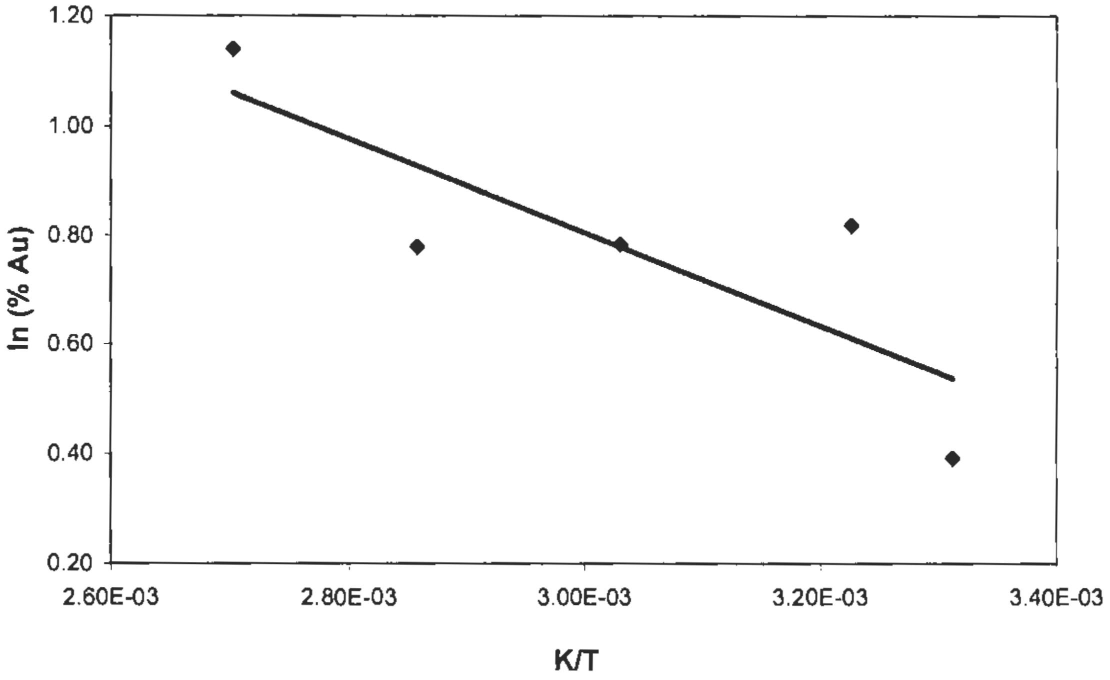

Figure 6.7 ln (% Au) versus 1/T for calculation of enthalpy of recovery by TBP-HNO_3

The conclusion that gold removal by TBP-HNO_3 most likely occurs by physical desorption (probably ion-dipole interaction as explained below) explains why only a limited amount of gold can be removed from the carbon surface. The recoverable gold probably resides in the outer layer(s) of $KAu(CN)_2$ attached to the primary monolayer on the carbon surface by weak physical forces (intermolecular, adhesion, electrostatic). This outer layer(s) is probably removed by ion-dipole attraction between opposite charges (negatively charged ion $Au(CN)_2^-$ and positively charged end of polar TBP molecule) as described by Coulomb's law. The energy associated with such interaction is generally called solvation energy, a quantity which can in certain instances (especially solvation by water, referred to as hydration) be more substantial than the value obtained here. Once the outer layer(s) is removed, TBP is incapable of recovering any more gold, and the process is limited accordingly.

6.3 Dynamic Extraction of $KAu(CN)_2$ from Activated Carbon

In all previous work in this chapter a static mode of extraction was employed. To remove a maximum amount of adsorbate from a matrix a dynamic extraction mode is required. In this mode fresh solvent is continuously introduced to dissolve/desorb material from the matrix. In the end all adsorbate will be removed from the matrix.

It was shown earlier in this chapter that TBP is soluble in *sc*-CO_2 and that $KAu(CN)_2$ can be extracted by TBP (TBP-HNO_3). This opened up the possibility to continuously introduce TBP-HNO_3 with the modifier pump of the supercritical extractor into the *sc*-CO_2 stream. The *sc*-CO_2 then acts as a carrier which constantly introduces fresh TBP-HNO_3 to exhaustively extract $KAu(CN)_2$ from the activated carbon, regardless of how long such a recovery may take. Unfortunately, in view of the detrimental effect TBP and TBP-HNO_3 have on the flow lines, valves and seals of the supercritical extractor, such a run could not be conducted. However, since there was no difference in the amount of gold extracted from activated carbon with TBP-HNO_3 in the absence or presence of *sc*-CO_2, it was possible to mimic a dynamic extraction run of this nature outside the supercritical extractor. This was done in duplicate by allowing TBP-HNO_3 to react with a sample of loaded activated carbon for a limited period of time (in this instance 1 h), after which the gold containing TBP-HNO_3 was separated from the gold loaded activated carbon before a fresh amount of TBP-HNO_3 was introduced. The procedure was repeated continuously for 6 h. The results in **Table 6.4** show that, even with a dynamic extraction with regularly added extractant, only ca. 10 % of the loaded gold could be recovered.

Table 6.4 Dynamic recovery of $KAu(CN)_2$ from activated carbon byTBP-HNO_3 adduct

Time / min	% Au	
60	3.98	3.79
120	2.17	2.43
180	1.49	1.31
240	1.19	1.03
300	0.79	0.60
340	0.41	0.30
Total	9.68	9.13

In all experimental work performed no more than 10 % of the loaded gold could be recovered, immaterial whether a static mode establishing equilibrium conditions or a dynamic mode warranting exhaustive recovery was employed. This proved that 10 % of gold recovered was the only amount of retrievable gold by TBP on the surface of the activated carbon and that this was the limiting factor in the recovery process. In order to substantiate this conclusion, experiments were performed in which the surface area of the activated carbon sample and thus the amount of retrievable gold was increased and the resulting gold recovery monitored.

In the first experiment a larger amount of loaded activated carbon (0.2 g instead of 0.1 g) was used to which 2 mL TBP-HNO_3 was added. The results obtained for a static extraction of 10 h indicated that almost twice the amount of gold had been extracted.

In the second experiment a larger carbon surface area was obtained by crushing the activated carbon sample of 0.1 g into very fine particles before 2 mL TBP-HNO_3 was added to it for a static recovery of 10 h. An amount of gold substantially larger than the amount recovered in all previous experiments was recovered.

In both experiments a larger surface area of activated carbon was exposed to the extractant and correspondingly more of the adsorbate could be extracted. From the results of these two experiments it could be concluded that the retrievable gold on the surface of the activated carbon was indeed the limiting factor for the recovery of loaded $KAu(CN)_2$ by TBP, TBP-HNO_3 and *sc*-CO_2 entrained with these substances.

In an effort to explain why gold could be recovered only from the surface and not from the inner pore structure of the activated carbon matrix, the pore size distribution of the activated carbon was determined using the mercury porosimeter referred to in **Paragraph 3.3.5**. In **Figure 6.8** the pore size distribution in relation to the intrusion volume of Hg is shown. From this result it was possible to determine the percentages of micropores (8 Å - 100 Å), mesopores (100 Å - 500 Å) and macropores (500 - 20 000 Å). **Figure 6.9** indicates that ca. 95 % of the activated carbon consisted of micropores. It was argued that the limitation to 10 % recovery could be ascribed to the abundance of micropores and the possibility that a $Au(CN)_2.p$TBP assembly was probably too large to exit a micropore. However, by simply adding bond lengths taken from the literature,[8] an approximate diameter of 20 Å for the assembly could be determined, indicating that it could exit micropores quite easily.

The most plausible explanation for the small amount of gold recoverable from activated carbon thus remains the presence of multilayers of $KAu(CN)_2$ on the surface of the activated carbon. When multilayer adsorption occurs, the initial layer acts as a substrate for further adsorption. This is usually associated with weaker physical forces interacting.[7] Probably only these weaker bonded layers are extracted with TBP or TBP-HNO_3. The primary layer of $KAu(CN)_2$ is too strongly attached to the activated carbon surface to be desorbed by TBP or TBP-HNO_3. The low isosteric enthalpy of desorption is a good indication that this explanation is indeed plausible.

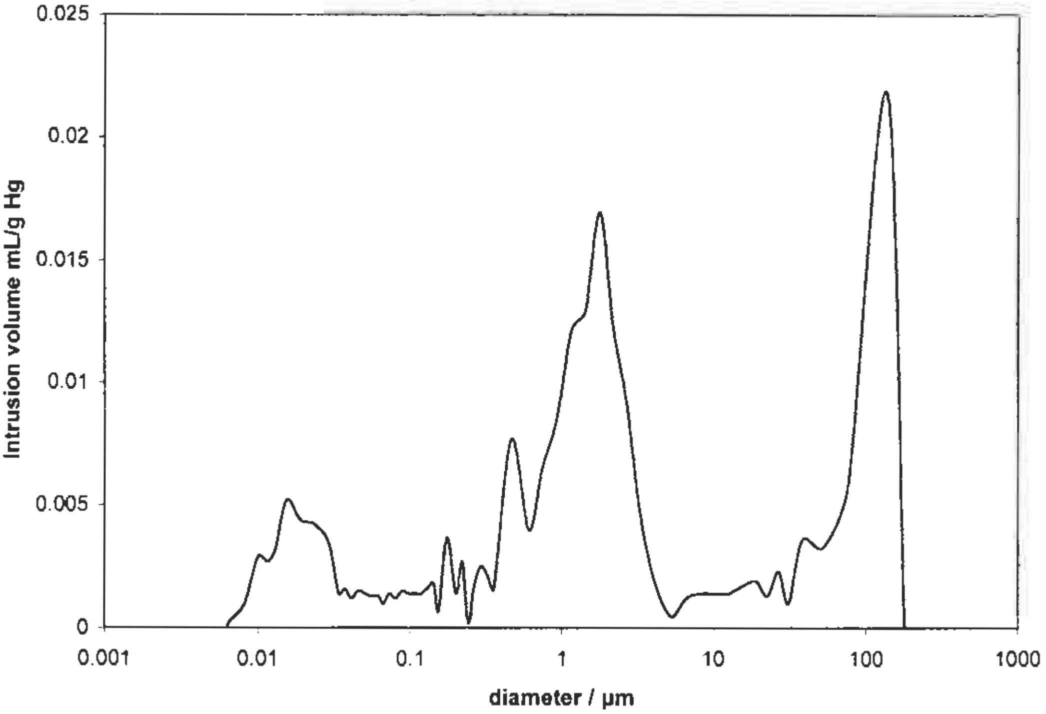

Figure 6.8 Pore size distribution of activated carbon

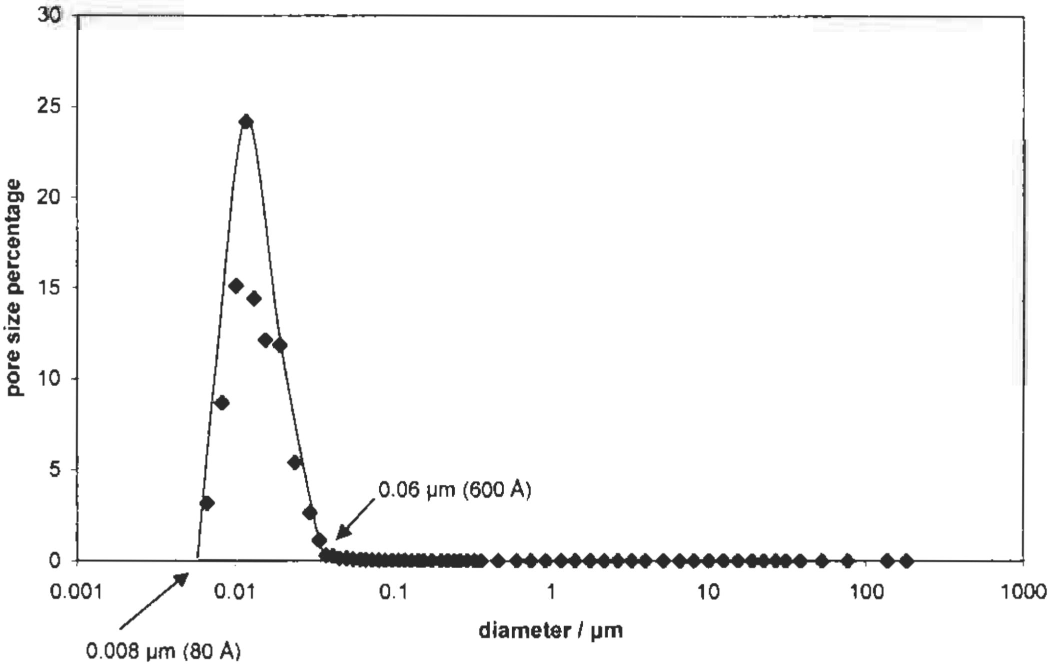

Figure 6.9 Pore size percentage of activated carbon

The amount of recoverable gold was quite different for *sc*-CO_2 and TBP (< 1 % versus ~10 %). This indicates that the extractant is an important variable and that other substances should be considered in an attempt to recover larger amounts of gold from activated carbon.

There are reports in literature on higher percentages of Au recovered by *sc*-CO_2, TBP and TBP-HNO_3[1-3,9-10] than obtained in this investigation. However, in the majority of these studies gold was not recovered from a matrix such as activated carbon where strong Van der Waals forces played a crucial role in the recovery. Another important factor not taken into consideration was sufficient precaution to prevent liquid samples from being swept from the extraction thimble by the incoming high-pressure fluid. Special methods need to be developed to deal with *sc*-CO_2 extraction of liquid samples as was shown in this investigation.

References

1 Miller, J.D.; Wan, R.Y.; Mooiman, M.B.; Sibrell, P.L., *Separation Science and Technology*, **1987**, *22*, 487.

2 Mooiman, M.B.; Miller, J.D., *Hydrometallurgy*, **1991**, *27*, 29.

3 Wang, J.S.; Wai, C.M., *Industrial and Engineering Chemistry Research*, **2005**, *44*, 922.

4 Enokida, Y.; Tomioka, O.; Lee, S.; Rustenholtz, A.; Wai, C.M., *Industrial and Engineering Chemistry Research*, **2003**, *42*, 5037.

5 Enokida, Y.; El-Fatah, S.A.; Wai, C.M., *Industrial and Engineering Chemistry Research*, **2002**, *41*, 2282.

6 SF-Solver™: Software for Supercritical Fluid Analysis, Copyright© Isco Inc., **1995**.

7 Atkins, P.W., *Physical Chemistry 8th Edition*, Oxford University Press: Oxford, **2006**.

8 Lide, D.R., *CRC Handbook of Chemistry and Physics 84th Edition*, CRC Press LLC: Washington, D.C., **2003**.

9 Otu, E.O., *Separation Science and Technology*, **1997**, *32 (6)*, 1107.

10 Otu, E.O.; Wilson, J.J., *Separation Science and Technology*, **2000**, *35 (12)*, 1879.

CHAPTER 7

Conclusion and Future Perspective

The key hypothesis to be proven in this investigation was the viability to recover gold preloaded onto activated carbon by *sc*-CO_2, either as a pure fluid or entrained by a suitable cosolvent. In this chapter the project is evaluated by considering and weighing up the successes and shortcomings encountered. A few future perspectives drawn from the results are also discussed.

7.1 Successes and Shortcomings

A first accomplishment was the conversion of Au(0) to $HAuCl_4$ in order to synthesise various gold complexes, namely $KAu(CN)_2$, $[Au\{CS(NH_2)_2\}_2]ClO_4$, $[Au(phen)Cl_2]Cl$ and $[Au(en)_2]Cl_3$. The complexes were analysed for gold content by AA, and uv/visible spectra were recorded, in a few instances for the first time ever, to further characterise the complexes. Spectral data (λ_{max}, ε_{max}) of the complexes were established, and good agreement with literature values was obtained in cases where such values were available. Moreover, spectral data could be reported that have not been published before.

The solubility in *sc*-CO_2 of the different complexes was investigated, but with the exception of $KAu(CN)_2$, none of the complexes were soluble. This was confirmed by AA and uv/visible analysis of the extracts collected. In the case of $[Au(phen)Cl_2]Cl$ and $[Au(en)_2]Cl_3$ unreacted free ligand (1,10-phenanthroline and ethylenediamine) present as an impurity or contaminant was dissolved by *sc*-CO_2, resulting in an experimental gold content closer to the theoretical value as a result of the *sc*-CO_2 removal of the unreacted ligand. This result led to a new application possibility whereby *sc*-CO_2 can be used as an alternative method to the classical recrystallisation of a substance from solution as a means of purifying the substance. The solubility of 1.10-phenanthroline in *sc*-CO_2 was formally measured in view of the foregoing result, and a value of 6×10^{-4} g per gram of CO_2 (2.8×10^{-3} mol/L) at 40 °C and 300 atm was obtained. This value turned out to be in good agreement with solubilities determined for similar ligands by other authors.

$KAu(CN)_2$ could be successfully loaded onto granular activated carbon. In a typical run 99.9 % of the available gold in solution could be adsorbed. The elemental composition (mass percent) of the surface of the gold containing activated carbon could be determined before and after exposure to *sc*-CO_2 by SEM-EDS. The analysis was performed by examining the surface of a number of selected granules at randomly selected sites to guarantee a high level of accuracy and reproducibility. The technique was capable of detecting changes of up to 3.5 % in the elemental composition of the surface of the activated carbon as a result of exposure to *sc*-CO_2. The recovery of gold indicated by these changes could be confirmed by the presence of gold in the *sc*-CO_2 extracts as detected by ICP-MS. These results proved that a limited amount of gold (< 1 %) preloaded as $KAu(CN)_2$ could be retrieved from activated carbon by *sc*-CO_2.

Tributyl phosphate (TBP) was shown to be capable of extracting more $KAu(CN)_2$ from activated carbon both as a stand-alone extractant or as a cosolvent introduced into the *sc*-CO_2 flow line, but maximally 10 % of the gold loaded onto a sample of activated carbon could be extracted. The compatibility of TBP with *sc*-CO_2 served as a motivation to formally measure its solubility in *sc*-CO_2, and the value of 1.5×10^{-2} g per gram of CO_2 (5.1×10^{-2} mol/L) at 200 atm and 40 °C turned out to be in good agreement with the solubilities of similar compounds in *sc*-CO_2 reported in the literature.

A TBP-HNO_3 adduct was prepared to improve gold recovery through oxidation of gold(I) to gold(III), but as in the case of pure TBP, no more than 10% of the adsorbed gold could be recovered. *sc*-CO_2 neither improved nor deteriorated the yield of gold recovery, regardless of whether TBP or TBP-HNO_3 adduct was used or whether *sc*-CO_2 was used in static or dynamic mode. Although the effect of continuously adding fresh extractant could be successfully mimicked outside the supercritical extractor, the amount of gold recovered could not be improved beyond 10 % of the loaded material. This figure turned out to be the maximum amount of gold removable from the activated carbon since not a single other parameter (amount of extractant, mode of extraction) could improve the extent of recovery. It could therefore be concluded that the amount of removable gold on the surface of the activated carbon was the limiting factor in all recovery attempts. This conclusion could be confirmed by experiments in which an increase in the surface of the activated carbon indeed resulted in improved recovery by TBP-HNO_3. The amount of recoverable gold was quite different for *sc*-CO_2 and TBP, indicating that the extracting agent is important and that other substances may be capable of recovering larger amounts of gold from activated carbon.

The influence of different process parameters (temperature, pressure and density) on the TBP-HNO_3 assisted *sc*-CO_2 recovery of gold from activated carbon could be resolved by utilising surface response analysis. Since pressure, and thus density at constant temperature, had no effect on the process, it could be concluded that TBP-HNO_3 rather than *sc*-CO_2 was the principal extracting agent. Temperature was shown to have a slight positive effect on gold recovery. A small positive isosteric enthalpy of recovery of 8.6 kJ mol^{-1} could be calculated, a value which pointed towards physical desorption of the outer layers of adsorbed gold on the activated carbon surface.

An innovative sample handling procedure for liquid samples in the thimbles of the supercritical extractor was implemented in this study. It prevented the sample from being swept out of the extraction thimble as a result of the entrance of the high-pressure *sc*-CO_2 and entailed placement of the liquid sample in a glass tube stabilised by high-density pulp tablets to retain the liquid effectively. The high recoveries of gold from solution by *sc*-CO_2 claimed in the literature cast some doubt on the efficiency with which liquid samples were protected against instantaneous displacement from a sample holder equipped with porous frits at both end-caps. The procedure was successfully used in this study to measure the solubility of TBP as mentioned earlier.

It would be scientific naïve and optimistic to regard the entire project successful in view of the achievements listed above. There were indeed many difficulties to overcome and, although most could be dealt with fairly successfully, a few shortcomings remained that can only be attended to in a follow-up investigation of a different scope.

Firstly, pure *sc*-CO_2 could only recover a small amount (< 1 %) of adsorbed gold from the activated carbon. Although this amount could be improved to 10 % of adsorbed gold by entraining *sc*-CO_2 by TBP or TBP-HNO_3, it was disappointing to realise that the same extent of recovery could also be achieved by pure TBP and TBP-HNO_3 and that *sc*-CO_2 was not the primary extractant.

Secondly, the solubility of complexes (and other types of substances, such as polymers[1]) in *sc*-CO_2 is disappointingly low, and more imaginative methods to improve solubility in *sc*-CO_2 need to be explored. Solubility plays an important role in recovery, and as long as solubility is low, no large scale recovery can be anticipated.

Finally, activated carbon was shown to play a decisive role in limiting the recovery process. This was contrary to initial expectations, where attention was much more given to *sc*-CO_2 as primary extractant and to a gold complex soluble in *sc*-CO_2 as a model compound to be adsorbed onto and to be recovered from activated carbon.

7.2 Future Perspective

The range of metal complexes by virtue of which gold can be stored on activated carbon and from which it can be recovered by *sc*-CO_2 should be extended in order to establish a database of suitable compounds. In particular, ligands yielding electrically neutral complexes, like fluorinated β-diketones or macrocyclic ligands, need to be selected to prepare complexes which are more readily soluble in *sc*-CO_2 according to the rule “like dissolves like”.[2]

The recovery of $KAu(CN)_2$ from granular activated carbon by TBP and TBP-HNO_3 entrained *sc*-CO_2 showed efficiencies of maximally 10 % of the gold loaded onto the activated carbon. Although this figure is surface determined, further investigation is required to identify alternative modifiers/cosolvents which, together with *sc*-CO_2, may extract higher percentages of gold as a result of improved counteraction of Van der Waals forces on the activated carbon surface. As in the case of TBP-HNO_3 adduct, which is a new form of "complex" soluble in *sc*-CO_2 and capable of extracting metals, new types of extractants need to be developed. The process of *in situ* chelation, where *sc*-CO_2 carries suitable ligands or extractants to the matrix containing the metal in order to form soluble species in *sc*-CO_2, offers yet another technique for the recovery of metals, which can also be environmentally friendly.

Van der Waals forces are probably the reason why $KAu(CN)_2$ is so strongly bound to activated carbon that recovery of gold is surface limited. Alternative matrices (ion-exchange resins or cellulose membranes) with weaker attractive forces should be considered for more efficient recovery of gold by *sc*-CO_2. Further experimentation is also needed with regard to other types of activated carbon, larger surface areas for exposure to *sc*-CO_2 and various complex species adsorbed onto the same type of activated carbon in order to better understand the limitation of recovery by the surface of the adsorbent.

There are claims in the literature of high percentages of metal recovery by *sc*-CO_2, but in most cases it is highly probable that liquid samples were swept from the extraction thimble as no precautions were taken to prevent that. The innovative procedure for handling liquid samples in this investigation proved to be an effective way to solve the problem, but more attention to this topic is necessary to obtain even more reliable results.

A limitation was the reluctance to use the supercritical extractor for gold recovery by TBP-HNO_3 entrained *sc*-CO_2 due to the harshness of the cosolvent. A more industrial type extractor that can withstand tough conditions would be ideal to perform such an experiment. Moreover, attention is currently given to an extruder design[3,4] which may replace batch type extraction by continuous extraction to handle large volumes of metal-bearing material for recovery purposes.

References

1 Moolman, S.F.; Labuschagne, P.W.; Thantsha, M.S.; Van der Merwe, T.L.; Cloete, T.E., *South African Journal of Science*, **2006**.

2 Kotz, J.C.; Treichel, P.M.; Weaver, G.C., *Chemistry and Chemical Reactivity 6th Edition*, Thomson Brooks/Cole: Canada, **2006**.

3 Research News: Supercritical extrusion - extraction, Agrotechnology & Food Innovations, Wageningen, **2004**.

4 Phelps, C.L.; Smart, N.G.; Wai, C.M., *Journal of Chemical Education*, **1996**, *73*, 1168.

ABSTRACT

The feasibility of recovering gold preloaded onto activated carbon by supercritical carbon dioxide (*sc*-CO_2) was investigated in view of the actuality of a more environmentally friendly process for the retrieval of gold from real-world matrices (ion-exchange resin, cellulose, activated carbon) than the harsh elution methods currently employed.

Several complexes of gold(I) and gold(III) were synthesised and characterised (AA, uv/visible), and their solubility in *sc*-CO_2 investigated, to identify a suitable compound for loading onto activated carbon and subsequent retrieval by *sc*-CO_2.

$KAu(CN)_2$ was successfully loaded onto activated carbon. The mass percentage of gold relative to that of other elements on the carbon surface was monitored (SEM-EDS) before and after exposure to *sc*-CO_2 using a laboratory-size supercritical extractor of the latest design. A decrease in ca. 3.6 % in the mass percentage of gold on the carbon surface, and the presence of gold in the resulting extracts (ICP-MS), confirmed that a small amount (< 1 %) of the loaded gold could be recovered. Since the same results were obtained regardless of whether *sc*-CO_2 extraction was performed in static mode (to establish equilibrium conditions for solubility measurement) or dynamic mode (to warrant exhaustive extraction), it could be concluded that the limiting factor was not the solubility of the adsorbate in the fluid but the amount of removable gold in the outer layer(s) of the adsorbed material on the surface of the activated carbon.

The extent of gold recovery was improved to ca. 10 % of the loaded gold by entraining *sc*-CO_2 with tributyl phosphate (TBP) or TBP-HNO_3 (a Lewis-acid-Lewis-base-adduct supposed to improve recovery by oxidising gold(I) to gold(III) species), but the results revealed, just as with pure *sc*-CO_2, that there was a surface related limitation and not a TBP related limitation to the amount of recoverable gold. This conclusion could be substantiated by enlarging the surface either by larger samples of loaded carbon or by crushing samples of loaded carbon to very small particles, and in both cases correspondingly higher recoveries were obtained.

The influence of different variables on the recovery of $KAu(CN)_2$ from activated carbon by TBP-HNO_3 entrained *sc*-CO_2 was studied by surface response analysis based on a statistical design. The independence of density and thus solvent strength suggested that *sc*-CO_2 was not the primary extractant, and a comparison between gold recovery in the absence and presence of *sc*-CO_2 revealed that the supercritical fluid neither improved nor deteriorated the extent of recovery by TBP-HNO_3. The slight positive effect of temperature allowed a small positive enthalpy of recovery to be calculated which could be interpreted in terms of physical desorption of gold from the carbon surface. The recoverable gold probably resided in the outer or secondary layer(s) attached to the primary monolayer on the carbon surface from where it could be desorbed by ion-dipole interaction between opposite charges ($Au(CN)_2^-$ and positive end of polar TBP), explaining why the process was found to be surface-limited.

The pore size distribution of the activated carbon was determined (mercury porosimetry) to find an explanation why gold was removed only from the surface. Although the activated carbon consisted for 95 % of micropores (8 - 100 Å), the molecular diameter of $Au(CN)_2.p$TBP was found to be ca. 20 Å so that it could easily exit a micropore and thereby warranted that, in principle, gold could be removed from the inner pore structure as well.

In the course of investigating the central hypothesis, valuable additions to existing knowledge were achieved. The spectral data acquired for a few gold complexes either confirmed existing literature data or represent new data published for the first time. The uv-visible spectra of the complexes were not only recorded but also interpreted in terms of different types of transitions (d-d, charge-transfer, $\pi^* \leftarrow \pi$, $\pi^* \leftarrow n$). The solubility in *sc*-CO_2 of an organophosphorous compound (TBP) was determined with the available supercritical extractor using a self-invented procedure which prevented liquid samples from being swept away instantaneously by *sc*-CO_2 on entering the extraction thimble. The solubility so obtained was in excellent agreement with values reported in the literature for similar type compounds at comparable conditions. The proved solubility of 1.10-phenanthroline in *sc*-CO_2 opened up the possibility of purifying a phenanthroline complex of gold(III) containing some unreacted ligand as an impurity by *sc*-CO_2 instead of recrystallising the substance from solution.

The investigation drew the attention to the decisive role played by activated carbon in limiting the recovery of gold regardless of which extractant (sc-CO_2, TBP or TBP-HNO_3) was used. This encourages investigation of alternative matrices (ion-exchange resins, cellulose membranes) with weaker attractive forces in future if an efficient gold recovery process need to be developed.

OPSOMMING

Die uitvoerbaarheid om goud wat vooraf op koolstof gelaai is met superkritieke koolstofdioksied (*sc*-CO_2) te herwin, is ondersoek in die lig van die aktualiteit van 'n omgewingsvriendeliker proses om goud vanaf reële matryse (ioonuitruilhars, sellulose, geaktiveerde koolstof) te verwyder as die harde elueringsmetodes wat tans gebruik word.

Verskeie goud(I)- en goud(III)komplekse is berei en gekarakteriseer (AA, uv/sigbare), en hulle oplosbaarheid in *sc*-CO_2 is ondersoek, ten einde 'n geskikte verbinding te identifiseer wat op geaktiveerde koolstof gelaai en in 'n daaropvolgende stap met *sc*-CO_2 herwin kan word.

$KAu(CN)_2$ is suksesvol op geaktiveerde koolstof gelaai. Die massapersentasie goud relatief tot dié van ander elemente op die koolstofoppervlak is voor en na blootstelling aan *sc*-CO_2 gemonitor (SEM-EDS) deur van 'n laboratorium-grootte superkritieke ekstraktor van die jongste ontwerp gebruik te maak. 'n Afname van ca. 3.6 % in die massapersentasie goud op die koolstofoppervlak, en die teenwoordigheid van goud in die ooreenstemmende ekstrakte (ICP-MS), het bevestig dat 'n klein hoeveelheid (< 1 %) van die gelaaide goud herwin kon word. Aangesien dieselfde resultate verkry is ongeag daarvan of ekstraksie met *sc*-CO_2 in statiese modus (om ewewigskondisies vir oplosbaarheidsmeting daar te stel) of dinamiese modus (om uitputtende ekstraksie te verseker) uitgevoer is, kon afgelei word dat die beperkende faktor nie die oplosbaarheid van die adsorbaat in die fluïed was nie maar die hoeveelheid verwyderbare goud in die buitenste laag (lae) van die geadsorbeerde materiaal op die oppervlak van die geaktiveerde koolstof.

Die omvang van die goudherwinning is tot ca. 10 % van die gelaaide goud verbeter deur tributielfosfaat (TBP) of TBP-HNO_3 ('n Lewis-suur-Lewis-basis-adduk wat veronderstel is om herwinning te verbeter deur goud(I)-verbindinge na gold(III)-verbindinge te oksideer) as ko-oplosmiddel saam met *sc*-CO_2 in te voer, maar die resultate het, soos in die geval van ongemodifiseerde *sc*-CO_2, getoon dat daar 'n oppervlakverwante beperking, en nie 'n TBP-verwante beperking nie, op die hoeveelheid herwinbare goud was. Hierdie gevolgtrekking kon gestaaf word deur die oppervlak te vergroot deur óf groter monsters gelaaide koolstof te gebruik óf monsters gelaaide koolstof tot baie klein deeltjies fyn te maal, en in albei gevalle is ooreenstemmende hoër herwinnings verkry.

Die invloed van verskillende veranderlikes op die herwinning van $KAu(CN)_2$ vanaf geaktiveerde koolstof met TBP-HNO_3 gemodifiseerde *sc*-CO_2 is met behulp van oppervlakresponsanalise gebaseer op 'n statistiese ontwerp bestudeer. Die onafhanklikheid van digtheid en dus van oplosmiddelsterkte het die vermoede laat ontstaan dat *sc*-CO_2 nie die primêre ekstraheermiddel was nie, en 'n vergelyking van die goudherwinning in die afwesigheid en teenwoordigheid van *sc*-CO_2 het aan die lig gebring dat die superkritieke fluïed die omvang van die herwinning met TBP-HNO_3 nóg verbeter nóg benadeel het. Die geringe positiewe effek van temperatuur het dit moontlik gemaak om 'n klein positiewe herwinningsentalpie te bereken wat geïnterpreteer kon word in terme van fisiese desorpsie van goud vanaf die koolstofoppervlak. Die herwinbare goud kom waarskynlik voor in die buitenste of sekondêre laag (lae) bo-op die primêre monolaag op die koolstofoppervlak vanwaar dit deur ioon-dipool-wisselwerking tussen teenoorgestelde ladings $Au(CN)_2^-$ en positiewe pool van polêre TBP), gedesorbeer word en sodoende verklaar waarom die proses oppervlak-beperk is.

Die poriegrootteverspreiding van die geaktiveerde koolstof is bepaal (kwikporosimetrie) ten einde 'n verklaring te probeer vind waarom goud slegs vanaf die oppervlak verwyder word. Alhoewel die geaktiveerde koolstof vir 95 % uit mikroporieë (8 - 100 Å) bestaan, is die molekulêre deursnee van $Au(CN)_2.p$TBP ca. 20 Å sodat dit maklik 'n mikroporie kan verlaat en daardeur verseker dat goud in beginsel ook vanaf die binneste poriestruktuur van die koolstof verwyder kan word.

Terwyl die sentrale hipotese ondersoek is, is waardevolle toevoegings tot bestaande kennis gemaak. Die spektraaldata wat vir 'n aantal goudkomplekse bepaal is, het óf bestaande literatuurdata bevestig óf nuwe gegewens verteenwoordig wat vir die eerste keer gepubliseer is. Die uv-sigbare spektra van die komplekse is nie slegs geregistreer nie maar ook geïnterpreteer in terme van verskillende tipe oorgange (d-d, ladingoordrag, $\pi^* \leftarrow \pi$, $\pi^* \leftarrow n$). Die oplosbaarheid in *sc*-CO_2 van 'n organofosforverbinding (TBP) is met die beskikbare superkritieke ekstraktor bepaal deur van 'n eie oorspronklike prosedure gebruik te maak wat verhoed dat vloeistofmonsters oombliklik uitgeforseer word sodra *sc*-CO_2 die ekstraksiehouer binnekom. Die oplosbaarheid wat só gemeet is, is in uitstekende ooreenstemming met waardes wat in die literatuur vir soortgelyke tipe verbindings by vergelykbare kondisies gerapporteer word. Die bewese oplosbaarheid van 1.10-fenantrolien in *sc*-CO_2 het die moontlikheid geskep om 'n fenantrolienkompleks van goud(III) wat ongereageerde ligand as onsuiwerheid bevat met *sc*-CO_2 te suiwer in plaas daarvan om die stof uit oplossing te rekristalliseer.

Die ondersoek het die aandag gevestig op die deurslaggewende rol wat geaktiveerde koolstof in die beperking van goudherwinning speel ongeag watter ekstraheermiddel (*sc*-CO_2, TBP of TBP-HNO_3) gebruik word. Dit dien as aansporing om in die toekoms alternatiewe matryse (ioonuitruilharse, sellulose membrane) met swakker aantrekkingskragte te ondersoek indien 'n doeltreffende goudherwinningsproses ontwikkel moet word.

ACKNOWLEDGEMENTS

First of all I would like to thank God Almighty for giving me the strength, patience and inspiration to could have completed this investigation. Without Him nothing is possible.

I would like to also thank the following people and institutions:

My wife Cecile for her enduring love, encouragement and unconditional support.

My parents, Buks and Lettie, for the foundation they gave me and for their inspiration and guidance to grow as an individual.

My parents-in-law, Don and Annette, for their encouragement and understanding.

Prof. Ernst Breet for his invaluable contribution as promoter and for his enthusiasm and guidance to successfully complete this study.

Dr. Charles Williams for his assistance during the investigation and his indispensable contribution and inputs to the project.

Dr. Colin Read for help with AA analyses and for being a good and encouraging friend.

Dr. Casper Steenkamp for his assistance and support as a colleague in comprehending supercritical technology and for his friendship.

Dr. Louwrens Tiedt for help with SEM-EDS analysis.

Mr. Peet Jansen van Rensburg for ICP-MS analysis.

Mr. Hertzog Bissett for his help with porosimetric measurements.

Rand Refinery for their generous sponsorship of metallic gold for the investigation.

Mr. Deon van Rensburg and ChemQuest who donated activated carbon for the research project.

The staff of the Separation Science and Technology (SST) workshop.

Support staff of the SST and the School of Chemistry.

NRF and North-West University for research funding.